Politecnico di Torino

Master's Degree in Aerospace Engineering

Master's Degree Thesis

Minimum-Propellant Direct, Assisted, and Slingshot Return Trajectories from Mars, Jupiter, and their moons

Supervisors:
Dr. Luigi Mascolo
Prof. Manuela Battipede

Candidate:
Alessio Patti

Academic Year 2022-2023

"What that perhaps suggest is that
this tiny candle of consciousness that is humanity
is all that exists in a vast darkness
and we should do everything we can
to ensure that the candle does not go out."
-Elon Musk

Contents

List of Figures

List of Tables

Acronyms

2BP Two-Body Problem.

3BP Three-Body Problem.

4BP Four-Body Problem.

AU Astronomical Unit

BDE Best Direct Escape.

BCFB Best Combined Fly-By.

BC Boundary Condition.

CR3BP Circular Restricted 3-Body Problem.

DE Direct Escape.

DU Distance Unit.

FBPh Fly-By Phobos.

FBDe Fly-By Deimos.

ECI Earth-Centered Inertial.

EOM Equation of Motion.

LEO Low Earth Orbit.

LMO Low Mars Orbit.

MSR Mars Sample Return

PBCR4BP Planar Bicircular Restricted 4-Body Problem.

SOI Sphere Of Influence.

S/C Spacecraft.

VU Velocity Unit.

Abstract

For future space missions, exploiting planet's moons to escape from its sphere of influence can significantly improve the performance of the mission itself. In fact, being able to return to Earth while saving the maximum amount of propellant possible allows, at the preliminary stage, to design the mission with more mass to be allocated to the payload, which means being able to carry out more scientific explorations that will allow us to gain a greater understanding of our planetary system.
This study focuses on identifying the minimum-propellant mission architectures for future return missions from planets with moons to Earth. In particular, Mars and Jupiter are selected as the central bodies, and their moons, including Phobos, Deimos, and the four most massive moons of Jupiter, are taken into consideration. The analysis explores various escape strategies, such as direct escape trajectories from each gravitational body and either gravity assists or powered flybys. The study considers more than 100 different mission architectures, which include direct escape trajectories and all the possible permutations with one or two additional moons. A detailed analysis narrows the search space for the best gravitational body combinations and identifies the most promising candidate strategies for escape. Different dynamical models are implemented, including a three-body dynamical model and a bi-circular four-body problem, respectively for when one or two moons are considered along with the more massive primary. The heliocentric phase follows Keplerian motion and is patched to the escape conditions from the primaries at the sphere of influence. JPL's DE432s ephemerides are implemented to retrieve the celestial bodies' states over time. A Lambert's problem for the return trajectory explores launch windows between January 1, 2025, and December 31, 2050. Results show significant differences between the Mars and Jupiter frameworks, with an evident cut-off convenience threshold for considering moons to escape when a bigger primary to smaller primary flyby is implemented. In contrast, solutions that exploit trajectories from a smaller primary towards the bigger one to take advantage of its gravitational pull or the Oberth effect are promising regardless of the specific primary's mass ratio. Notably, the solutions exhibit periodicity over the years due to the combined planetary ephemerides.

Chapter 1

Introduction

The exploration of Mars represents an ambitious goal of humanity in our journey through a better understanding of the cosmos. This planet has always held an irresistible attraction for past and present generations. Recent missions, such as those of the Curiosity and Perseverance rovers, have contributed significantly to our understanding of the red planet and paved the way for future human missions. In particular, Curiosity found that early Mars could have supported life. It also found traces of organic molecules preserved in rock layers 3.5 billion years old and that the amount of methane in the Martian atmosphere varies with the seasons [1]. Also the key objective for Perseverance's mission on Mars is astrobiology, including the search for signs of ancient microbial life. The rover will characterize the planet's geology and past climate, pave the way for human exploration of the red planet, and be the first mission to collect and cache Martian rock and regolith [2].
In the field of human space exploration, one of the most daring and widely debated initiatives of recent years has been the Mars One mission. This visionary undertaking, first announced in 2012, aimed to establish a permanent colony on Mars, opening the door to a momentous chapter in the evolution of the human race. Beginning in 2025, the program plans to land four people on Mars every 26 months via a series of one-way missions, using exclusively existing technology [3]. Mars One has been enthusiastically hailed by some as the symbol of a multiplanetary future, but it has also generated intense debates about its feasibility, sustainability, and the scientific rigor of its ambitions.
But the Mars One mission is not alone in setting such an ambitious goal: in the context of space exploration, the Mars Sample Return (MSR) mission emerges as an outstanding and critically important undertaking. This ambitious mission aims to take a momentous step in the study of Mars by planning to collect and return soil and rock samples from this planet. MSR's primary goal is to refine our scientific understanding of Mars, but its scope goes far beyond the boundaries of a single planet. MSR represents the pinnacle of international cooperation between space

agencies and scientific institutions, bringing together the best in space engineering and scientific research. In fact, ESA is working with NASA to explore mission concepts for an international Mars Sample Return campaign between 2020 and 2030 [4, 5].
The return of Martian samples to Earth represents an unprecedented technical and logistical challenge, requiring sophisticated sampling systems, highly specialized spacecraft and meticulous planning. However, the expected scientific results and the promise of laying the groundwork for future human missions to Mars make MSR a key milestone in the exploration of our solar system. A feasibility study was conducted of a potentially simple and low cost approach to Mars Sample Return mission enabled by the use of new commercial capabilities [6, 7].
One of the most significant challenges in this journey is the return from the surface of Mars. Developing safe and reliable systems for launch and return from Mars represents a complex technological barrier that will require significant resources and ingenuity. However, despite the challenges and costs, Mars exploration is vital to humanity's future. It is not only about discovering new scientific information, but also about considering the long-term survival of our species. Mars could become a future human colony, a resource for Earth's resource reserves, and a springboard for further exploration in the solar system.
In conclusion, the possibility of being able to getting to and from Mars in the near future is becoming more and more concrete especially in recent years. The difficulties in accomplishing such a mission are not only related to how to get to the red planet, but, if we want to get human beings there, we also have to pose the problem of how to get the astronauts safely back to Earth.
This thesis aims to identify the best possible maneuver that will allow a space probe located on a low orbit of a generic solar system planet to return to Earth while consuming the least amount of propellant. Therefore, to achieve this, a four-body planar bicircular model ($PBCR4BP$) will be used to evaluate whether and how fruiting, via flyby maneuvers, a planet's moons can actually be an advantage.
In particular, this implemented four-body model makes it possible to simulate any ternary system, thus allowing the creation of a system with a generic primary body while also including in the analysis the perturbative actions of any two moons, so that possible gravitational assist maneuvers with them can be evaluated.
Within this framework, the ternary system consisting of Mars and its two moons Phobos and Deimos will be presented and considered as a specific case and the main topic of this paper.
Therefore, four different types of maneuvers will be presented: a direct escape, an assisted escape by flyby of Phobos, an assisted escape by flyby of Deimos, and finally, a combined flyby maneuver with both Mars moons will also be evaluated. The analyses performed in this paper should not be exclusively applicable only to

the Mars-Phobos-Deimos tertiary system; rather, a parametric study was conducted in which as the gravitational parameter of the binary system, the mass of the tertiary body and the distance between the secondary and tertiary body vary, it is possible to describe all existing three-body systems.
In fact, since Phobos and Deimos are very small and not very massive moons [8], it would be possible to conclude, even before results are obtained, that their gravitational aids to the probe are actually negligible; for this reason, the parametric study consists of simulating, in steps of an order of magnitude each, an increase in the gravitational parameter of the binary system, so that it is possible to investigate what the minimum mass ratio between primary and secondary must be in order for it to make sense to speak of a gain of at least 1 m/s over the ΔV that is needed to implement a direct escape maneuver without exploiting the gravitational assistance of a planet's moons.
Therefore, in the first chapter the aim is to briefly summarize the purpose of this work so as to provide a general overview and the logical flow followed. In the second chapter a reminder of the fundamentals of spaceflight mechanics will be given, with a focus on the differential equations of dynamics that describe spacecraft behavior in space and the various types of maneuvers that can be implemented. The third chapter will go into more detail about the mission both from a theoretical point of view, going into an analysis of the fundamental quantities describing the Mars-Phobos-Deimos synodic system, and from a practical point of view in terms of the implementation in the *Matlab* environment of the code used to simulate in this particular case the Mars-Phobos-Deimos synodic system but, by appropriately varying the three parameters described above, it would be possible to simulate any tertiary system existing in nature.
The core of this code consists of a genetic algorithm, which will be described and analyzed in detail in the fourth chapter: its purpose is to find the best possible combination of initial conditions that, integrated over time according to the equations of motion (EOMs) of the *PBCR4BP*, allow minimizing the errors defined as constraints imposed on the final conditions.
The results obtained for the Martiocentric system will be explained and commented on in the fifth chapter, while the sixth and last chapter will present the final conclusions.

Chapter 2

Fundamentals of orbital mechanics

It is intended to present in this chapter a brief overview of the essential theoretical concepts on which the physics of the problem analyzed in the thesis is based. The fundamental laws governing motions in space will then be described, moving on to the key aspects of defining orbits. Then, propulsion-related parameters will be introduced in order to present the main characteristics of orbital maneuvers, reference systems and the most common types of maneuvers will be described in order to provide a general overview of the context in which this thesis work focused, paying particular attention to the restricted circular three-body model and then moving on to the more accurate, as well as the model implemented in this work, bicircular and planar four-body model. For the realization of this chapter, use was made of reference books [9, 10, 11, 12, 13, 14].

2.1 Gravitational force of attraction

Gravitational force of attraction. *Two material points A and B of masses m_A and m_B separated by a distance r, exert on each other an attractive force F directed as the segment AB; the modulus of this force F is directly proportional to the product of the two masses and inversely proportional to the square of their mutual distance $r = |AB|$*, that is:

$$\vec{F_g} = -\frac{Gm_A m_B}{r^2}\frac{\vec{r}}{r} \tag{2.1}$$

where $G = 6{,}673 \times 10^{-11}\,\mathrm{m^3/(kg\,s^2)}$ is the constant of universal gravitation (2.1). The universal term means that this law is valid both on Earth and in celestial space. The negative sign present in the equation (2.1) is due to the fact that the force is of the attractive type so in the opposite direction with respect to the vector $\vec{r}$. Note that the $\vec{F_G}$ is the same for both bodies, however, due to the different mass possessed, it will cause a different acceleration $\frac{F}{m}$ for the two bodies.

2.2 Mention of the N-body problem

The N-body problem means the study of the motion of a set of N masses $m_1, m_2, \ldots, m_N$, distributed in a Euclidean space and interacting with each other only by gravitational forces. It represents in a general way the problem under consideration, where the satellite is the i-th mass subjected to the gravitational forces of the other N-1 celestial bodies.

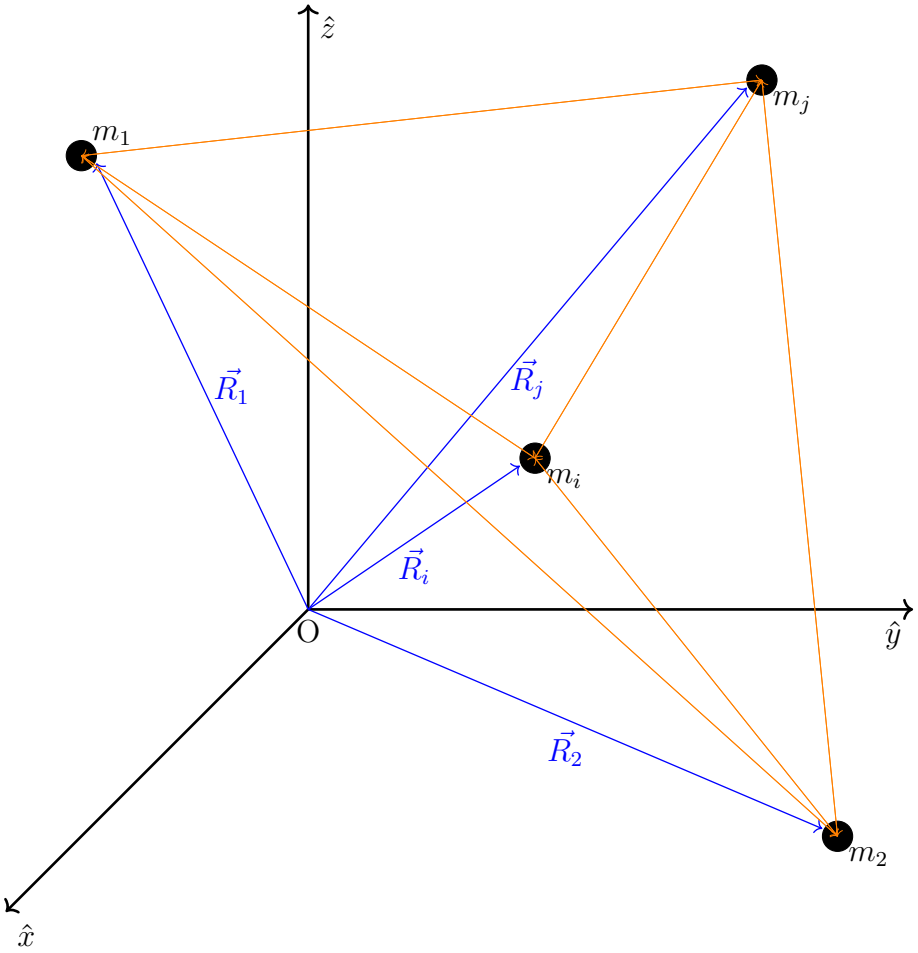

Figure 2.1: N-body problem

The following assumptions are made:

1. Bodies are point masses.
2. Bodies have constant, homogeneous masses.

3. Only the contribution of the gravitational force is considered.

Defining an inertial reference system centered at any point O (such as the one in figure 2.1): it is possible to describe a position vector $\vec{R_i}$ relative to the i-th mass and consequently the distance vector of body j relative to body i as $\vec{R_{ij}} = \vec{R_i} - \vec{R_j}$. With these definitions, now it is possible to evaluate the force exerted by mass i on mass j using Newton's second law of dynamics:

$$\vec{F} = \frac{d}{dt}(m\dot{\vec{r}}) \tag{2.2}$$

where $\dot{\vec{r}}$ is the velocity of the body and, in the case where the mass is constant over time, takes the form:

$$\vec{F} = m\ddot{\vec{r}} \tag{2.3}$$

In the present case the gravitational force can be expressed as:

$$\vec{F_g} = -G\frac{m_i m_j}{||\vec{R_i} - \vec{R_j}||^2}\frac{\vec{R_i} - \vec{R_j}}{||\vec{R_i} - \vec{R_j}||} \tag{2.4}$$

Using the equation (2.3) in the (2.4) and simplifying the i-th mass is ultimately obtained:

$$\ddot{\vec{R}}_i = \sum_{i \neq j} -G\frac{m_j}{||\vec{R_i} - \vec{R_j}||^2}\frac{\vec{R_i} - \vec{R_j}}{||\vec{R_i} - \vec{R_j}||} \tag{2.5}$$

Thus there will be N vector equations that will have to be solved all at once since it is a system of equations coupled together. One could decompose $\vec{R_i}$ into the three components along the principal axes so as to work with scalars and no longer with vectors however, in this way one would have 3N coupled equations. The main problem remains, however, that this set of equations does not have an analytic solution in closed form (except for the N=2 case), so it will be necessary to resort to numerical methods.
Subtracting from all the equations that of the j-th body, whose relative motion one want to study, it is possible to obtain N-1 vector equations, and assuming that the mass of the satellite is m_j it is possible to make the following assumption:

$$m_j << m_1, m_2, \ldots, m_{N-2} \tag{2.6}$$

By doing so, is talking about the problem of N bodies *restricted*.

2.3 Two-body problem

The simplest case of the N-body problem is the one with N=2. The condition just presented is ideal and in some cases introduces a strong simplification, but

when two masses are very close to each other relative to each other, the gravitational disturbances of the other bodies become negligible, and the two-body problem describes the physics of the system with good approximation.

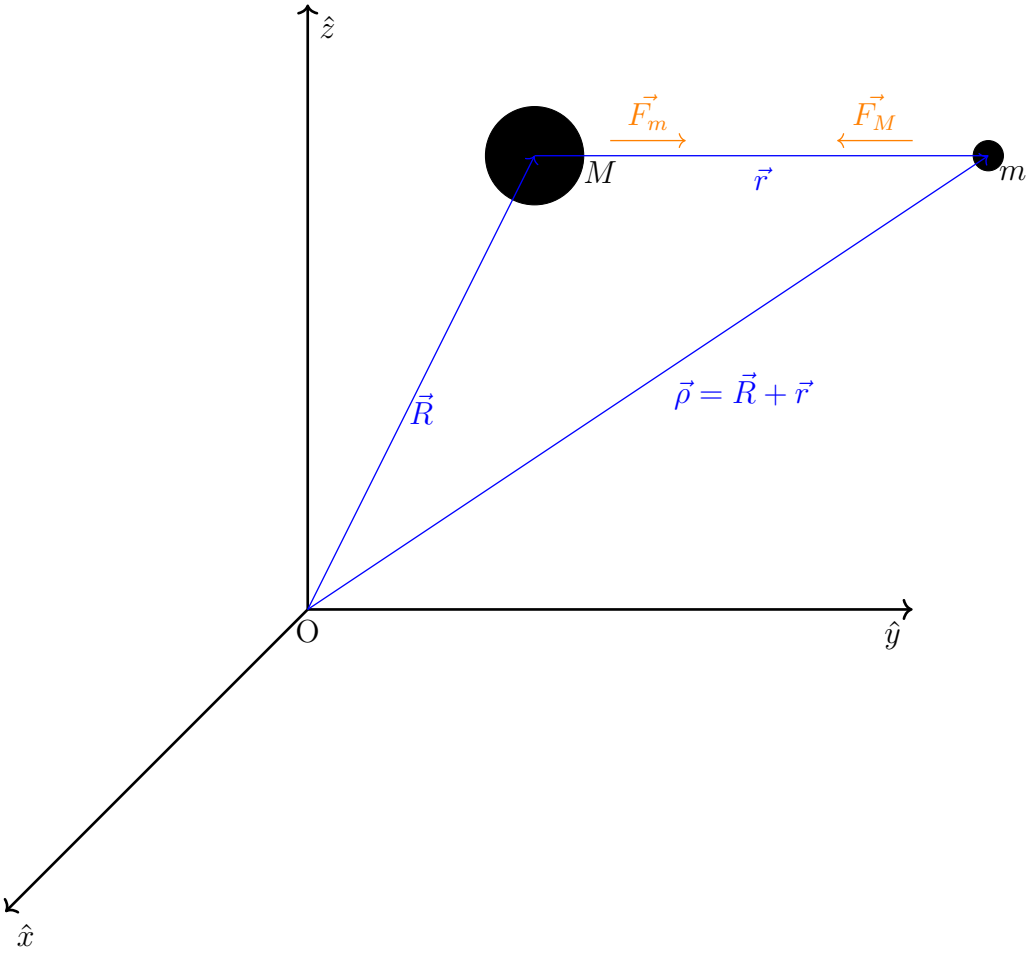

Figure 2.2: Two-body system

Defining an inertial reference system centered at any point O (like the one in the figure 2.2): consider two bodies of masses M and m $\vec{r}$ away from each other and consider the following assumptions to be valid:

1. The two bodies are point masses.
2. The two bodies have masses such that m $\ll$ M.
3. Only the contribution of the gravitational force is considered.
4. The influence of the generic smaller body is not considered.

In particular, if one considers, in accordance with Hypothesis 2, one of the two masses to be much less than the other, the problem is further simplified: the force that the small body exerts on the large body is irrelevant, and it is possible to place the origin of the reference system at the center of the large body of mass M, which will be considered inertial. This is called the *restricted two-body problem*. It is possible to define the absolute value of the gravitational forces as follows:

$$|\vec{F_m}| = |\vec{F_M}| = G\frac{mM}{r^2} \tag{2.7}$$

Considering the body m:

$$m\ddot{\vec{\rho}} = -G\frac{mM}{r^2}\frac{\vec{r}}{r} \tag{2.8}$$

Considering the body M:

$$M\ddot{\vec{R}} = +G\frac{mM}{r^2}\frac{\vec{r}}{r} \tag{2.9}$$

Evaluating the relative motion of m with respect to M so from (2.8) - (2.9):

$$\ddot{\vec{\rho}} - \ddot{\vec{R}} = -G\frac{M+m}{r^2}\frac{\vec{r}}{r} \tag{2.10}$$

Using hypothesis 2 one can neglect the mass m and write:

$$\ddot{\vec{r}} \simeq -\frac{GM}{r^2}\frac{\vec{r}}{r} \tag{2.11}$$

This gives the equation of motion in the two-body problem:

$$\ddot{\vec{r}} + \frac{\mu}{r^2}\frac{\vec{r}}{r} = 0 \tag{2.12}$$

Where the planetary gravitational constant $\mu = GM$ was introduced. It is valid for the Earth $\mu = 398\,600\,\mathrm{km}^3/\mathrm{s}^2$, for the Sun $\mu = 1{,}327 \times 10^{11}\,\mathrm{km}^3/\mathrm{s}^2$ but can be defined for any planet in the solar system.
Given the great importance of this parameter within this thesis work and, more specifically, in view of what will be the subsequent considerations, it is to get an idea from the outset of the orders of magnitude of the gravitational parameter μ for the various planets of the solar system, which can be visualized by the table 2.1:

	Sun	**Mercury**	**Venus**	**Earth**	**Mars**
$\boldsymbol{\mu}$ **[km³/s²]**	$1{,}3271 \times 10^{11}$	$2{,}2032 \times 10^{4}$	$3{,}2486 \times 10^{5}$	$3{,}986 \times 10^{5}$	$4{,}2828 \times 10^{4}$
	Jupiter	**Saturn**	**Neptune**	**Pluto**	
$\boldsymbol{\mu}$ **[km³/s²]**	$1{,}2669 \times 10^{8}$	$3{,}7931 \times 10^{7}$	$5{,}7940 \times 10^{6}$	$6{,}8366 \times 10^{6}$	

Table 2.1: Planetary gravitational constant

2.4 Sphere of influence

The purpose of this section is to analyze when the restricted two-body model is sufficiently accurate. Consider the satellite in question (of negligible mass) subject to the gravitational fields of Earth and Sun. In addition to this, the presence of a centrifugal force related to the Earth's rotation around the Sun must be taken into account; as the probe takes off from the Earth, it too will be subjected to the centrifugal force and this will change as a function of distance from the Sun, less as it approaches and more as it moves away. There will exist in space the locus of the points where the vector sum of the three forces will be zero, and it is shown that, with good approximation, it is a sphere centered in the lesser body (in this case Earth) of radius:

$$r_{SOI} = a_{ES}\left(\frac{m_{Earth}}{m_{Sun}}\right)^{\frac{2}{5}} \tag{2.13}$$

where a_{ES} is the average distance between the Earth and the Sun and is worth one astronomical unit (AU) or about 149.6 million kilometers.
This means that when the satellite is sufficiently outside of this sphere, the Sun's gravity will be the predominant force and the two-body model narrow satellite-Sun becomes valid, while inside it, it will be necessary to use the satellite-Earth model. At the boundaries of the sphere, all three bodies will need to be analyzed.

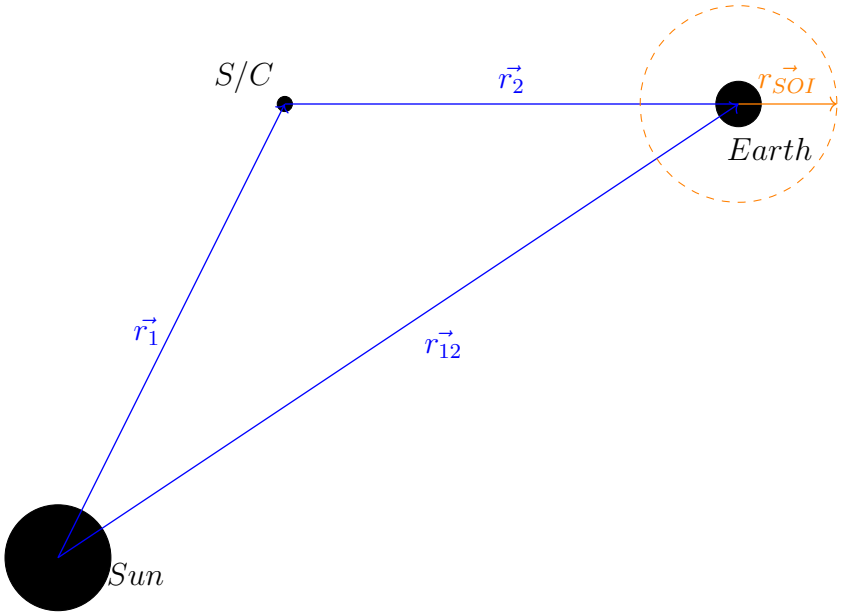

Figure 2.3: Earth's sphere of influence - not to scale

In the problem at hand, typically the probe will move away rather significantly

from the Earth, effectively making the two-body restricted satellite-Sun model a sufficiently accurate approximation of the real case.
A graphic representation of the earth's sphere of influence relative to the sun can be visualized in figure 2.3.

2.5 Gravitational energy

A gravitational field is a conservative field, in fact, a body moving under the influence of the gravitational force does not lose or gain energy but there is a continuous exchange between kinetic energy and potential energy. In order to vary the angular momentum of a system rotating about its center of rotation, it is necessary for a force to act on the system that has a tangential component; the gravitational force has only a radial component so the angular momentum will also remain constant.
Since the gravitational field is conservative it is permissible to define the gravitational potential energy of a body, which will not depend on the path taken by the mass m but only on the initial and final position.

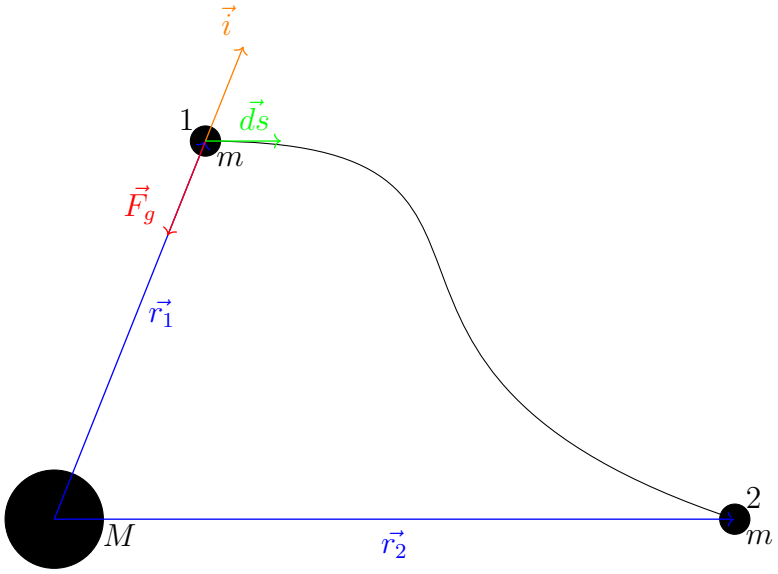

Figure 2.4: Potential energy in a gravitational field

Calculating the work done to move the body of mass m from position 1 to position 2 as shown by the figure 2.4, counteracting the force of gravity acting in

the radial direction $\hat{i}$ and is attractive:

$$\mathcal{L} = \int_1^2 \frac{\vec{F}}{m}\vec{ds} = \int_1^2 \frac{\mu}{r^2}\frac{\vec{r}}{r}\vec{ds} = \int_1^2 \frac{\mu}{r^2}\vec{dr} = \Big[-\frac{\mu}{r} \Big]_1^2 = -\frac{\mu}{r_2} + \frac{\mu}{r_1} = Eg_2 - Eg_1 \quad (2.14)$$

Evaluating the potential energy at a generic point in the gravitational field:

$$Eg_P = -\frac{\mu}{r} + C \quad (2.15)$$

where C is an arbitrary integrative constant, assumed by convention to be zero: this means that the body will have zero potential energy when it is at an infinite distance from the main body, while in other cases it will be negative by definition.

2.6 Specific angular momentum

The velocity of a body rotating in a plane has two components, a radial v_r and a tangential v_t:

$$\vec{\dot{r}} = \begin{Bmatrix} v_r \\ v_r \end{Bmatrix} = \begin{Bmatrix} \dot{r} \\ r\dot{\nu} \end{Bmatrix} \quad (2.16)$$

As for the acceleration $\vec{\alpha}$, on the other hand, the one in the two-body problem has only the radial component $\hat{i}$:

$$\vec{\ddot{r}} + \frac{\mu}{r^2}\frac{\vec{r}}{r} = 0 \rightarrow \vec{\alpha} = -\frac{\mu}{r}\hat{i} \quad (2.17)$$

Specifically, the radial α_r and tangential α_t components will be:

$$\alpha_r = \ddot{r} - r\dot{\nu}^2 \quad (2.18)$$

$$\alpha_t = 2\dot{r}\dot{\nu} + r\ddot{\nu} = 0 \quad (2.19)$$

Looking for the integrand function that derivative makes α_t cancel, the equation (2.19) can also be written in the form:

$$\frac{1}{r}\frac{d}{dt}(r^2\dot{\nu}) = 0 \quad (2.20)$$

Using the equation (2.9) we can therefore conclude that:

$$r \cdot v_t = constant \quad (2.21)$$

that is, at each point in the trajectory the scalar product $r \cdot v_t$, representing the angular momentum vector, is held constant:

$$\vec{h} = \vec{r} \times \vec{v} = rvcos\varphi \cdot \hat{w} = constant \quad (2.22)$$

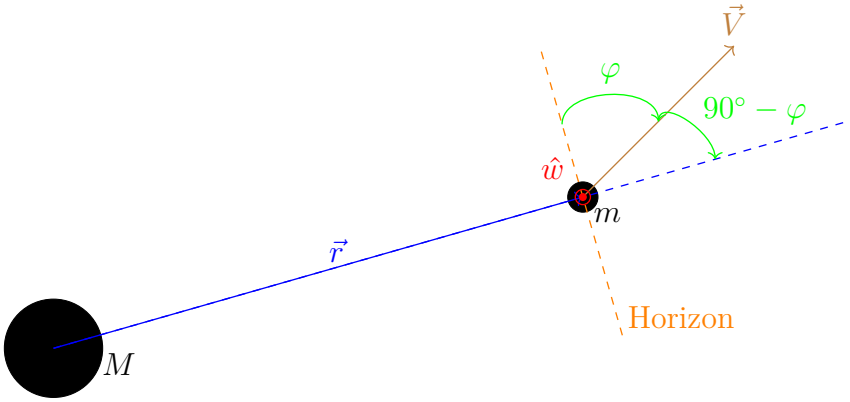

Figure 2.5: Potential energy in a gravitational field

φ is the flight path angle, i.e., the angle between the horizon and the velocity vector, while $\hat{w}$ is the verse perpendicular to the plane of motion of the body of mass m. The momentum vector $\vec{h}$ is constant in modulus, direction, and direction at every point of the trajectory, and this means that the trajectory of the body m around M will be a plane trajectory because $\vec{h}$ always remains perpendicular to the plane of motion of m around M. This property is of fundamental importance since it leads to the conclusion that all trajectories, under the hypothesis of the two-body problem, are planar.
Please note that the momentum vector $\vec{h}$ is a specific quantity, that is, per unit mass.

2.7 Mechanical energy

Starting from the equation (2.12), through appropriate algebraic steps the following relationship can be obtained:

$$\frac{d}{dt}\left(\frac{v^2}{2} - \frac{\mu}{r}\right) = 0 \tag{2.23}$$

this equation represents the conservation of mechanical energy: inside the brackets appear specific kinetic and potential energy, respectively, the sum of which must be constant over time in the absence of other disturbances.

$$\varepsilon = \frac{v^2}{2} - \frac{\mu}{r} = constant \tag{2.24}$$

N.B. Mechanical energy ε is a specific quantity, that is, per unit mass.
Supposing to give a constant impulse in an infinitesimal time dt, then is it possible to consider r constant and derive the following formula:

$$d\varepsilon = vdv \tag{2.25}$$

This equation is of fundamental importance because it shows that, since one pay in terms of propellant for changes in velocity (the amount of propellant is related to dv and not to $d\varepsilon$), fixed the change in energy one want to achieve through a certain maneuver, the dv and therefore the amount of propellant that is going to use will be small if this maneuver is done where the velocity is high; conversely, if the velocity is low, a large dv will be needed for the same energy jump one want to achieve. Similarly, if the aim is to vary the energy of the orbit, it is better to perform the maneuver and push at the low radii where the velocity is high (reason why the ΔV is better to give it at perigee and not at apogee): this is because the same $d\varepsilon$ costs less if it is obtained by pushing at the low radii than at the high radii.

2.8 Reference system

The previous sections introduced the concept of a reference system, but it is now appropriate to give a more rigorous definition of it; first of all, a system of reference means a system with respect to which a given phenomenon is observed. There are different types of them, with different types of coordinates, but we will just introduce a simple Cartesian tern defined by:

- an origin O;
- the orientation of the plane $\hat{x}$ - $\hat{y}$;
- the principal direction $\hat{x}$;
- the direction of the normal to the plane, that is, the direction of $\hat{z}$.

Clearly, $\hat{y}$ is chosen to be perpendicular to $\hat{x}$ and $\hat{z}$ and such as to generate a right-handed triad.
A reference system can then be inertial, that is, not subject to acceleration, or not. In reality all systems are noninertial, but in most cases the accelerations to which they are subject are negligible and the system can be considered as inertial.
The reference systems that will be used in the following are now presented.
All the reference systems presented below are characterized by an origin, a fundamental plane and a positive z-axis direction: they are all right-handed systems so these three elements are sufficient to describe them completely.

2.8.1 Geocentric-equatorial system

The origin of the reference system is the Earth's center of mass while the fundamental plane is the equatorial plane. The direction of the principal direction

$\hat{I}$ is again chosen directed toward the Sun on the day of the vernal equinox, also known as the First point of Aries or Vernal point; the axis $\hat{k}$ is chosen directed toward the North Pole. Note, therefore, that the system is not rotating with the Earth, which rotates about the $\hat{z}$ axis, and is not properly inertial since it is subject to the motion of revolution, as well as the gravitational disturbances of other celestial bodies.

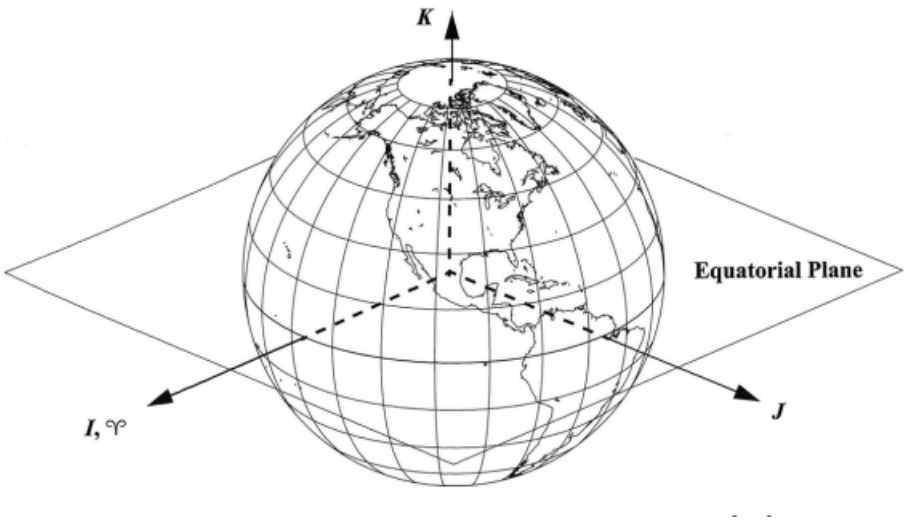

Figure 2.6: Geocentric-equatorial system

2.8.2 Heliocentric-ecliptic system

The origin of this system is located in the center of the Sun; the fundamental plane is the ecliptic, i.e., the imaginary plane containing the Earth's orbit in its motion around the Sun (this is indeed a plane since $\vec{h}$ = constant).
By definition, the x-axis (also called $\hat{g_1}$) is defined as the intersection of the Earth's equatorial plane and the plane of the ecliptic during the spring equinox (these two planes are inclined to each other by 23,27°). It is important to emphasize the fact that the y-axis (also called $\hat{g_2}$), which represents the line joining the Earth's positions at the two solstices, does not correspond with the line of apses, i.e., the line joining periapsis and apoapsis; this is because the periapsis does not coincide with the day of the winter solstice (21/12). Instead, the positive direction of z is directed toward the hemisphere that contains the pole star.

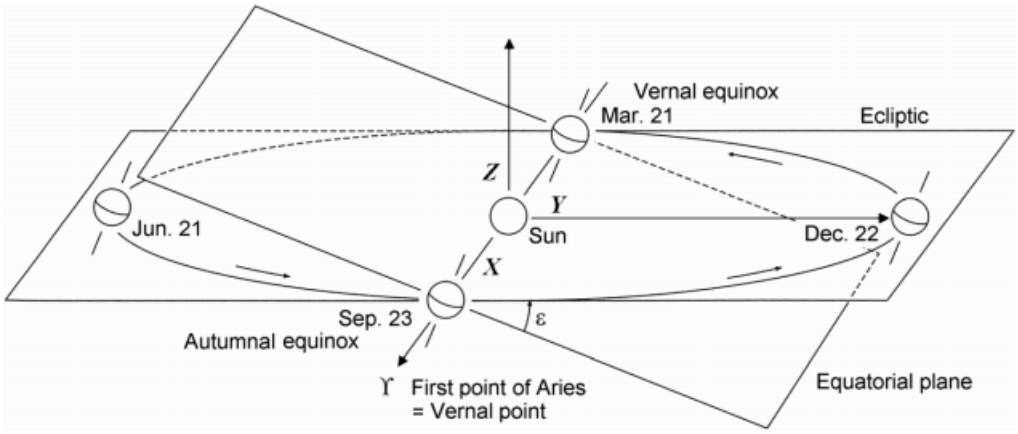

Figure 2.7: Heliocentric-ecliptic system

2.8.3 Orbital parameters

The classical orbital parameters are:

1. semi-major axis a, it represents half the maximum distance between the periapsis and apoapsis of an elliptical orbit. This parameter defines the physical size of the orbit and determines the orbital period of the celestial body.

2. eccentricity e, it measures the shape of the orbit. It is a number between 0 and 1, where 0 represents a perfectly circular orbit and 1 indicates a highly elliptical orbit. Eccentricity determines how far an orbit deviates from the circular shape and affects the speed with which the celestial body moves along the orbit.

3. inclination i, it represents the angle between the plane of the orbit and a conventional reference plane, usually the plane of the ecliptic (the plane in which the planets of the solar system orbit). The inclination determines the orientation of the orbit relative to the reference plane and can range from 0° (equatorial orbit) to 90° (polar orbit).

4. topic of the periapsis ω, it describes the angle between the ascending node and the periapsis of an orbit. The ascending node is the point at which the orbit crosses the reference plane in upward motion. The periapsis argument indicates the direction in which the periapsis lies with respect to the ascending node.

5. longitude of the ascending node Ω, it represents the point at which the orbit crosses the upward-moving reference plane. It is the angular distance between the inertial I-axis (or g_1) and the position of the ascending node.

6. true anomaly ν, it describes the position of a celestial body along its elliptical orbit with respect to the periapsis. It represents the angle between the periapsis and the current position of the celestial body measured in the plane of the orbit.

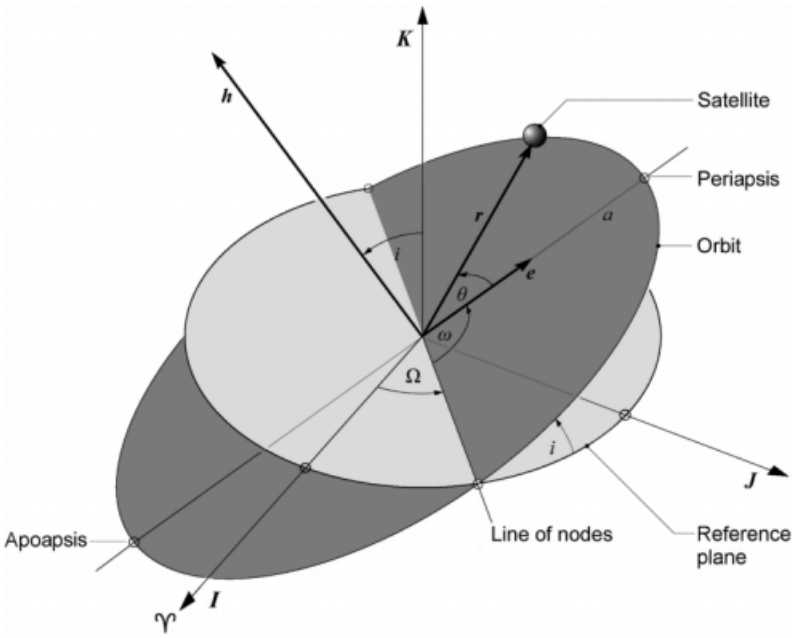

Figure 2.8: Orbital parameters

Given these orbital parameters, it is possible to derive position and velocity of the satellite at each time instant and at each point in the orbit and vice versa. The period of an orbit can be evaluated as:

$$T = 2\pi\sqrt{\frac{a^3}{\mu}} \tag{2.26}$$

If the semi-major axis increases, the orbital period will increase not only because we have a greater distance to travel but also because we will be slower. In the two-body problem the orbital parameters remain constant, apart from $\nu(t)$ which depends on time, unless we introduce perturbative actions e.g. accelerations due

to propulsive thrusts. In particular, when traveling through an elliptical orbit, the velocity will be tangent to the trajectory and can be decomposed into the tangential component in the V_T plane, the radial component in the V_R plane, and the component normal to the V_N orbital plane; likewise, the acceleration can be decomposed into its radial component α_R, tangential α_T, normal to the plane of the orbit α_W, or along the direction of the velocity vector α_V, in the plane and normal to the velocity vector α_N and normal to the plane of the orbit α_W.
In this context it is also useful to introduce the Gauss equations, which are a set of equations used to calculate the position and motion of an object in space. They are based on the Keplerian laws of motion and make it possible to determine the orbital parameters and the variations of these elements over time:

$$\dot{a} = \frac{2\alpha^2}{\sqrt{\mu p}}[(e\sin\nu)\alpha_R + \left(\frac{p}{r}\right)\alpha_T] = \left(\frac{2\alpha^2 V}{\mu}\right)\alpha_V \tag{2.27a}$$

$$\begin{aligned}\dot{e} &= \sqrt{\frac{p}{\mu}}[\sin\nu\alpha_R + \left(\frac{r}{p}\right)(e\cos^2(\nu) + 2\cos\nu + e)\alpha_T] = \\ &= \left(\frac{1}{V}\right)[2(e+\cos\nu)\alpha_V - (\alpha\sin\nu/r)\alpha_N]\end{aligned} \tag{2.27b}$$

$$\dot{i} = \left(\frac{r}{\sqrt{\mu p}}\right)[\cos(\omega+\nu)]\alpha_W \tag{2.27c}$$

$$\dot{\Omega} = \left(\frac{r}{\sqrt{\mu p}}\right)\left[\frac{\sin(\omega+\nu)}{\sin(i)}\right]\alpha_W \tag{2.27d}$$

$$\begin{aligned}\dot{\omega} &= -\dot{\Omega}\cos(i) - \left(\frac{\frac{p}{\mu}}{e}\right)[\cos\nu\alpha_R - \sin\nu\Big(1+\frac{r}{p}\Big)\alpha_T] = \\ &= -\dot{\Omega}\cos(i) + \left(\frac{1}{eV}\right)[2\sin\nu\alpha_V + \left(\frac{r}{p}\right)(2e + \cos\nu + e^2\cos\nu)\alpha_N]\end{aligned} \tag{2.27e}$$

These are Gauss differential equations and show that:

1. To change the semi-major axis α (thus the energy of the orbit) one must push parallel to the velocity so as to change the modulus of $\vec{V}$ as shown by the equation (2.27a).

2. Applying a force parallel to $\vec{V}$ will change both the semi-major axis but also the eccentricity (perhaps unintended effect).

3. Thrusting in the plane of the orbit, in addition to changing eccentricity, ω will also change (equation (2.27b) and (2.27e)). Typically, however, the change in ω and eccentricity are not important and can be neglected with respect to the change in the semi-major axis.

4. The normal component α_N changes the eccentricity of the orbit but not the value of energy and thus of its semi-axis α (equations (2.27a) and (2.27b)).

5. In particular, the equation (2.27a) shows that the same acceleration changes the semi-axis to a greater extent if the velocity is large. Since one pay for the thrust and thus the acceleration in terms of propellant, if the goal is to change α it is possible to find that if one push where the velocity is high then will change the semi-axis to a greater extent.
   This implies that as often as one need to change α it is convenient to do so where the velocity is large, and since the energy $\varepsilon = \frac{V^2}{2} - \frac{mu}{r}$ is constant, this implies that it is convenient to make such a maneuver where the radii are low.

6. To change the direction of the angular momentum $\vec{h}$ (i.e., vary the plane of the orbit), one need to use the out-of-plane acceleration component α_W that goes to change both i and Ω, depending on where one is located in the orbit (groundtrack). For the same out-of-plane acceleration, the change in i and Ω is greatest at large radii and thus where the velocity is low (equations (2.27c) and (2.27d))

2.8.4 Perifocal reference system

It is the most convenient system for studying the motion of a body along its orbit since it is easy to define the orbital parameters just presented. The origin is placed at the center of mass of the main celestial body, which occupies one of the two foci of the orbit. The main direction $\hat{p}$ is the line of the apsides, from the origin toward the periapsis. In contrast, the axis $\hat{w}$ is oriented as the angular momentum of the body itself.
The usefulness of the perifocal plane is that it greatly simplifies the analysis of the orbital motions of celestial bodies. Indeed, in this plane, it is easier to deal with orbital parameters such as orbital inclination and perigee argument. Another important feature of the perifocal plane is that it reduces the three-dimensional analysis to a two-dimensional plane. This is useful because many orbits are very close to two-dimensional planes. For example, a geostationary orbit is almost perfectly contained in a two-dimensional plane, which greatly simplifies calculations. In addition, the perifocal plane is often used to define the reference coordinate system for orbit analysis. This coordinate system includes classical orbital coordinates such as the semi-major axis, eccentricity and true anomaly, which are fundamental to fully describing an orbit.

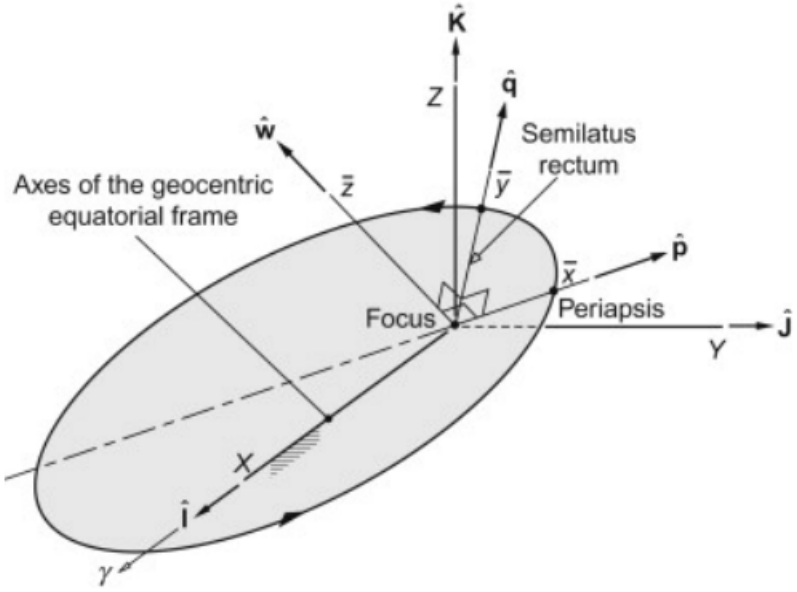

Figure 2.9: Perifocal system

It represents the plane containing the trajectory of the satellite, the $\hat{p}$ direction points toward the periapsis, the $\hat{q}$ direction toward the semilatus rectum, and the $\hat{w}$ direction according to the direction of the angular momentum vector $\vec{h}$. It is important to note that the perifocal plane is not static, but rotates together with the orbiting object due to conservation of angular momentum. This means that the perifocal plane will constantly change its orientation relative to the central object during the orbit. In this reference system, we can easily calculate the position and velocity of the satellite as the true anomaly ν changes according to the following formulas:

$$\vec{r}_{pqw} = \begin{Bmatrix} r\cos\nu \\ r\sin\nu \end{Bmatrix} \tag{2.28}$$

$$\vec{v}_{pqw} = \begin{Bmatrix} -\frac{\mu}{h}\sin\nu \\ -\frac{\mu}{h}(e+\cos\nu) \end{Bmatrix} \tag{2.29}$$

In particular, the true anomaly ν will be defined as positive when between 0° and 180° so that, since the flight path angle φ and the true anomaly ν have the same sign, it is possible to conclude that if $\varphi > 0$ then the satellite will be moving away from the periapsis, conversely if $\varphi < 0$ it will be approaching the periapsis.

2.8.5 Synodic system

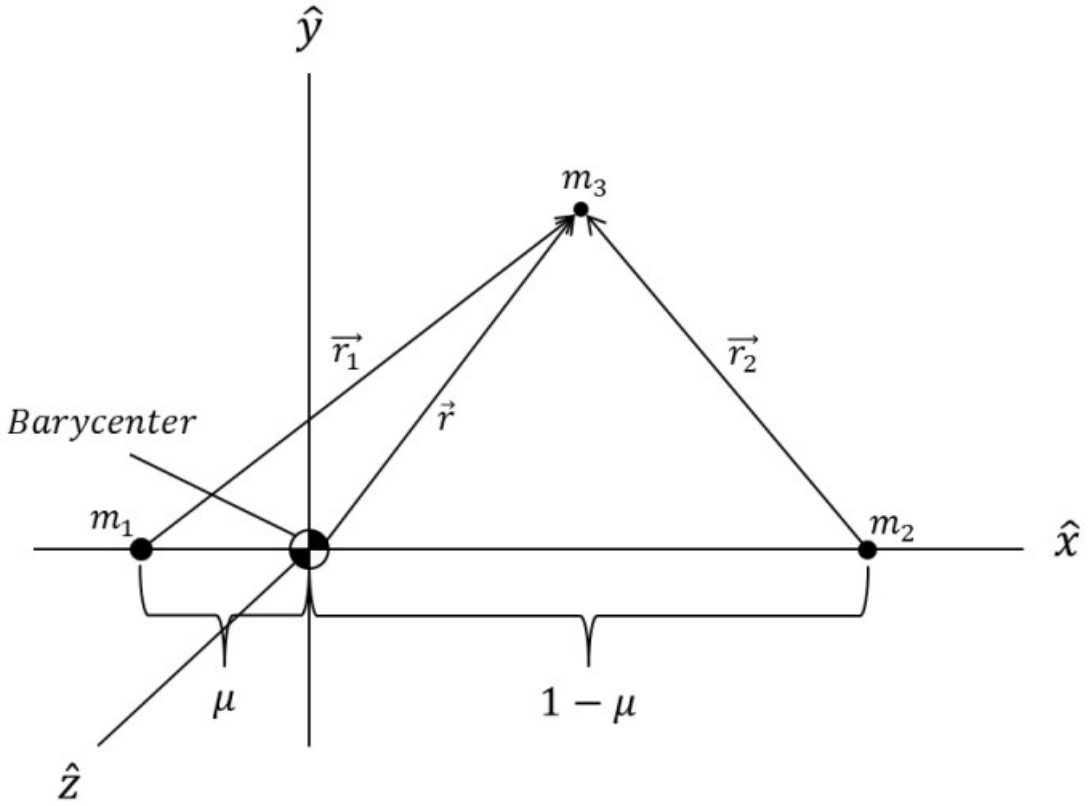

Figure 2.10: Synodic system

Particularly important especially for the following discussion is the synodic system, in this example shown in figure 2.10 the Earth-Moon synodic system is shown, that is, a dual system in which the center of mass is located at a distance x from the center of the Earth. To find the position of the center of mass of the system it is possible to impose null on the sum of the static moments:

$$\mu_{Earth} \cdot x = \mu_{Moon}(R - x) \tag{2.30}$$

$$x = \frac{\mu_{Moon} \cdot R}{\mu_{Earth} + \mu_{Moon}} = 4671\,\text{km} \tag{2.31}$$

Attention must therefore be paid to the fact that it is not true that the Moon revolves around the Earth; in fact they both revolve around the center of mass of the system, even though that point falls within the Earth.

The amount of time it takes the Moon to pass through the same point in its orbit twice is called the orbital (or draconic) period and is worth about 27.3 days. However, because of the Earth's motion along its orbit around the Sun, the Moon's relative position to the Sun varies slightly with each lunar revolution.
The synodic period, which is the time required for the Moon to return to the same relative position with respect to the Sun, is slightly longer than the orbital period. This is because, in the time it takes the Moon to return to the same position relative to the fixed stars in the night sky, the Earth has also completed part of its orbit around the Sun. As a result, it takes about 29.5 days for the Earth-Moon system to return to the same alignment between Earth, Moon and Sun. The synodic period is important in determining the duration between Moon phases, such as lunar phases, lunar and solar eclipses.

2.9 Circular Restricted Three-Body Problem

The following simplifying assumptions are valid in this case:

1. Consider 3 bodies of which 2 are main bodies (m_1 and m_2), this means we do not consider the effect of the Sun.

2. Restricted means that m « m_1,m_2 i.e. the mass of the satellite is much less than that of the 2 main bodies.

3. Circular means that the 2 main bodies are assumed to follow circular orbits relative to their center of mass.

Considering that $m_1 >> m_2 >> m$ and define $M = m_1 + m_2$:

$$\mu = \frac{m_2}{M} \tag{2.32}$$

Beware that in this case μ is not a gravitational parameter but only shows how massive the second primary body is. As seen above, it is possible to calculate the distance x of the center of mass of the primary body (Earth) from the center of mass of the synodic system as follows:

$$m_1 \cdot x = m_2 \cdot (R - x) \tag{2.33}$$

$$(1 - \mu)M \cdot x = \mu M \cdot (R - x) \tag{2.34}$$

$$Mx - \cancel{\mu M x} = \mu MR - \cancel{\mu M x} \tag{2.35}$$

$$x = \mu R \tag{2.36}$$

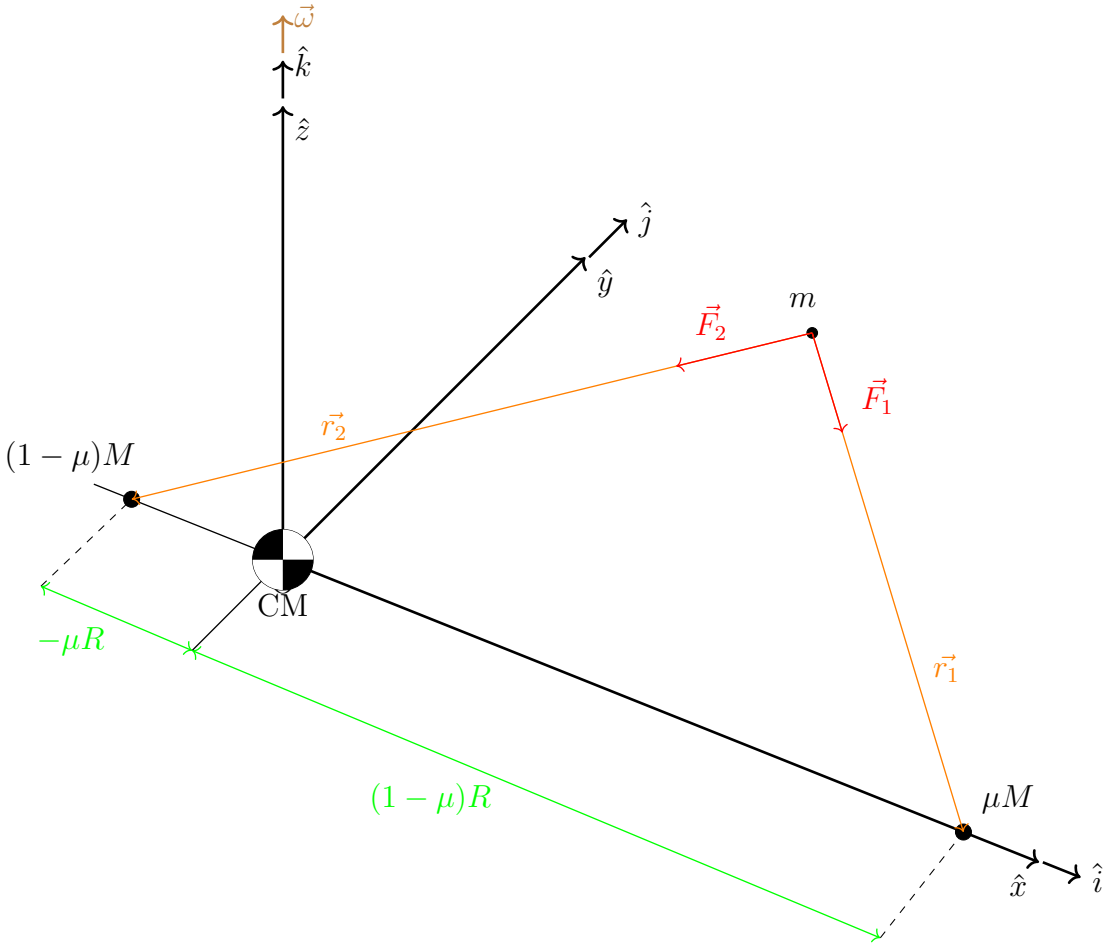

Figure 2.11: Earth-Moon Synodic

The period of revolution of the two bodies with respect to the center of mass of the system is defined by the symbol τ and holds:

$$\tau = 2\pi\sqrt{\frac{R^3}{GM}} = 2\pi\sqrt{\frac{R^3}{\mu_{Earth} + \mu_{Moon}}} \tag{2.37}$$

and consequently the angular velocity of the synodic system will be:

$$\omega = \frac{2\pi}{\tau} = \sqrt{\frac{\mu_{Earth} + \mu_{Moon}}{R^3}} \tag{2.38}$$

At this point we need to make a clarification: the equations of dynamics $\vec{a} = \frac{\vec{F}}{m}$ are valid only when stretched in an inertial reference system, but the synodic system is a non-inertial rotating system, so one have to include the so-called apparent forces,

i.e., non-real forces that are introduced when studying the equations of motion in non-inertial systems precisely to make the accounts add up with respect to the physical forces being measured.

$$\ddot{\vec{r}} + \vec{\omega} \times (\vec{\omega} \times \vec{r}) + 2\vec{\omega} \times \dot{\vec{r}} = \frac{1}{m}(\vec{F_1} + \vec{F_2}) \tag{2.39}$$

where the first term represents inertial relative acceleration, the second and third terms constitute the apparent forces: centripetal acceleration and Coriolis acceleration, respectively, and the terms to the right of equal represent the accelerations due to gravitational forces.
Analyzing the various terms individually:

$$\vec{F_1} = -G \cdot \frac{m_1 m_2}{r_1^2} \frac{\vec{r_1}}{|r_1|} = -G \cdot \frac{(1-\mu)Mm}{r_1^3} \vec{r_1} \tag{2.40}$$

$$\vec{F_2} = -G \cdot \frac{m_1 m_2}{r_2^2} \frac{\vec{r_2}}{|r_2|} = -G \cdot \frac{(1-\mu)Mm}{r_2^3} \vec{r_2} \tag{2.41}$$

where:

$$|r_1| = \sqrt{[x + \mu R]^2 + y^2 + z^2} \tag{2.42}$$

$$|r_2| = \sqrt{[x - (1-\mu)R]^2 + y^2 + z^2} \tag{2.43}$$

$$\vec{\omega} \times \vec{r} = \begin{vmatrix} \hat{i} & \hat{j} & \hat{k} \\ 0 & 0 & \omega \\ x & y & z \end{vmatrix} = \begin{bmatrix} 0 & -\omega & 0 \\ \omega & 0 & 0 \\ 0 & 0 & 0 \end{bmatrix} \begin{Bmatrix} x \\ y \\ z \end{Bmatrix} = \begin{Bmatrix} -\omega y \\ \omega x \\ 0 \end{Bmatrix} \tag{2.44}$$

$$\vec{\omega} \times (\vec{\omega} \times \vec{r}) = \begin{bmatrix} 0 & -\omega & 0 \\ \omega & 0 & 0 \\ 0 & 0 & 0 \end{bmatrix} \begin{Bmatrix} -\omega y \\ \omega x \\ 0 \end{Bmatrix} = \begin{Bmatrix} -\omega^2 x \\ -\omega^2 y \\ 0 \end{Bmatrix} \tag{2.45}$$

$$2\vec{\omega} \times \dot{\vec{r}} = 2 \begin{bmatrix} 0 & -\omega & 0 \\ \omega & 0 & 0 \\ 0 & 0 & 0 \end{bmatrix} \begin{Bmatrix} \dot{x} \\ \dot{y} \\ \dot{z} \end{Bmatrix} = \begin{Bmatrix} -2\omega\dot{y} \\ 2\omega\dot{x} \\ 0 \end{Bmatrix} \tag{2.46}$$

Putting it all together results in:

$$\begin{cases} \ddot{x} - \omega^2 x - 2\omega\dot{y} = -\frac{GM(1-\mu)(x+\mu R)}{r_1^3} - \frac{GM\mu[x(1-\mu)R]}{r_2^3} \\ \ddot{y} - \omega^2 y + 2\omega\dot{x} = -\frac{GM(1-\mu)y}{r_1^3} - \frac{GM\mu y}{r_2^3} \\ \ddot{z} = -\frac{GM(1-\mu)z}{r_1^3} - \frac{GM\mu z}{r_2^3} \end{cases} \tag{2.47}$$

At this point it is convenient to proceed with the following dimensionalizations:

$$\vec{\rho} = \frac{\vec{r}}{\vec{R}} \tag{2.48}$$

Dimensionless coordinates will therefore be:

$$\xi = \frac{x}{R} \quad \eta = \frac{y}{R} \quad \zeta = \frac{z}{R} \tag{2.49}$$

Similarly, it is possible to dimensionalize time in the following way:

$$\tau = t \cdot \omega \tag{2.50}$$

Substituting these into the equation (2.51) will yield the final dimensionless system representing the equations of motion in the restricted circular three-body problem:

$$\begin{cases} \ddot{\xi} - \xi - 2\eta = -(1-\mu)\frac{\xi+\mu}{\rho_1^3} - \mu\frac{[\xi-(1-\mu)]}{\rho_2^3} \\ \ddot{\eta} - \eta + 2\dot{\xi} = -(1-\mu)\frac{\eta}{\rho_1^3} - \mu\frac{\eta}{\rho_2^3} \\ \ddot{\zeta} = -(1-\mu)\frac{\zeta}{\rho_1^3} - \mu\frac{\zeta}{\rho_2^3} \end{cases} \tag{2.51}$$

where:

$$\rho_1 = \sqrt{[\xi+\mu]^2 + \eta^2 + \zeta^2} \tag{2.52}$$

$$\rho_2 = \sqrt{[\xi-(1-\mu)]^2 + \eta^2 + \zeta^2} \tag{2.53}$$

These are three second-order differential equations that are nonlinear because of ρ_1^3 and ρ_2^3 plus sibi all three are coupled so the only way to solve them is through numerical integration. The state vector containing the unknowns of the problem will be defined as:

$$\overline{x} = \left\{\dot{\xi} \quad \dot{\eta} \quad \dot{\zeta} \quad \ddot{\xi} \quad \ddot{\eta} \quad \ddot{\zeta}\right\} \tag{2.54}$$

while the initial condition will be given by the vector:

$$\overline{CI} = \left\{\dot{\xi}_0 \quad \dot{\eta}_0 \quad \dot{\zeta}_0 \quad \ddot{\xi}_0 \quad \ddot{\eta}_0 \quad \ddot{\zeta}_0\right\} \tag{2.55}$$

which are associated with the speed at the bornout ($\vec{V}_{BO}$) that the S/C will be to arrive in a lunar orbit starting from a LEO orbit around the Earth, so it is possible to deduce that once the impulse is given and the vector of initial conditions is defined in this way, the trajectory accomplished by the satellite will be fully determined.

2.10 Types of maneuvers

In general, there may be two types of maneuvers: impulsive in the case of chemical propulsion where one give large ΔV pulses for a brief moment of time (compared to the time of the transfer) or low-thrust maneuvers but continuously and gradually for long times (comparable to transfer times and therefore not negligible)

changing the ΔV by little at a time as in the case in electric propulsion.
Particularly, this thesis work is going to focus on chemical propulsion, going to investigate the most common maneuvers such as the Hohmann, direct escape and assisted escape, concepts that will come in handy in future discussions present in the following chapters.

2.10.1 Hohmann transfer

Hohmann transfer is a maneuver between two circular and coplanar (e=0, i=0) two-pulse orbits. The Hohmann ellipse must intersect or be tangent to the two orbits and it must hold that:

$$\begin{cases} r_p = \frac{p}{1+e} \leq r_1 \\ r_a = \frac{p}{1-e} \geq r_2 \end{cases} \tag{2.56}$$

where r_p represents the radius of the periapsis, r_a the radius of the apoapsis, p is the semilatus rectum and e is the eccentricity. Among all possible ellipses that must satisfy these constraints, the Hohmann transfer is the one that arrives exactly tangent to the two orbits, which means it satisfies the constraints $r_p = r_1$ and $r_a = r_2$. Among all two-pulse transfers between two circular, coplanar orbits, the Hohmann transfer is the one with the minimum ΔV but also the one with the longest duration.

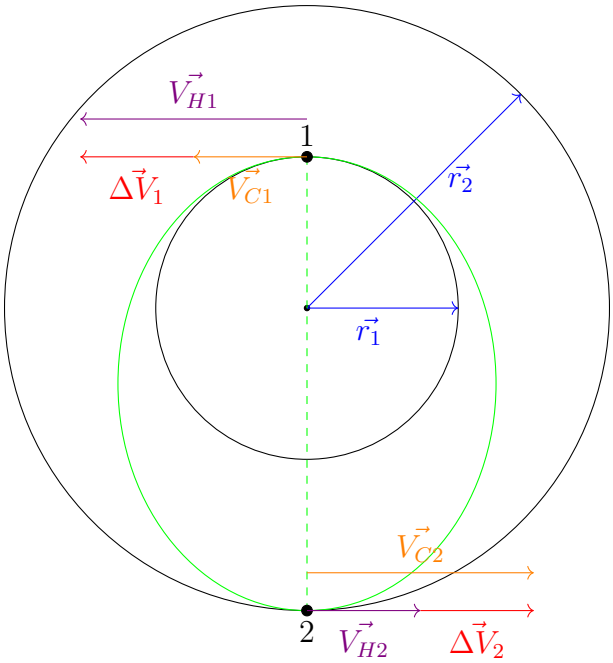

Figure 2.12: Hohmann transfer

The circular velocities of the departure and arrival orbits can be easily calculated through conservation of specific energy:

$$\varepsilon = \frac{V_{C1}^2}{2} - \frac{\mu}{r_1} = \frac{V_{C2}^2}{2} - \frac{\mu}{r_2} = -\frac{\mu}{2a} \tag{2.57}$$

$$V_{C1} = \sqrt{\frac{\mu}{r_1}} \quad \text{and} \quad V_{C2} = \sqrt{\frac{\mu}{r_2}} \tag{2.58}$$

all velocities are parallel to each other precisely because the Hohmann ellipse is tangent to both orbits.
Similarly, by estimating the specific energy of the Hohmann maneuver at perigee and apogee, it is possible to estimate the velocities that will occur at those points:

$$\varepsilon_H = \frac{V_{H1}^2}{2} - \frac{\mu}{r_1} = \frac{V_{H2}^2}{2} - \frac{\mu}{r_2} = -\frac{\mu}{2a_H} = -\frac{\mu}{r_1 + r_2} \tag{2.59}$$

$$V_{H1} = \sqrt{2\mu\Big(\frac{1}{r_1} - \frac{1}{r_1 + r_2}\Big)} \quad \text{and} \quad V_{H2} = \sqrt{2\mu\Big(\frac{1}{r_2} - \frac{1}{r_1 + r_2}\Big)} \tag{2.60}$$

the pulses to be provided will therefore be:

$$\Delta V_1 = V_{H1} - V_{C1} \quad \text{and} \quad \Delta V_2 = V_{C2} - V_{H2} \tag{2.61}$$

Please note that both of ΔV, in this case, are to accelerate!

2.10.2 Biparabolic Transfer

The biparabolic transfer is a three-pulse maneuver formed by a typically large ΔV_{1P} that allows the S/C to enter a parabolic orbit that will cause it to travel infinitely far with zero velocity (or better said infinitesimal ε). At this point with a practically zero ΔV_∞ (or better said equal to 2ε) it will be possible to change the direction of the velocity and transform the outgoing parabola into an incoming parabola that will carry the S/C as far as the radius r_2, where we will give a ΔV_{2P} this time to braking, so as to circularize the orbit.
At an ideal level this maneuver is therefore very convenient because it could allow a free change of plane to be made if done at the point where the S/C is at the infinite radius point, but in practice this maneuver cannot be implemented because it would take an infinite amount of time to reach that point.
Please note that, in this case, the ΔV are one to accelerate and one to brake!

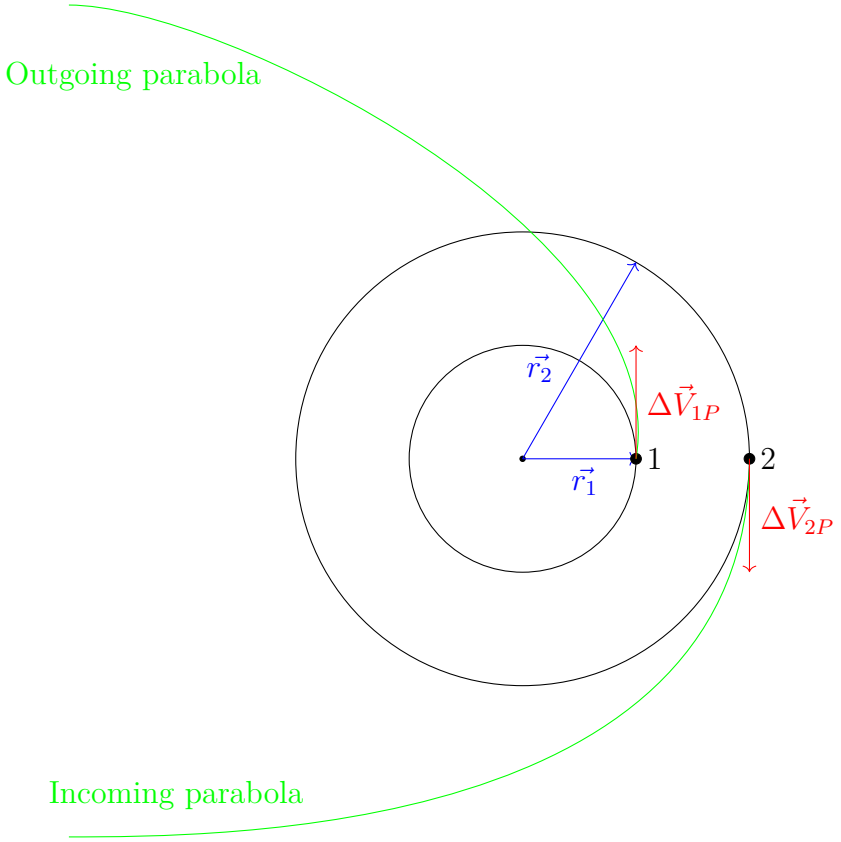

Figure 2.13: Biparabolic Transfer

Evaluate the pulses to be delivered by analyzing the energy of the parabolic orbit:

$$\varepsilon_P = \frac{V^2}{2} - \frac{\mu}{r} = 0 \tag{2.62}$$

escape velocities to enter the outgoing and incoming parabola respectively will be:

$$V_{Exit1} = \sqrt{2\frac{\mu}{r}} = \sqrt{2}V_{C1} \quad and \quad V_{Exit2} = \sqrt{2\frac{\mu}{r}} = \sqrt{2}V_{C2} \tag{2.63}$$

the impulses to be provided will therefore be:

$$\Delta V_{1P} = V_{Exit1} - V_{C1} = (\sqrt{2} - 1)V_{C1} \tag{2.64}$$

$$\Delta V_{2P} = V_{Exit2} - V_{C2} = (\sqrt{2} - 1)V_{C2} \tag{2.65}$$

The biparabolic maneuver is classified as a three-pulse maneuver even though in reality the ΔV one give to $r \to \infty$ (where the S/C will be found to have a velocity $V \to 0$) to return to the orbit at radius r_2 is not paid. For this reason, the biparabolic maneuver would ideally be perfect for accomplishing any plane change. The impulse required to perform a simple plane-change maneuver is in fact:

$$\Delta V_{\Delta i} = 2V_{C1} \sin\left(\frac{\Delta\psi}{2}\right) \tag{2.66}$$

the equation (2.66) basically shows two things:

1. is better to do a plane change maneuver at the nodes because only at those points of the orbit it will be possible to have $\Delta\psi = \Delta i$, while at all other points of the orbit the $\Delta\psi$ will be greater than the Δi, which means that for the same useful effect (Δi) one should spend more in terms of ΔV.

2. the faster one is, the more expensive the plane change maneuver is, so it is better to do it at apogee because it is the farthest and therefore slowest point of the orbit.

The ideal case in which the change of plane would cost zero would be precisely if went to $r \to \infty$, that is, if used a biparabolic maneuver only to avoid paying the Δi, in that case in fact the cost would be only that necessary to enter and exit the parabolic trajectories but once arrived at $r \to \infty$ it will be possible to obtain a Δi as large as one like totally free.
Please note that the biparabolic maneuver always costs more than the hyperbolic escape maneuver while it is cheaper than the Hohmann maneuver from $\frac{r_2}{r_1} = 11.94$ onwards.

2.10.3 Bielliptical Transfer

Ideally the biparabolic move takes an infinite amount of time because one have to go to $r \to \infty$ so in practice what is done is to make a bielliptic trajectory represented in figure 2.14 in which essentially the two parabolas are replaced into two elliptic Hohmann trajectories.
Compared to the biparabolic the ΔV_1 is reduced so the gain in pushing at low altitudes (it will have more gravity losses) and one have to add the ΔV_i (which in the biparabolic at $r \to \infty$ became zero) so at the propulsive level it is a bit worse than the biparabolic but the more one use an orbit of radius r_i high, the more convenient the bielliptical maneuver will be, approaching the performance of the biparabolic maneuver (which it can be seen in fact as a bielliptical maneuver with $r_i \to \infty$).

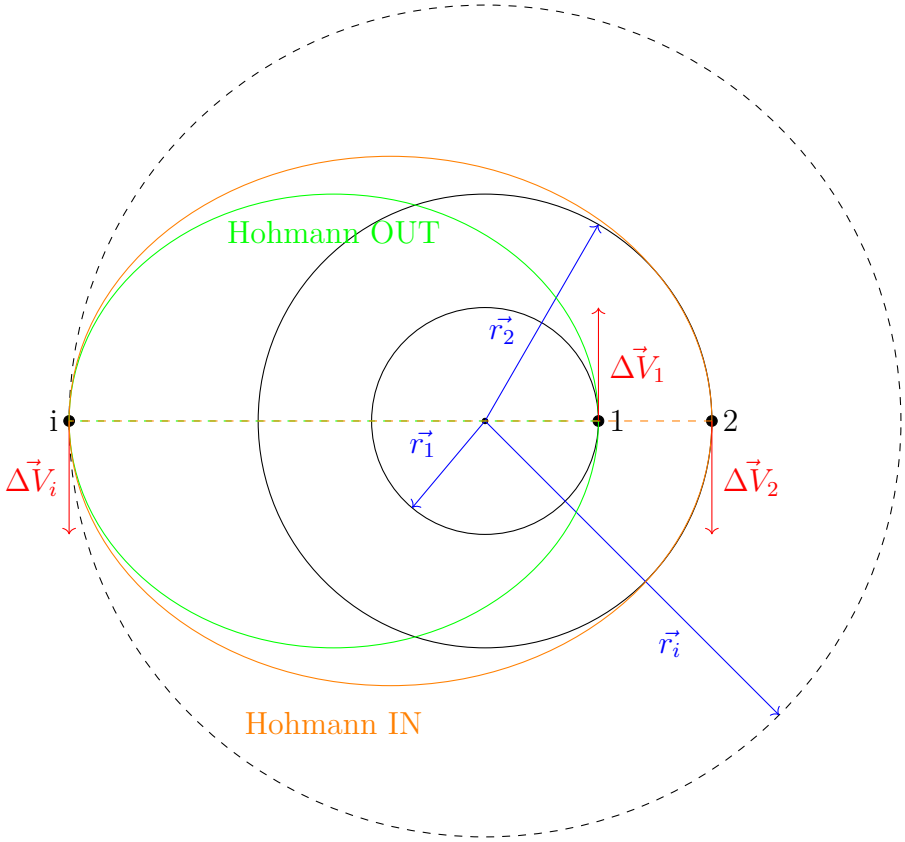

Figure 2.14: Bielliptical Transfer - not to scale

2.10.4 Direct escape

The parabola is the minimum-energy trajectory that allows to make an escape maneuver. Hyperbolic trajectories, in fact, are characterized by potisive energy ($\varepsilon > 0$) so that even if for $r \to \infty$ the potential energy contribution cancels out, there will be a positive kinetic contribution:

$$\varepsilon_i = \frac{V^2}{2} - \frac{\mu}{r} > 0 \tag{2.67}$$

$$V_\infty = \sqrt{2\varepsilon_i} \tag{2.68}$$

such velocity is called the hyperbolic excess velocity. From the conservation of the energy of the hyperbolic orbit we can derive the V_i that is the velocity that the S/C will have to have in order to enter a hyperbolic orbit that will take it to $r \to \infty$ with exactly the V_∞.

$$\varepsilon_i = \frac{V_\infty^2}{2} = \frac{V_i^2}{2} - \frac{\mu}{r_1} \tag{2.69}$$

$$V_i = \sqrt{V_\infty^2 + 2\frac{\mu}{r_1}} = \sqrt{V_\infty^2 + 2V_{C1}^2} = \sqrt{V_\infty^2 + V_{Exit1}^2} \tag{2.70}$$

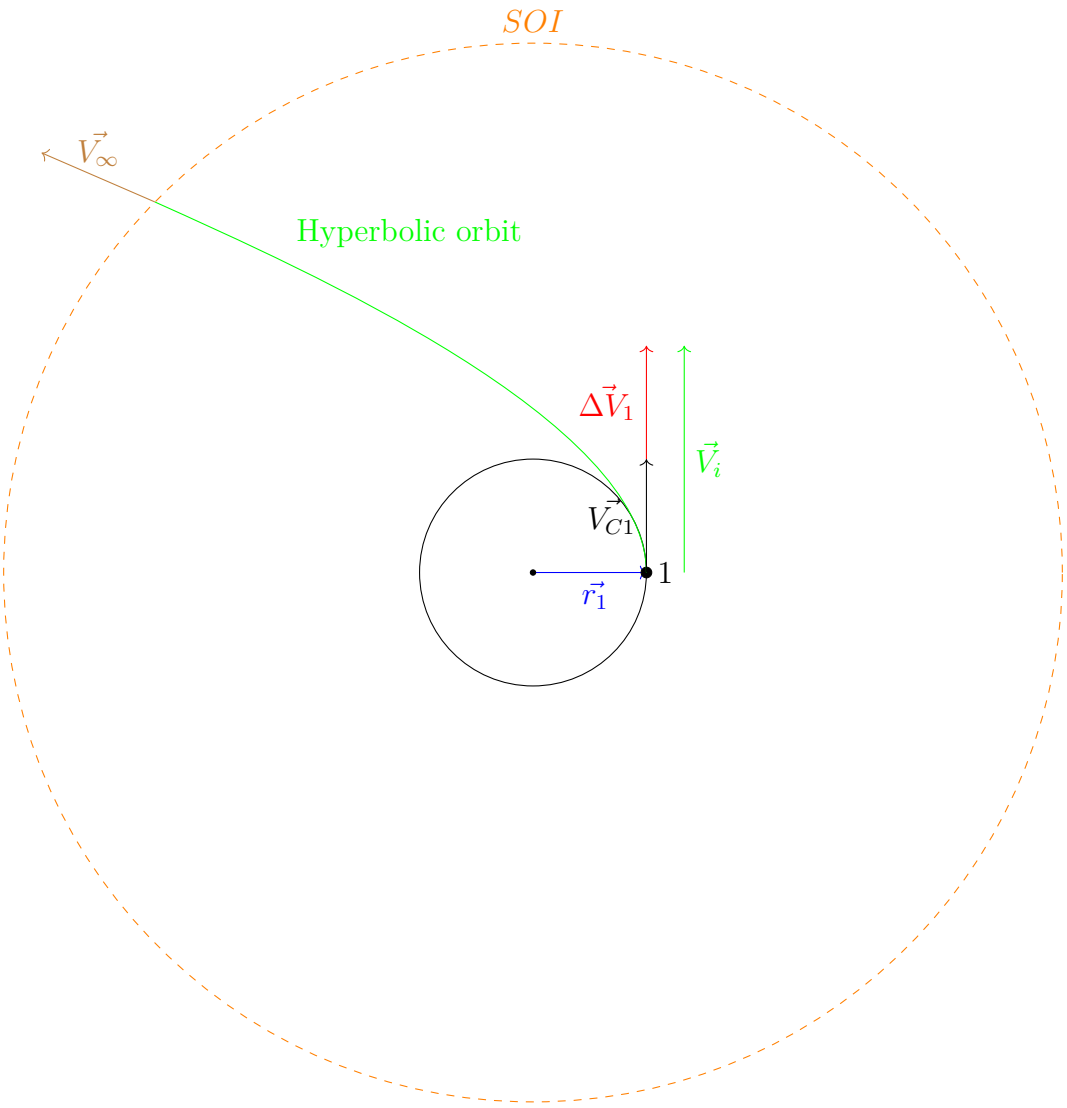

Figure 2.15: Direct escape

At this point it is good to make an observation; supposing to get to $r \to \infty$, theoretically this can be done in two distinct ways:

1. parabolic escape plus a ΔV at $r \to \infty$ so as to go from zero velocity to V_∞ through two pulses.

2. hyperbolic escape so as to obtain the V_∞ once arrive at $r \to \infty$ by making a single impulse.

Well, in order to minimize gravity losses it is convenient to push at low altitudes so, without doing math, it is possible to say right away that giving an impulse at $r \to \infty$ where the velocity is practically zero, from the propulsive point of view is the worst thing that can be done. This implies that it is always better to evade on a hyperbola than to evade on a parabola!
A final observation is that hyperbolic escaping can have a cost even smaller than the V_∞ one want to achieve, this is because the larger the V_∞ is the larger the ΔV_1 will be and the less gravity losses one will have; if, on the other hand, the V_∞ is small it is possible to provide a small ΔV_1 and, consequently, one will have as many gravity losses: in fact, the limiting case is that of the parabolic orbit where one will arrive at $r \to \infty$ with $V \to 0$, so all the ΔV_1 provided at the beginning of the maneuver is lost, and this is due precisely to gravity losses. Therefore, it is possible to conclude that, although it may seem a counter-intuitive concept, obtaining very large V_∞ can cost much less than obtaining small V_∞.

2.10.5 Oberth effect

In this kind of maneuver instead of making an immediate escape on a hyperbola, since, as mentioned, it is convenient to push at low radii, first one will give a ΔV to brake (ΔV_{O1}) so as to descend in altitude (and begin to accelerate) through a Hohmann and then, one will give a ΔV to accelerate (ΔV_{O2}) that will bring the S/C onto a hyperbola that will make it arrive at $r \to \infty$ with the V_∞.
The cost of this maneuver will therefore be:

$$\Delta V_{TOT} = \Delta V_{O1} + \Delta V_{O2} \tag{2.71}$$

where

$$\Delta V_{O1} = V_{C1} - V_{H1} \tag{2.72}$$

$$\Delta V_{O2} = \sqrt{V_\infty^2 + V_{Exit2}^2} - V_{H2} \tag{2.73}$$

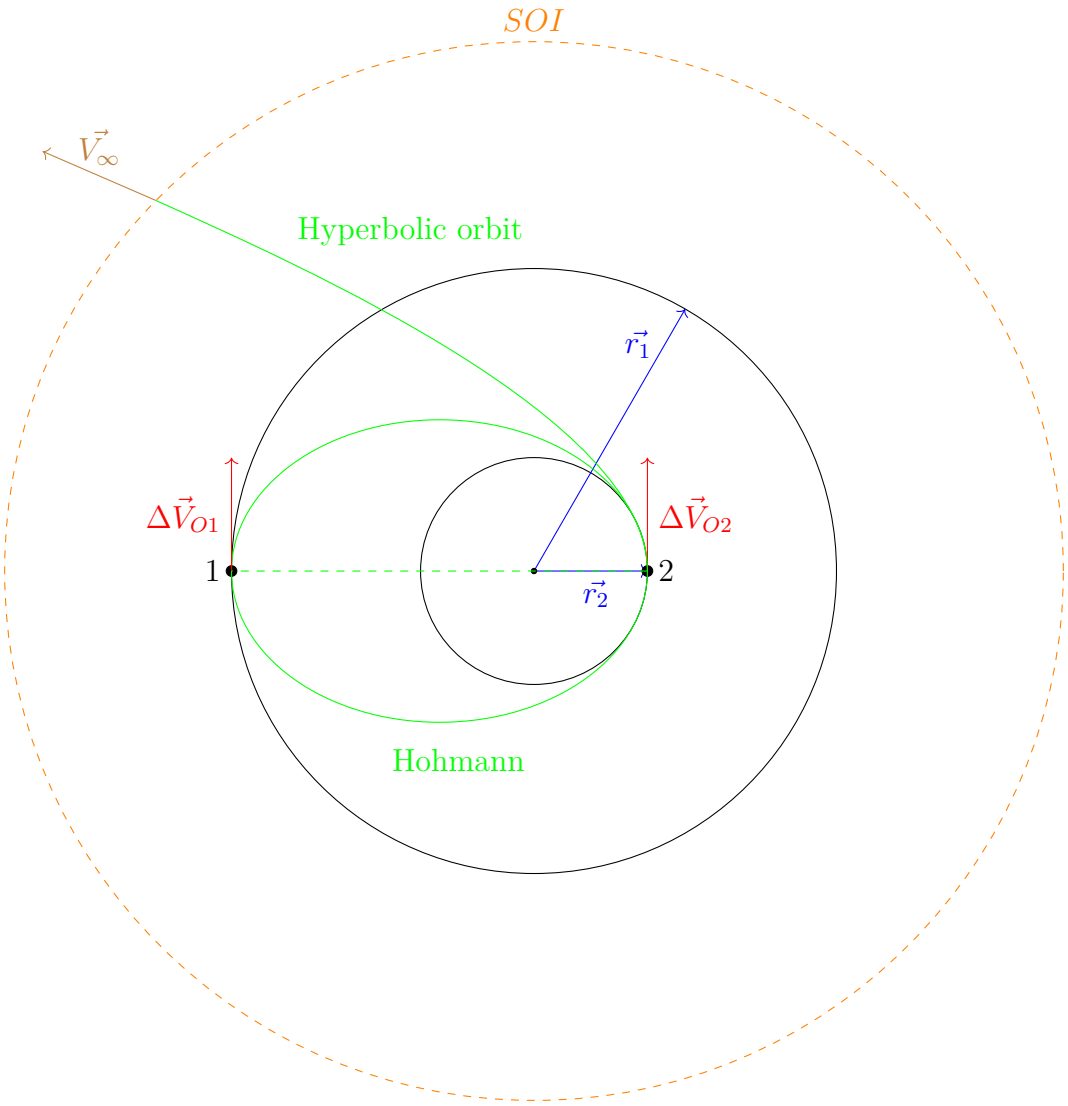

Figure 2.16: Oberth maneuver

In particular, the ΔV_{O2} will typically be small but, propulsively, very effective because the radius r_2 will be small (it is advisable to get attracted as close as possible to the main planet to take advantage of this maneuver) while the velocity will be large. Indeed, it will be the case that when $V_\infty > \sqrt{2}V_{C1}$, Oberth's maneuver becomes more convenient than direct escape (conversely, it will be more convenient to escape by direct escape than by Oberth's maneuver) and it will be the more convenient the smaller the radius r_2 at which one maneuver, i.e., the more one get accelerated by the main body before giving the ΔV_{O2}.

2.10.6 Interplanetary maneuvers

Typically, interplanetary maneuvers are studied by the method of *Patch-Conics*, which is an approximate method that allows the feasibility of the interplanetary mission to be evaluated by studying the order of magnitude of the ΔV needed. A more detailed evaluation will require numerical integration of the momentum ledds, which, however, need an initial condition to be solved. A possible initial condition can be, for example, the approximate one derived by this method.
As a first step, the method involves going to identify the sphere of influence of the various planets: in order to figure out whether the body of mass m (typically the S/C) is under the influence of the main body or the secondary body of mass m_1 and m_2, respectively, the aim is to estimate the radius of the sphere of influence of the various bodies involved, according to the equation (2.13).
For example, the Earth's SOI radius is worth about one million km, while the Earth-Sun distance is worth about 150 million km, this means that the Earth's sphere of influence in interplanetary missions (which see the Sun as the focus of trajectories) is $\frac{1}{150}$ so for all intents and purposes it can be considered as a point and not a sphere.
The method of the *patch conics* predicts that while one is inside a planet's sphere of influence it is considered a two-body problem with Keplerian trajectories (planeto-centric starting phase), as soon as one leave instead it is the Sun that becomes the focus of the trajectories and no longer the planet under consideration, this phase is also studied as a two-body problem with Keplerian trajectories (heliocentric phase), finally, as soon as one enter the sphere of influence of the target planet (planetocentric arrival phase) a two-body problem will be studied in which the center of the Keplerian trajectories will be the center of mass of the target planet. As often as the focus of the Keplerian trajectories changed the energy content will change because the gravitational parameters G and μ will change accordingly. This is a very important aspect because it implies that the energy possessed by a trajectory and expressed by the formula (2.24) will be evaluated by including a gravitational parameter μ which may be that of the sun if a heliocentric phase is considered, or that of one of the planets in the solar system if one is within a planetocentric phase.
Please note that, in general, all planets have a non-zero inclination with respect to the eccliptic, but this effect will be neglected in the following discussion. For the realization of this section, use was made of Refs. [15, 16, 17].

1. Heliocentric phase

The longest phase is definitely the heliocentric phase so that is the one that will need to be investigated first. The purpose of the analysis of this phase is to evaluate three quantities: V_{1H}, V_{2H} and φ.
In this first phase will go to discuss, for example, two cases one in which the aim is to go to Venus and one in which the aim is to go to Mars, starting from Earth, represented in figure 2.17 and 2.18.
For a better understanding of the following representations, the symbols used are summarized in the table 2.2.

Symbol	Planet
$V_{\earth}$	Earth
$V_{\venus}$	Venus
$V_{\mars}$	Mars
$V_{\sun}$	Sun

Table 2.2: Symbolic representation

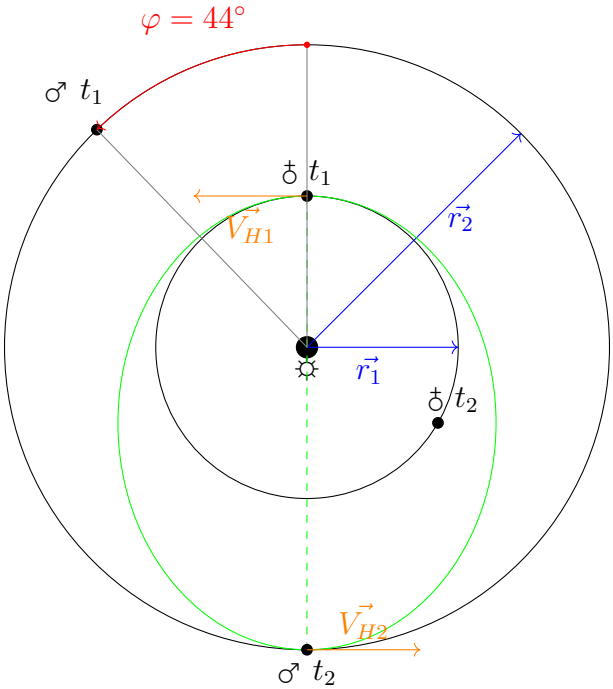

Figure 2.17: Outer planet

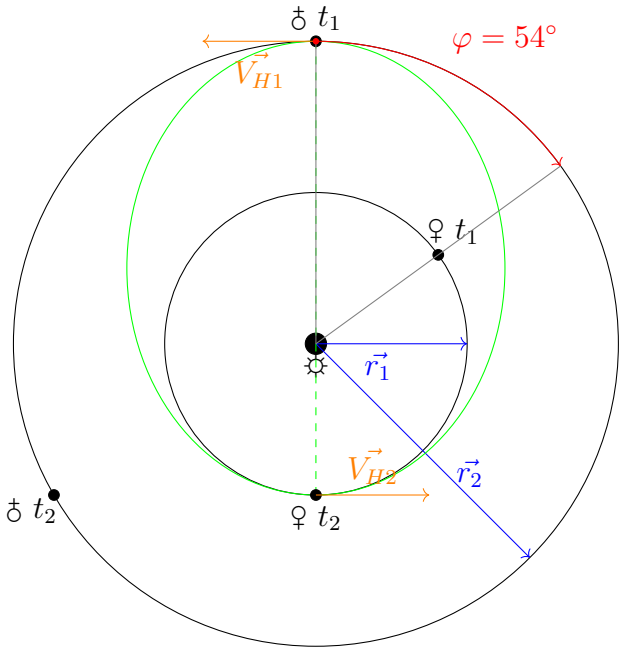

Figure 2.18: Inner planet

Table 2.3: Speed characteristics in the case of inner and outer planet

Inner planet	Outer planet
$V_{1H} < V_{♁}$	$V_{1H} > V_{♁}$
$V_{2H} > V_{1H}$	$V_{2H} < V_{1H}$
$V_{2H} > V_{♀}$	$V_{2H} < V_{♂}$

in both cases one have to phase with the arrival planet and would have to arrive with an $\varphi \neq 0$ to be intercepted by the sphere of influence of the planet that in the meantime is moving with its trailing velocity around the Sun.
Please note that in the case of terrestrial orbits one always had $\varphi_1 = 0$ and $\varphi_2 = 0$ in the Hohmann shift, here instead one will have a Hohmann shift with $\varphi_1 = 0$ and $\varphi_2 \neq 0$.
Let's give a numerical example in the inner planet case:

$$a_{TO} = \frac{r_{♁} + r_{♀}}{2} \tag{2.74}$$

$$E_{TO} = -\frac{\mu_{☼}}{2a_{TO}} = \frac{V_{1H}^2}{2} - \frac{\mu_{☼}}{r_{♁}} = \frac{V_{2H}^2}{2} - \frac{\mu_{☼}}{r_{♀}} \tag{2.75}$$

$$V_{1H} = V_{\sun}\sqrt{\frac{2 \cdot r_{\venus}}{r_{\venus} \cdot r_{\sun}}} < V_{\sun} \tag{2.76}$$

$$V_{2H} = V_{\venus}\sqrt{\frac{2 \cdot r_{\sun}}{r_{\venus} \cdot r_{\sun}}} > V_{\venus} \tag{2.77}$$

furthermore, remembering that $\vec{h}$ is a constant of motion, therefore at fixed orbit it is conserved, so it is possible to say that $\vec{h}$ is conserved during Hohmann's move. Evaluating $\vec{h}$ at perigee and apogee yields:

$$h = V_{1H} \cdot r_{\sun} = V_{2H} \cdot r_{\venus} \cdot \cos\varphi_2 \tag{2.78}$$

from which:

$$\varphi_2 = \cos^{-1}\left(\frac{V_{1H} \cdot r_{\sun}}{V_{2H} \cdot r_{\venus}}\right) \tag{2.79}$$

With this heliocentric phase therefore it is possible to evaluate V_{1H}, V_{2H} and φ.

2. Escape from the planetocentric sphere of influence

Consider, for example, the inner planet Earth-Venus case, the purpose of this step is to evaluate the ΔV and the initial ϕ_{IN} angle.
Earth is inclined about 0° relative to the eccliptic but the other planets are not, e.g. Venus is inclined about 3°, however, will neglect this effect and consider a planar maneuver.
To exit Earth's sphere of influence one must put on at least a parabolic open orbit, however, if exit with a parabolic orbit one would arrive at the boundary of the sphere of influence with a $V_\infty = 0$, instead the goal will be to arrive with a V_∞ that meets the following two requirements:

- $\vec{V_\infty}$ must be parallel to $\vec{V_{\sun}}$
- $\vec{V_{\sun}}$ - $\vec{V_\infty} = \vec{V_{1H}}$ [1]

to get a more complete idea, one can refer to the schematic shown in figure 2.19 representing the direct escape starting from a LEO orbit in case the purpose is to reach an inner planet, where ϕ_{IN} represents the angle of the phase shift between the Earth's direction and the satellite's position at the time of burnout, as well as the opening angle of the asymptote of the hyperbolic orbit.

[1] just the one found previously with the heliocentric phase

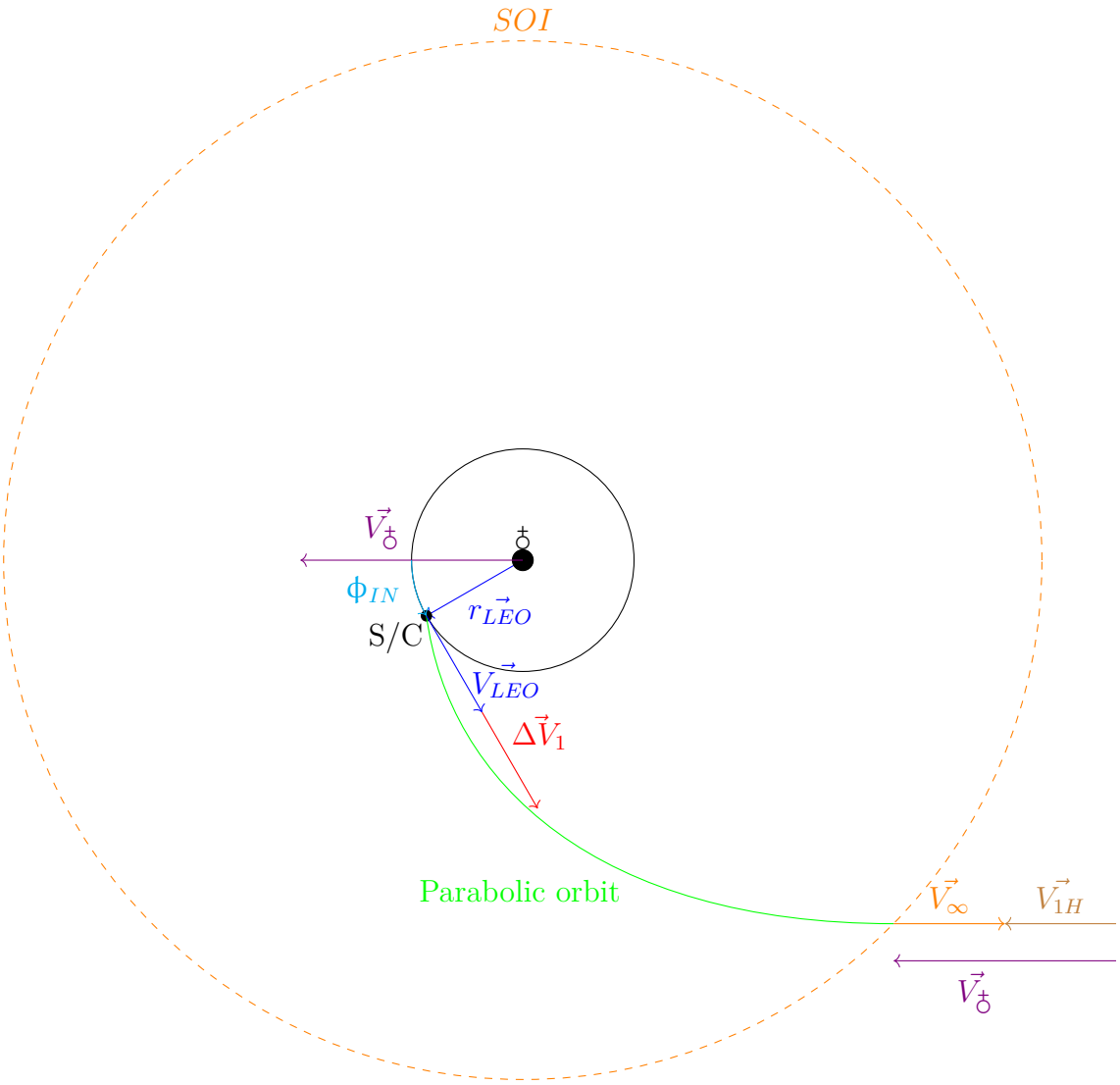

Figure 2.19: Escape inner planet

Let's give a numerical example in the outer planet case: supposing that at time t_0 the S/C leaves its LEO orbit to enter a parabolic or hyperbolic orbit that will take it to the boundaries of the Earth's sphere of influence and according to the pattern shown in figure 2.20 which this time represents the case of outer planet.

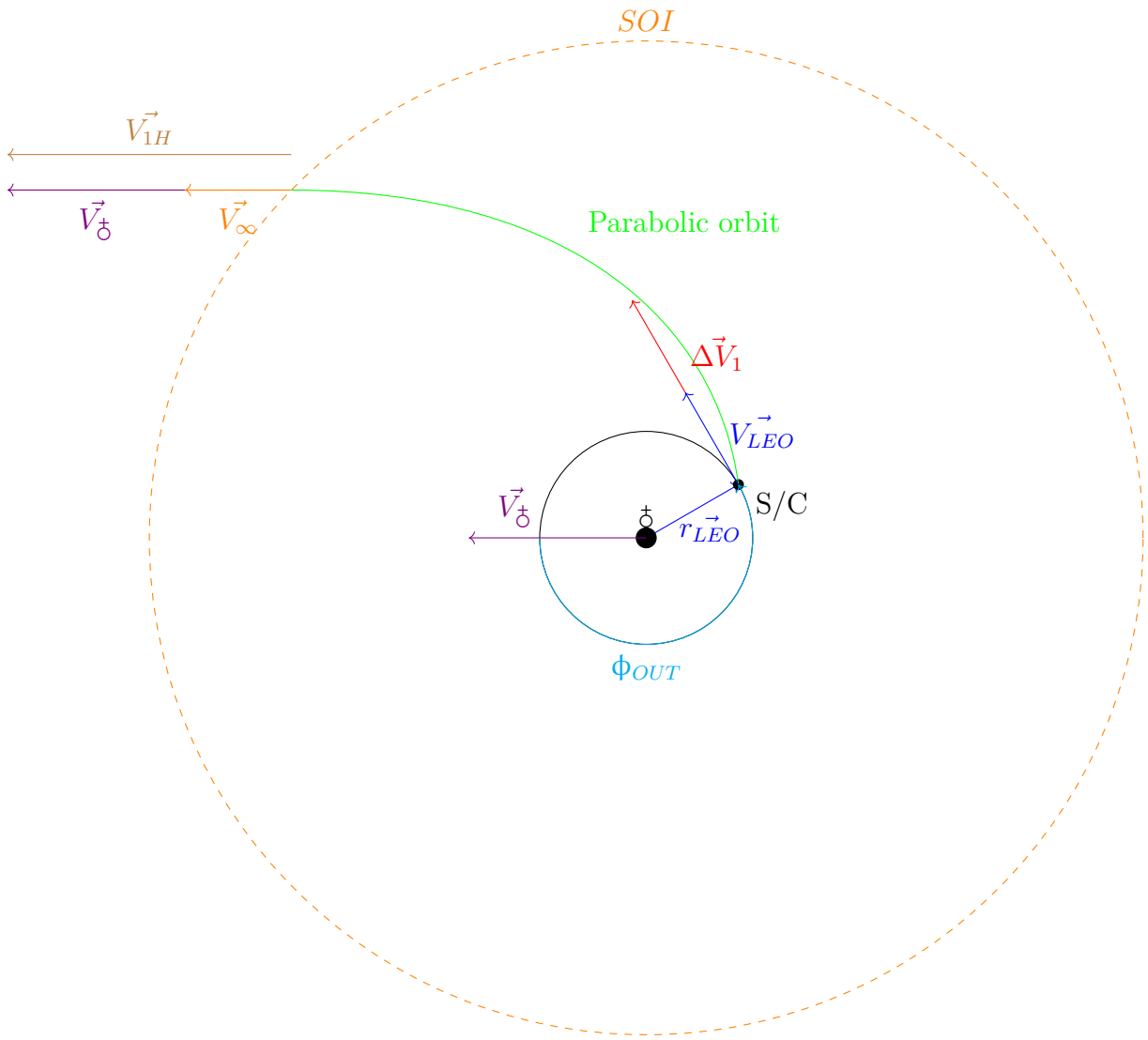

Figure 2.20: Escape outer planet

It is possible to say that the velocity at bornout V_0 will be:

$$V_0 = V_{LEO} + \Delta V_1 \tag{2.80}$$

where:

$$V_{LEO} = \sqrt{\frac{\mu_{\sun}}{r_{LEO}}} \tag{2.81}$$

for the calculation of ΔV_1 it is possible to rely on the conservation of energy by assuming that r $\rightarrow \infty$ once the S/C will arrive at V_∞ having arrived at the

boundaries of the sphere of influence:

$$E_g = \frac{V_\infty^2}{2} - \frac{\mu_{\cancel{\oplus}}}{\cancel{\infty}} = \frac{V_0^2}{2} - \frac{\mu_{\oplus}}{r_{LEO}} = -\frac{\mu_{\oplus}}{2a} \tag{2.82}$$

from which:

$$V_0 = \sqrt{2V_{LEO}^2 + V_\infty^2} \tag{2.83}$$

$$\Delta V_1 = V_0 - V_{LEO} \tag{2.84}$$

eccentricity and characteristic angles can also be evaluated:

$$p = \frac{h^2}{\mu_{\oplus}} = a(1-e^2) = r_{LEO}(1+e) \tag{2.85}$$

$$e = \frac{h^2}{\mu_{\oplus} \cdot r_{LEO}} - 1 = \frac{V_0^2 \cdot r_{LEO}}{\mu_{\oplus}} - 1 \tag{2.86}$$

from which one can easily derive the opening angles of the asymptotes in the case of hyperbolic trajectory in the inner case and in the outer planet case:

$$\phi_{IN} = \arccos\left(\frac{1}{e}\right) \quad \text{and} \quad \phi_{OUT} = \arccos\left(\frac{1}{e}\right) + \pi \tag{2.87}$$

So summarizing, in a case where the aim is going to an inner planet starting from a LEO orbit, one need to provide a ΔV_1 to obtain the V_0 which is the velocity that the satellite will have at the periastral point of a hyperbolic orbit that will take it out of the Earth's field of influence with a V_∞ representing an velocity relative to the Earth (the latter moves with a $V_{\oplus}$ drag relative to the Sun) so, since the Earth also revolves around the Sun, the satellite's velocity relative to the Sun will be precisely V_{1H} (it is as if once one leave the Earth's sphere of influence and inherit its drag velocity).
This velocity V_{1H} will be such that the S/C will not be able to get out of the solar sphere of influence, so it will enter a closed elliptical orbit (typically a Hohmann ellipse) that with respect to the Sun does not have enough energy to get out of the solar sphere of influence.

3. Arrival on the target planet

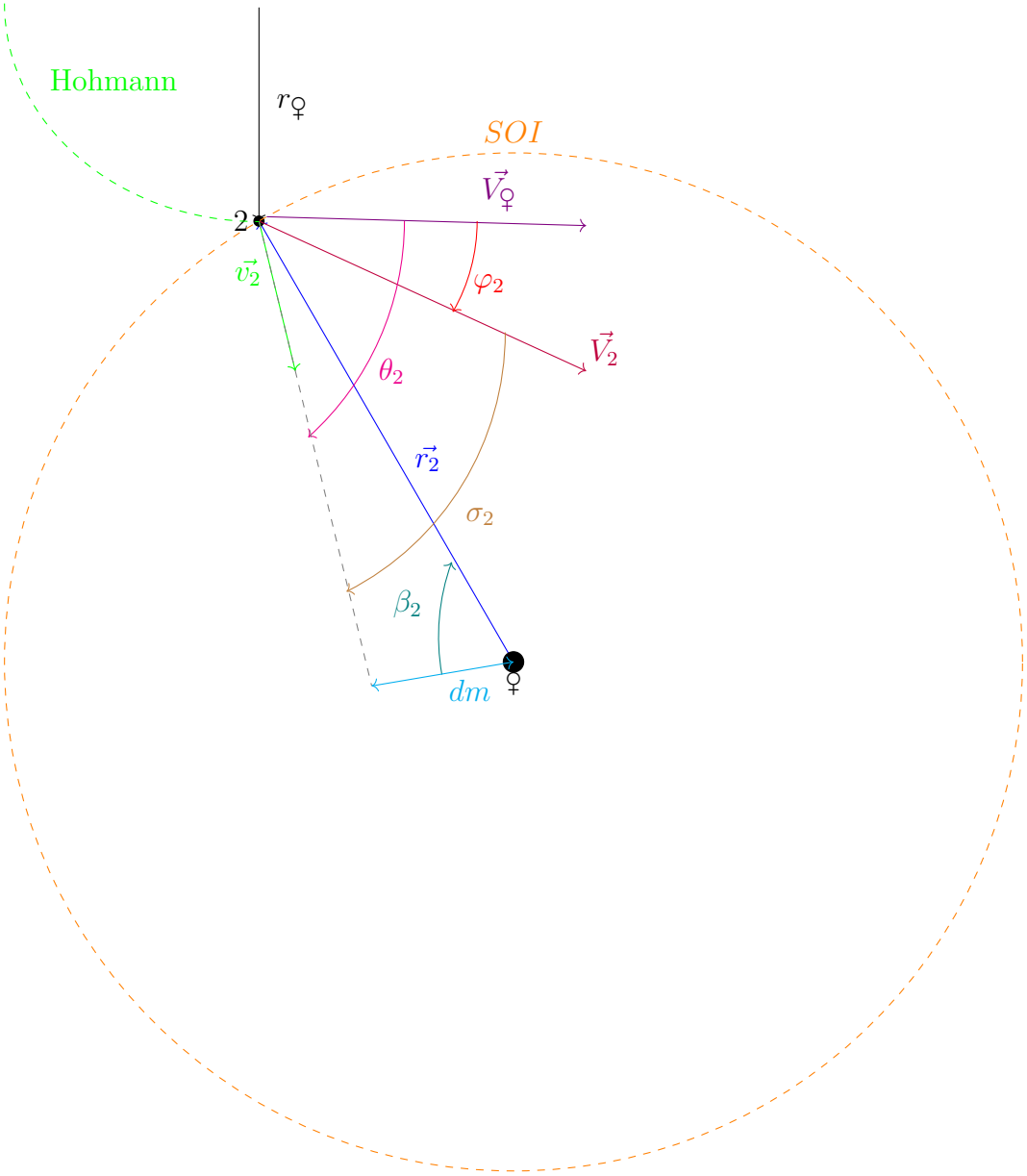

Figure 2.21: Entry into the sphere of influence: inner planet case of Venus

Consider the inner planet case, shown in figure 2.21, where the satellite arrives with a $V_{2H} > V_{♀}$, i.e. physically the S/C will arrive later and be caught by the planet because, being faster, it will catch up with it.
Special attention should be paid to the parameter dm that is the missing distance

defined as follows:

$$dm = r_2 \cos\beta \tag{2.88}$$

in particular, $\vec{V_2}$ is the velocity with which the satellite enters into the sphere of influence of Venus with respect to the Sun, but Venus will also have its own trailing velocity with respect to the Sun V_{φ}, so the velocity of the S/C with respect to Venus will be:

$$\vec{v_2} = \vec{V_2} - \vec{V_{\varphi}} \tag{2.89}$$

where $\vec{v_2}$ is the S/C velocity relative to the planet, $\vec{V_2}$ is the S/C velocity relative to the Sun, and $\vec{V_{\varphi}}$ is the velocity of the planet around the Sun.
Let's consider the outer planet case, shown in figure 2.22, where the satellite arrives with a $V_{2H} < V_{\sigma}$, i.e. physically the S/C will arrive first and the planet capturing the S/C will arrive later because it will be faster than the S/C itself.
It is important to note that once it enters the planet's sphere of influence, the S/C will head toward the center of the planet along the direction of $\vec{v_2}$ defined by the angle θ_2. Since the goal will be to avoid the crash into the planet one must have that the missing distance must be greater than the impact parameter β, which represents that value of missing distance for which the S/C arrives at the periapsis exactly on the surface of the target planet, that is with $r_{peri} = R_{target}$.

$$dm = \frac{h}{v_2} = \frac{r_{peri} \cdot v_{peri}}{v_2} \tag{2.90}$$

From the conservation of the energy of the trajectory followed by the S/C, it is possible to derive these two parameters:

$$\frac{v_2^2}{2} = \frac{\mu_{\sigma}}{\cancel{\infty}} = \frac{v_{peri}^2}{2} - \frac{\mu_{\varphi}}{r_{peri}} \tag{2.91}$$

From which it follows that:

$$dm = \frac{r_{peri}}{v_2}\sqrt{v_2^2 + 2\frac{\mu_{\varphi}}{r_{peri}}} \tag{2.92}$$

$$\beta = \frac{R_{\varphi}}{v_2}\sqrt{v_2^2 + 2\frac{\mu_{\varphi}}{R_{\varphi}}} \tag{2.93}$$

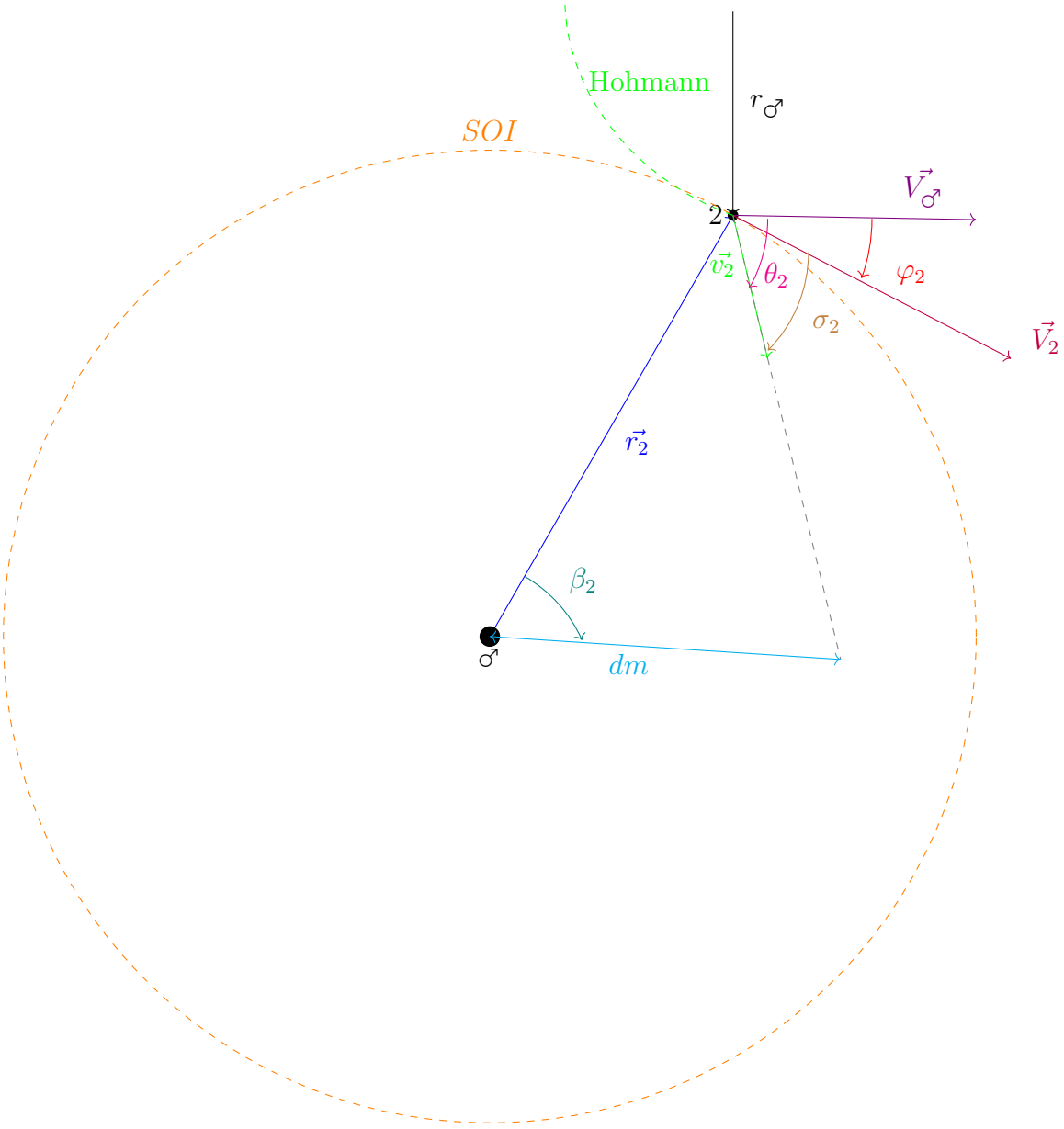

Figure 2.22: Entry into the sphere of influence: outer planet case of Mars

As said, to be able to complete the mission without crashing into the planet it is necessary to have dm $> \beta$ and at this point three things can happen:

1. capture at the periapsis of the arrival orbit with entry on a circular planetocentric orbit, i.e., once S/C arrives at perigee it is necessary to provide a ΔV_2 to be captured by the planet and enter a circular orbit useful for closely exploring the planet of interest.

2. fly-by behind the planet: this is a maneuver that allows to increase the energy of the trajectory exiting the planet without having to turn on the engines.

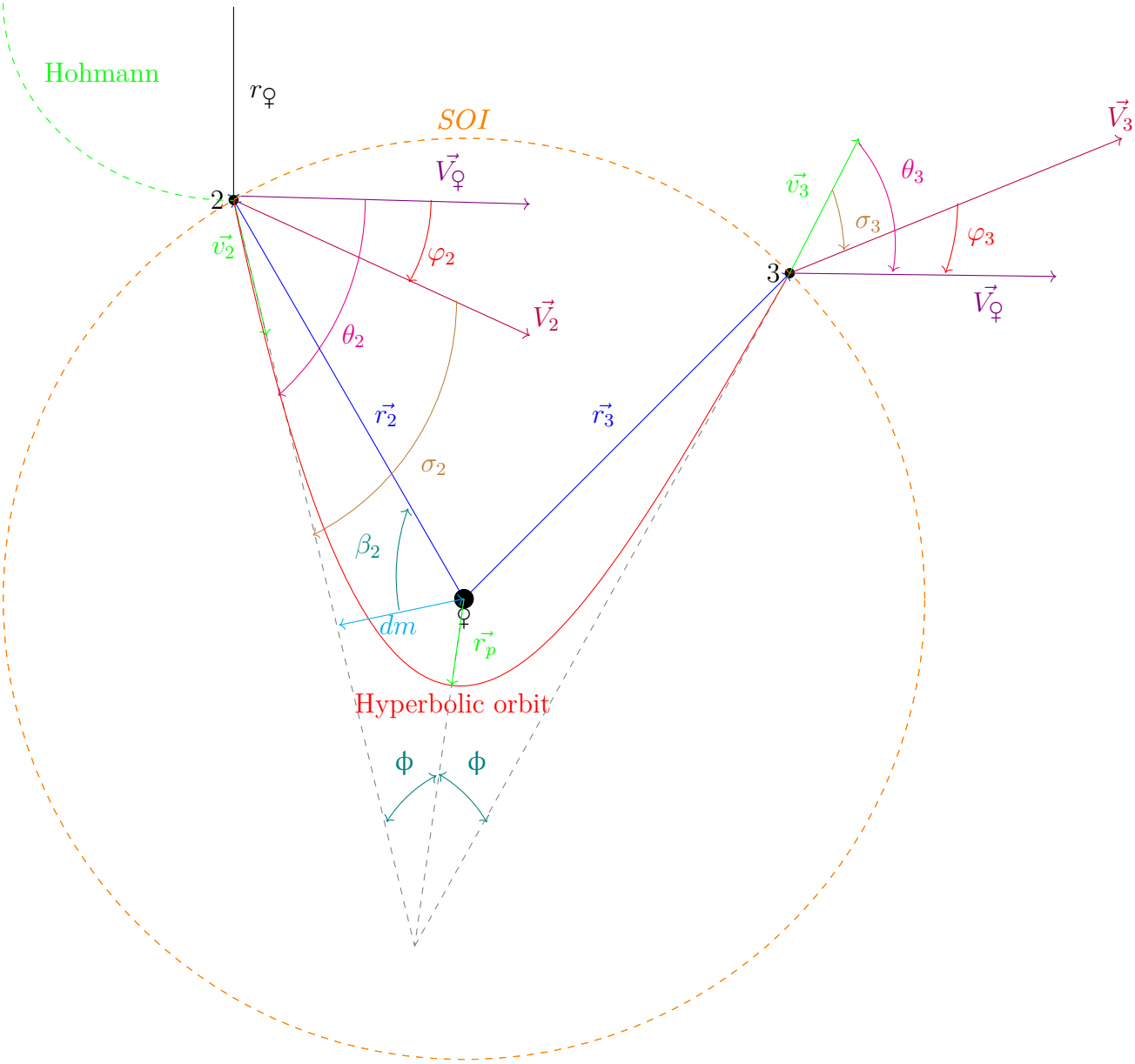

Figure 2.23: Fly-by behind the planet

In the flyby maneuver, in fact, the S/C enters with the $\vec{v_2}$, travel the hyperbolic orbit within the planet's sphere of influence without stopping, and will exit the sphere of influence with a velocity in modulus exactly equal to that

with which it started ($\vec{v_2}$ and $\vec{v_3}$ are equal in modulus and equal to the hyperbolic excess velocity) but with a different direction, as can be seen from the representation in the figure 2.23.

$$|\vec{v_2}| = |\vec{v_3}| = V_\infty \longrightarrow \vec{v_2} \neq \vec{v_3} \tag{2.94}$$

$$h_2 = v_2 r_2 \cos\varphi_2 \tag{2.95}$$

$$h_3 = v_3 r_3 \cos\varphi_3 \tag{2.96}$$

but $\varphi_3 < \varphi_2$ so it will have that $|v_3| > |v_2|$.
That is, without having maneuvered it obtained that $h_3 > h_2$, i.e., the momentum of the angular momentum of the orbit increased without having had to turn on the engines and expend propellant.

3. fly-by in front of the planet: instead, in this case the satellite will always have $|\vec{v_3}| = |\vec{v_2}|$ but will have $\varphi_3 > \varphi_2$ so it have lost energy having $h_3 < h_2$. This type of maneuver, analogous to the figure 2.23 with the only difference being that this time the satellite will not enter the planet's sphere of influence from behind but from the front, that is, in an angular range between $-90°$ and $90°$ with respect to the direction of the planet's drag speed, is in fact employed if the goal is to brake without the use of engines.
In general with the flyby maneuver one have the possibility of increasing or decreasing the momentum of the satellite at zero cost to us (because what actually happens is that this increase or decrease in the angular momentum vector is achieved at the expense of the planet). In fact, taking into account the huge difference between the masses involved, it can be said that this effect of changing angular momentum vector is negligible for the planet while the satellite can instead gain or lose a certain non-negligible amount of velocity.

2.11 Planar Bicircular Restricted 4-Body Problem (PBCR4BP)

In order to achieve the purpose of this dissertation, as well as to evaluate as consistently as possible the possible flyby maneuvers that a generic S/C can perform by exploiting the gravitational effects of the moons of the individual planets in the solar system, it is appropriate to introduce a model in which account is taken of the fact that there are three bodies in question that can significantly influence the trajectory of a spacecraft, such a model (implemented in this thesis work) is the *Planar Bicircular Restricted 4 Body Problem (PBCR4BP)* [18, 19, 20].
The model analyzed in this section is the *PBCR4BP* which describes the motion

of an infinite mass (P_3) under the influence of three massive bodies: the Earth (P_1), the Moon (P_2) and the Sun (P_4). Obviously, it will suffice to change the gravitational parameters of the bodies involved to fit this model on other systems centered in the various planets of the solar system, so that the interaction that the two main moons of the single planet analyzed will have on the final trajectory described by the S/C can be evaluated. In this model, the Earth and Moon move in circular paths around their mutual barycenters, denoted in the figure 2.24 by B_1. Similarly, the Sun and B_1 move in Keplerian circular motion around their mutual barycenter B_2.

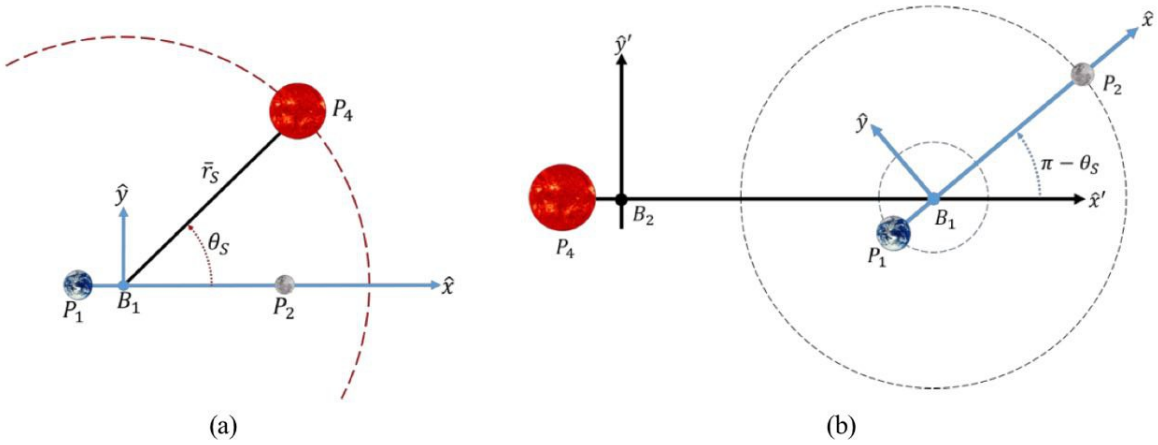

Figure 2.24: Rotating Earth-Moon system (left), rotating Sun-B_1 system (right)

This model is inconsistent since it is assumed that all primaries move on circular orbits, this strictly speaking is not true being that the eccentricities of the Earth and Moon orbits are 0.0167 and 0.0549, respectively, as well as the inclination of the lunar orbit with respect to the eccliptic is about 5°, so it is also assumed that the Earth-Moon orbital plane is the same as the Sun-B_1 orbit.
The model is defined with respect to a rotating coordinate system, where the positive direction of the x-axis is defined from the Earth to the Moon, the positive direction of the z-axis is defined in the direction of the orbital angular momentum for the Earth and Moon, and the positive direction of the y-axis completes the orthonormal triad.
Note that the *PBCR4BP* is a time-dependent system in which the position of the Sun in the Earth-Moon rotation frame is defined by a single angle called θ_S. The Sun moves clockwise around B_1 (i.e., the angle θ_S is negative), as illustrated in Figure 2.24(a); this effect is due to the fact that the Earth-Moon system centered in B_1 rotates with a unit angular velocity in accordance with the definition of the

CR3BP, while the Sun, rotating in turn around this rotating system will have a smaller angular velocity so that there will be this apparently clockwise circular motion.
The equations of motion describing the motion of the assumed massless particle (P_3), in the rotating Earth-Moon system, are described below:

$$\ddot{x} = 2\dot{y} + \frac{\partial \Upsilon}{\partial x} \tag{2.97}$$

$$\ddot{y} = -2\dot{x} + \frac{\partial \Upsilon}{\partial y} \tag{2.98}$$

$$\ddot{z} = \frac{\partial \Upsilon}{\partial z} \tag{2.99}$$

where Υ is the pseudo-potential in the rotating Earth-Moon system and is defined as:

$$\Upsilon = \frac{1-\mu}{r_{13}} + \frac{\mu}{r_{23}} + \frac{x^2+y^2}{2} + \varepsilon\Big(\frac{m_4}{r_{43}} - \frac{m_4}{a_4^3}(x_4 x + y_4 y + z_4 z)\Big) \tag{2.100}$$

where x_i, y_i and z_i are the components of the position of the point P_i with respect to the barycenter of the rotating Earth-Moon reference system, μ is the gravitational parameter of the Earth-Moon system, r_{ij} is the modulus of the position of P_i with respect to P_j, m_4 is the dimensionless mass of the fourth body P_4 defined as $\frac{M_4}{M_1+M_2}$, and a_4 is the semi-major axis of the circular orbit traveled by the Sun around the barycenter B_1. The ε term is a scaling parameter for the Sun's mass: $\varepsilon = 0$ reflects a restricted circular three-body problem *CR3BP* without solar gravity, while $\varepsilon = 1$ represents the *PBCR4BP*. Just as in *CR3BP* it is advantageous to study the motion of the satellite in the synodic system, similarly in this case it is advantageous to study the equations of motion in the rotating Sun-B_1 system: in this reference system the positive direction of the x-axis is directed from the Sun to the Earth-Moon barycenter B_1, the positive direction of the z-axis is defined as the direction of the angular momentum of the Sun-B_1 orbit, and the positive direction of the y-axis completes the triad. The rotating Sun-B_1 system is illustrated in the figure 2.24(b).
It is useful to know that there are instantaneous equilibrium solutions in the *PBCR4BP*; in fact, it can be shown that there is an instantaneous equilibrium solution for every angle of the Sun. Since the union of the points representing the equilibrium solutions depends on the angle of the Sun, a particle initialized at these positions will not remain there all the time, it will immediately move away as the position of the Sun changes over time having an angular velocity different from that of the rotating Earth-Moon system. This is a big difference from the *CR3BP* since both the equilibrium points and the Jacobi integral vanish.

Chapter 3

Mars-Phobos-Deimos System

The objective of this work is to quantitatively evaluate how convenient it is, in terms of ΔV and thus propellant consumed, to exploit a planet's moons to evaluate re-entry trajectories back to Earth by exploiting fly-by maneuvers with them, as opposed to the direct excape maneuver.
For this reason, it was necessary to implement in the *Matlab* environment a model containing the Mars-Phobos-Deimos system with the respective gravitational parameters of the celestial bodies considered, the equations of motion in the planar bicircular 4-body problem so that the perturbative actions of the two Mars moons can be simulated and possible flyby maneuvers can be implemented with them, the initial and final conditions, and the trajectory to be propagated by integrating the EOMs so as to start with the established initial conditions and arrive at the target final conditions. Once the model is set up, the next step will be to search for trajectories that reach as far as the sphere of influence of Mars: the purpose will be to compare the ΔV spent for the hyperbolic escape maneuver directed to the SOI of Mars with the ΔV needed to implement an assisted escape by exploiting the gravitational slingshot effect with Phobos individually, with Deimos individually, and finally, an assisted escape by a combined flyby of both Mars moons.
Strictly speaking, it is good to emphasize the fact that Mars moons are very unmassive and tiny in size as can be visualized from the gravitational parameters listed in table 3.1, so it could be immediately conclude that this gravitational slingshot effect will be negligible. For this reason, a parametric analysis was subsequently conducted in which, by varying the binary gravitational parameter μ within an appropriate range of values, any binary system could be simulated. In addition, by adding the possibility of also parametrically varying the mass of the tertiary body and its distance from the barycenter of the binary system, it was also possible to simulate any existing ternary system.
As explained of Chapter 2, in order to return to Earth starting from Mars (pacth conics method applied to an outer planet), one must in fact first exit the SOI in

the starting planet, and it must be done in a very precise way since, once exiting the SOI of Mars, the V_∞ will have to be parallel to the planet's trailing velocity and, in modulus, exactly equal to the V_{1H}, so as to begin the heliocentric phase that will see the S/C travel along a Hohmann that will take it all the way to the Earth's SOI. This work, therefore, will focus on the first planetocentric phase of the conics patch model that will see Mars as the main body, as the second heliocentric phase will go accordingly. The third planetocentric phase that sees Earth as the main body, however, will not be detailed.
It is therefore possible to evaluate the V_{1H} so as to uniquely define the constraints, both in terms of position and velocity once the satellite reaches the boundaries of the SOI, that the trajectories will have to respect.
By evaluating the energy of the Hohmann ellipse it is indeed possible to write:

$$\varepsilon_{GTO} = \frac{V_{1H}^2}{2} - \frac{\mu_{\odot}}{r_{MS}} = -\frac{\mu_{\odot}}{2a_{GTO}} \tag{3.1}$$

where $\mu_{\odot}$ is the gravitational parameter of the Sun which is worth $1{,}3271 \times 10^{11}\,\mathrm{km}^3/\mathrm{s}^2$, r_{MS} is the Mars-Sun distance which is worth $2{,}2793 \times 10^8\,\mathrm{km}$, and a_{GTO} is the semi-major axis of the Hohmann ellipse, which can be evaluated as:

$$a_{GTO} = \frac{r_{ES} + r_{MS}}{2} = 1{,}8876 \times 10^8\,\mathrm{km} \tag{3.2}$$

from which it follows that:

$$V_{1H} = \sqrt{2\left(\varepsilon_{GTO} + \frac{\mu_{\odot}}{r_{MS}}\right)} = 21{,}48\,\mathrm{km/s} \tag{3.3}$$

Thus, the constraints that valid trajectories will have to meet will be:

- final radius equal to the radius of the SOI of Mars ($r_{SOI} = 5{,}76 \times 10^5\,\mathrm{km}$),
- final velocity equal, in modulus, to the V_{1H}.

It is then appropriate to define and keep in mind (as they will be the subject of later evaluations) what are the gravitational parameters of the bodies in play, they will be summarized in the table 3.1 with the respective symbology used in the subsequent discussion.

Table 3.1: Gravitational Parameters

Body	**Mass [kg]**	**μ [km^3/s^2]**	**Radius [km]**
Mars	$6.39 \cdot 10^{23}$	$4.2828 \cdot 10^4$	3389
Phobos	$1.08 \cdot 10^{16}$	$7.112 \cdot 10^{-4}$	11.267
Deimos	$2 \cdot 10^{15}$	$9.85 \cdot 10^{-5}$	6.2

Before moving on to the 4-body (which is the actual model implemented), for greater understanding, it is good to give an overview starting with the restricted circular 3-body problem (*CR3BP*) following the logical path analyzed in Refs. [21, 22, 23, 24, 25, 26, 27]. In the Planar Circular Restricted Three-Body Problem two primary bodies P1, P2 of masses $m_1 > m_2 > 0$, respectively, move under mutual gravity on circular orbits about their common center of mass. The third body, P, assumed of infinitesimal mass, moves under the gravity of the primaries, and in the same plane. The motion of the primaries is not affected by P. In the present case, P represents a spacecraft, and P1, P2 represent the Mars and Phobos, respectively. In particular, assuming that the S/C starts from a low orbit around Mars (LMO) of altitude 400 km and study the evolution of the trajectory that an S/C would have to arrive on Phobos, it is appropriate to study the EOMs in the Mars-Phobos synodic system, i.e., a rotating reference system that allows to simplify the equations of motion by making them dimensionless in no small measure. In this reference system, the distance between Mars and Phobos ($DU = 9378$ km) is unitary, and the gravitational parameter of this binary system is defined as follows:

$$\mu_{syn} = \frac{\mu_{Phobos}}{\mu_{Mars} + \mu_{Phobos}} = 1{,}6606 \times 10^{-8} \tag{3.4}$$

The two bodies rotate around their common center of mass with a dimensional angular velocity equal to:

$$\omega_{syn} = \sqrt{\frac{\mu_{Mars} + \mu_{Phobos}}{DU^3}} = 2{,}2788 \times 10^{-4}\,\text{rad/s} \tag{3.5}$$

In the synodic system the center of mass is not coincident with the center of mass of the main planet but will be somewhat shifted toward the secondary body by a greater measure the more massive the latter body is. In the case of Phobos, as it can be seen from the table 3.1, its mass is seven orders of magnitude less than that of Mars, however, this does not detract from the fact that the center of mass of Mars **NOT** is coincident with the center of mass of the synodic system.
However, given the insignificant distance between the center of mass of Mars and that of the synodic system, it is possible, committing a more than negligible error, to consider Mars stationary at the center of the synodic system (in fact that distance from the origin of the synodic system would be $-\mu$) and Phobos revolving around it on a planar circular orbit of unit radius with a tangential velocity equal to:

$$VU = \sqrt{\frac{\mu_{Mars} + \mu_{Phobos}}{DU}} = 2{,}1370\,\text{km/s} \tag{3.6}$$

In the same way as distance and velocity, time must also be scaled in order to propagate the equations of motion of *CR3BP* correctly.
The scaled time defined as:

$$\tau = \frac{2\pi}{\omega_{syn}} \tag{3.7}$$

In the synodic system, time is in fact measured dimensionless through the use of radians: for example, a dimensionless period of time equal to 2π is equivalent to the dimensional time required for the secondary body (in this case Phobos), with its angular velocity, to make a complete 2π revolution around the primary body (in this case Mars), which is about 7 hours and 39 minutes.
Once the Mars-Phobos synodic system is properly defined, the perturbative effect of Deimos can be added by passing *PBCR4BP*.
The parameters to be provided as input to implement this model, in addition to those defined above are:

- the mass of the third body dimensionless from the sum of the primary and secondary body masses:

$$m_{Deimos} = \frac{M_{Deimos}}{M_{Mars} + M_{Phobos}} = 3{,}1299 \times 10^{-9} \tag{3.8}$$

- the distance of the third body from the center of the reference system (which with good approximation can be estimated as the distance between Mars and Deimos equal to $r_{MD} = 23\,459\,\text{km}$) dimensionless with respect to DU:

$$\rho_{Deimos} = \frac{r_{MD}}{DU} = 2.5015 \tag{3.9}$$

- the angular velocity of Deimos in its planar circular orbit relative to the dimensionless Mars-Phobos synodic system. The angular velocity of Deimos can be evaluated as:

$$\omega_{Deimos} = \sqrt{\frac{\mu_{Mars} + \mu_{Phobos}}{r_{MD}^3}} = 5{,}8073 \times 10^{-5}\,\text{rad/s} \tag{3.10}$$

  as mentioned, however, the magnitudes must be dimensionalized so it is possible to conclude that Phobos will rotate with unit angular velocity while Deimos with an angular velocity equal to $\omega_{Deimos}/\omega_{syn} = 0.2528$, which is approximately $\frac{1}{4}$ relative to that of Phobos. This means that, being by convention a positive angular velocity defined counterclockwise, Deimos, having an angular velocity less than 1, will appear to have an apparent clockwise circular motion with respect to the angular velocity with which the entire Mars-Phobos synodic system moves.

- the angle θ_{Deimos} representing the angular position of Deimos. In the synodic system in fact, Mars and Phobos will 'appear' to be stationary, while Deimos having an angular velocity less than 1 will rotate clockwise, so it will be important to define its angular position in time:

$$\theta_{Deimos} = \omega_{Deimos} \cdot t \tag{3.11}$$

3.1 Synodic vs inertial system

For further understanding, it is possible to visualize a 2D graphical representation of the Mars-Phobos-Deimos system in the synodic system in figure 3.1 in which it can be seen that the position of Phobos remains fixed in time while Deimos appears to rotate with negative angular velocity, i.e., clockwise.
In addition, using from [28] a code implemented in *Matlab* called *Syn2ECI* it was possible to convert quantities from the synodic system to the inertial system and vice versa, so that the trajectory of the S/C can be visualized in both reference systems thus having a more complete and detailed view.
In the figure 3.2 it is indeed possible how in the inertial system both Mars moons have a positive angular velocity (i.e., counterclockwise) different from zero and, in particular, how Phobos rotates faster than Deimos, leaving it behind.
Figures 3.1 and 3.2 also show the position of the center of mass of the respective reference systems (in both cases this point falls within Mars), the starting orbit of the S/C with altitude of 400 km from the Martian surface, and the planar circular orbits followed by Phobos and Deimos[1].
Please note that in the figures 3.1 and 3.2 the scale size of Mars is the correct one, while the sizes of Phobos and Deimos are not the real ones because it was preferred on purpose to increase the size of the two moons of Mars in order to have a clearer representation and be able to easily visualize their location at various time instants.

[1]The angular positions of Phobos and Deimos shown in both figures are representative of the moment of minimum distance with the space probe.

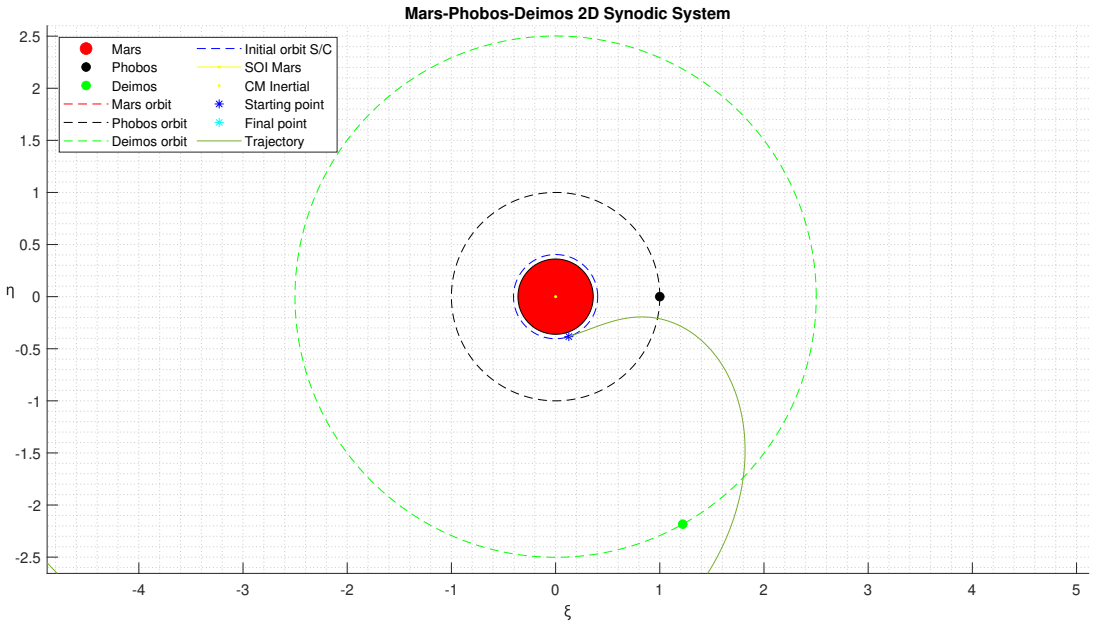

Figure 3.1: Mars-Phobos-Deimos synodic system

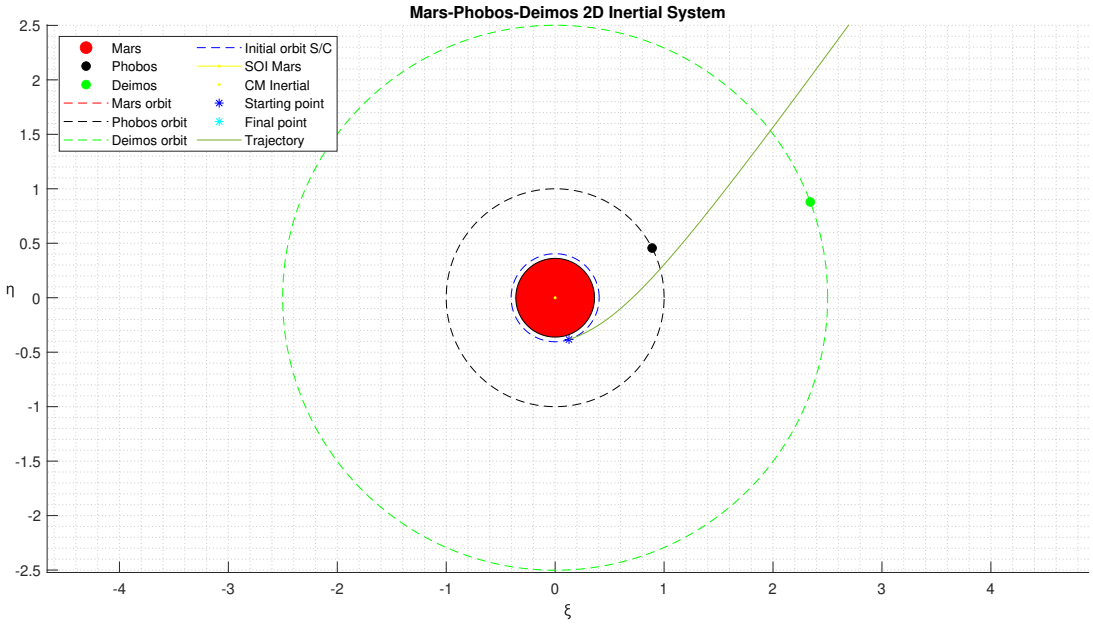

Figure 3.2: Mars-Phobos-Deimos Inertial system

By way of example only, a generic elliptical trajectory displayed in the inertial system 3.3 and the synodic system 3.5 is shown below, with the respective characteristic velocities reported in one and the other system (3.4 and 3.6 respectively): as can be clearly seen, the trajectory is the same but takes different forms depending on the reference system used.
Moreover, the trend of velocities is also completely different: viewing the graph in figure 3.7 it is also possible to notice a nontrivial singularity: the point of minimum velocity in the inertial system is the point of maximum velocity in the synodic system. This means that, between the two reference systems, in an elliptical trajectory the apogee is the same in terms of position but not in terms of velocity because from the synodic point of view the apogee will be the point at maximum velocity! This statement is not an absolute truth; it depend on the gravitational parameters characteristic of the various primary body-secondary body systems considered.

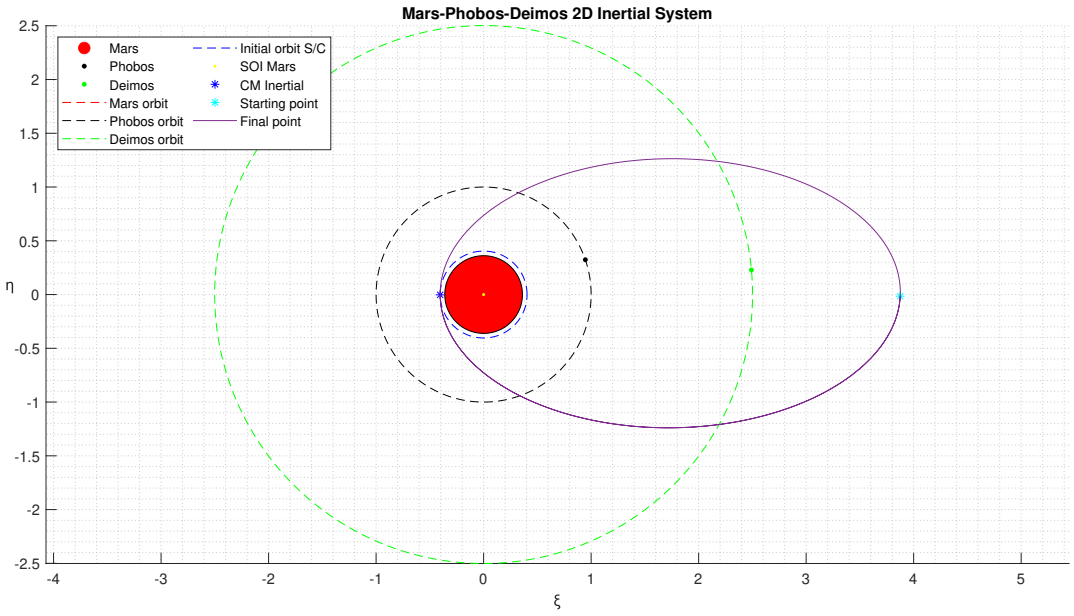

Figure 3.3: Elliptical trajectory in the inertial system

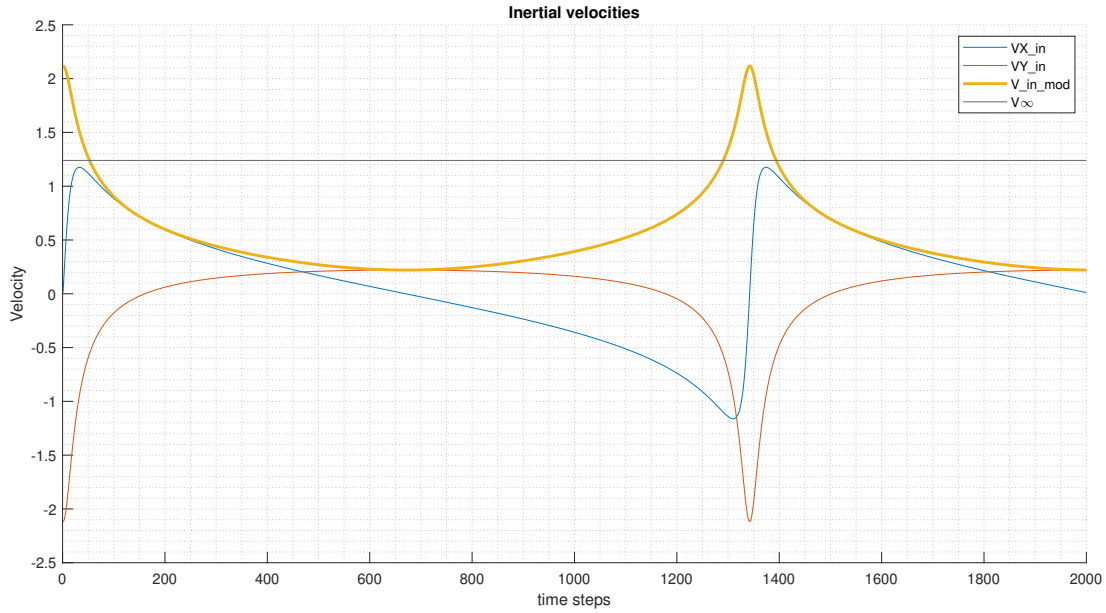

Figure 3.4: Characteristic velocities of an elliptical trajectory in the inertial system

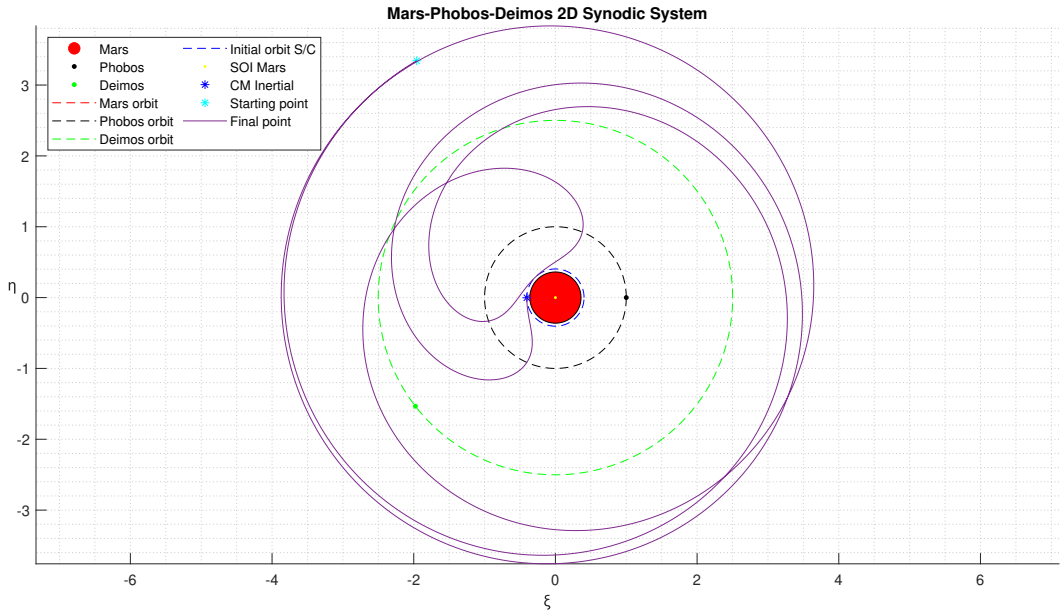

Figure 3.5: Elliptical trajectory in the synodic system

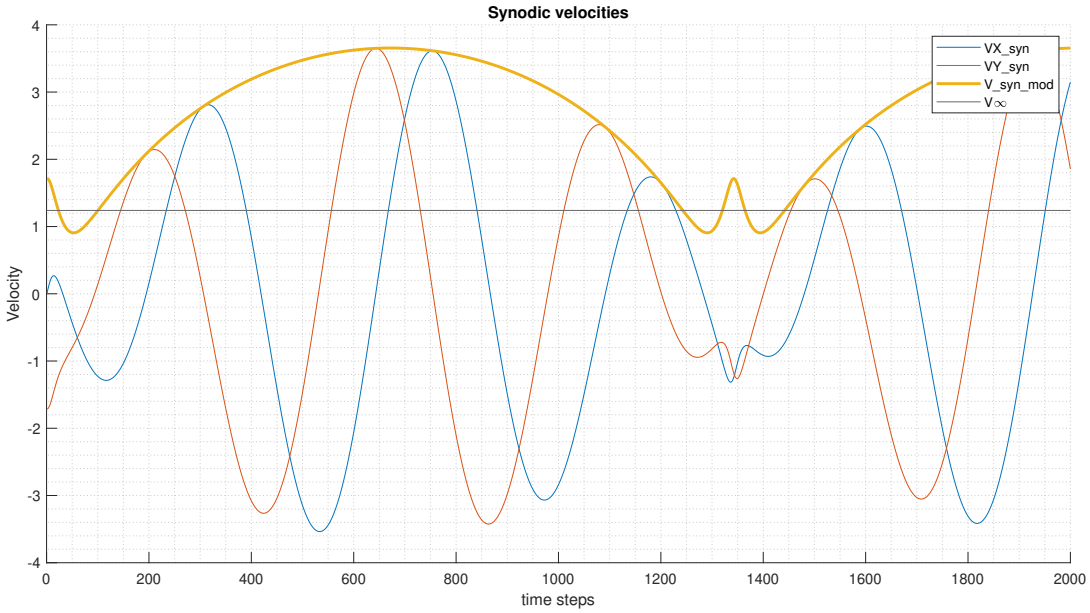

Figure 3.6: Characteristic velocities of an elliptical trajectory in the synodic system

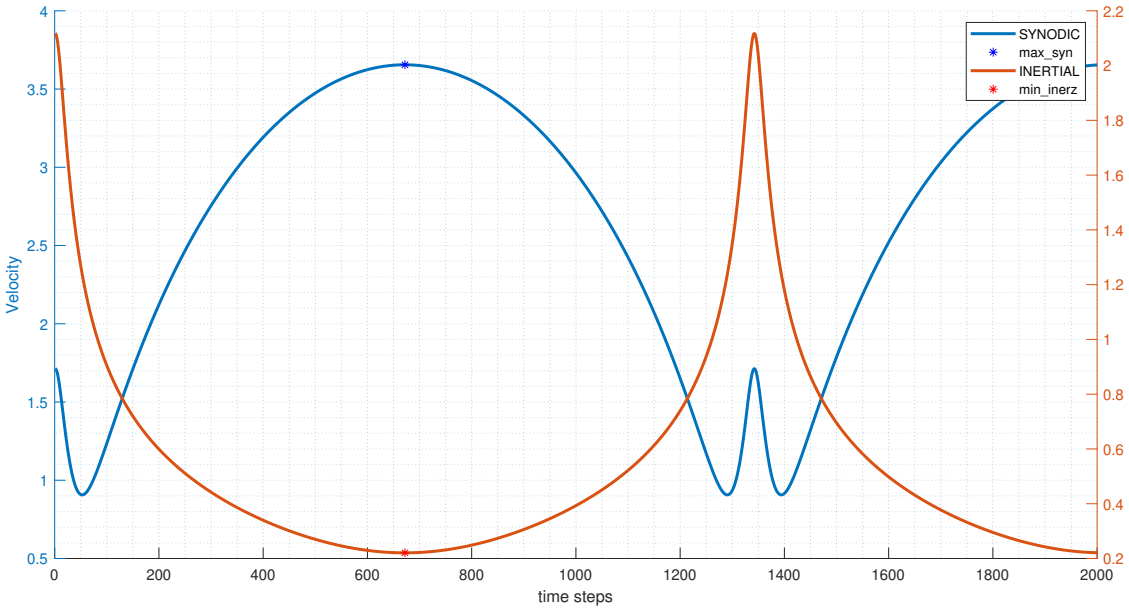

Figure 3.7: Comparison of elliptical velocities in inertial and synodic

At this point it is important to make two points regarding the use of one or the other reference system:

1. the equations of motion of the *PBCR4BP* are computed in the synodic system, while the variable V_∞ used as a constraint on the final velocity to be had by the probe is computed in the inertial system. Therefore, once the integration with *ode113* is done and the vector containing the positions of the S/C at each time step in the synodic system is obtained, it is possible to proceed in two ways:

   - move from the synodic system to the inertial system, through the use of a special function called *Syn2ECI*. In this way it will only be necessary to impose the constraint that the final velocity must be equal to V_∞,
   - to remain in the synodic system but at this point one will need to subtract from V_∞ the drag speed of the synodic system, that is, the tangential velocity with which Phobos moves in its circular orbit. It is possible to calculate this magnitude by a scalar product between the ω_{syn} that has component only along the *zi* axis and the distance between Mars and Phobos that has component only along *csi*, so as to obtain a resultant vector that has only the component along the *eta* axis, which in fact represents the tangential velocity of Phobos.

2. the synodic system, as mentioned, rotates around its center of mass with angular velocity ω_{syn}, but it also rotates in the heliocentric system, following the revolution of Earth and Mars around the Sun. For this reason, in the following analysis it was assumed an optimal phasing: as will be seen in the next chapter this optimal phasing assumption will prove more than valid.

Chapter 4

Genetic Algorithm

At this point it is appropriate to go on to investigate the genetic algorithm used to carry out the analyses during this thesis work. Once the initial conditions have been established, they must in fact be propagated over time, following the EOMs of the *PBCR4BP*, so as to arrive at the final conditions on which the two constraints in terms of position and velocity described above must be imposed.
Two possible avenues open up here (both lawful and viable): the first making use of *Matlab's fmincon* function, i.e., a tool that allows solving even very complex maximum and minimum problems as long as they are well constrained; the second making use of a genetic algorithm, i.e., a heuristic algorithm inspired by Darwin's theory of evolution. Since checking the optimum is not the goal of this paper the choice fell on the second option.
The genetic algorithm implemented consists of generating a population of 1000 individuals, each of which will be formed by 5 properties that are called genes (or alleles) and that represent the variables involved, in order they are:

1. the ΔV as the first gene, that is, the impulse that is given at the initial instant that is to be added vectorially (the ΔV will be given tangentially) to the circular velocity possessed by the S/C, which, being on an LMO orbit of altitude $h = 400\,\text{km}$ will have a tangential velocity equal to:

$$V_C = \sqrt{\frac{\mu_{Mars} + \mu_{Phobos}}{R_{Mars} + h}} = 3{,}3620\,\text{km/s} \tag{4.1}$$

2. the angle in the synodic plane θ as the second, i.e., the angular distance with respect to the x-axis of the Mars-Phobos synodic system at which the S/C is located at the time the impulse is given. This parameter can be changed from 0° to 360°, and in this way it is possible to simulate the start of the trajectory at any of the positions occupied by the satellite along its circular orbit in LMO.

3. the angle outside the synodic plane φ as the third. This angle has been made to explore freely between 0° and 360° but, for each trajectory implemented, the genetic algorithm has converged to the condition $\varphi = 0$, which is the one of interest, since, having implemented a planar model, the aim is precisely to simulate a trajectory that is as planar as possible, going to minimize the ΔV with respect to the nonplanar case.

4. the dimensionless time taken by the S/C to go from the starting point to the ending point, as well as the integration time as the fourth gene.
   For example, a dimensionless time equal to 2π means that the trajectory will have been integrated for a period of time equal to the amount of time it takes Phobos to make a complete rotation of 360° around Mars, that is, about 7 hours and 39 minutes.

5. the $\Delta\theta$ as the fifth and last gene. This parameter is defined as the difference between, respectively, the angular position possessed by Deimos θ_{Deimos} and Phobos θ_{Phobos} at the initial instant and is of fundamental importance since the synodic system is a rotating system with angular velocity equal to that possessed by Phobos, which is why it is defined with $\theta_{Phobos} = 0$ at any instant in time. By setting this variable with values between 0° and 360° it will therefore be possible to describe the relative position of Deimos in its circular orbit around Mars, as well as to go to identify the possible launch windows that will occur at the value $\Delta\theta = 0$, that is, when the two Mars moons are along the same conjunction.

These variables will thus determine what will be the random initial conditions that will be propagated by the genetic algorithm and, from this point on, the trajectory followed by the satellite will be uniquely defined.
To propagate the orbit in time, the *ode113* function of *Matlab* was used, which allows solving differential equations by giving as input the initial conditions and integration time. Once the vector containing the probe positions of the various time steps, output of integration with *ode113*, has been obtained, it is possible to impose constraints on the final position and velocity that the S/C will have to reach the boundaries of the Mars SOI with the right velocity, so as to enter with exactly V_{1H} on the Hohmann transfer and begin its heliocentric phase that will bring the probe of back to Earth.
Thus, the difference between the final position reached after integration and the target radius (r_{SOI}) and between the final velocity possessed by the S/C and the target velocity (V_{1H}) represent errors: the goal of the genetic algorithm is precisely to find the best individual that minimizes these errors.
It is also desirable to keep track of these errors so that they can be plotted obtaining the typical trend of genetic codes in which there is an error that decreases tending

to zero as generations pass with discontinuity jumps that may be caused by a crossover of the alleles of the individuals in the population or by a random mutation of one of the 5 genes in an individual as is shown in figure 4.1.

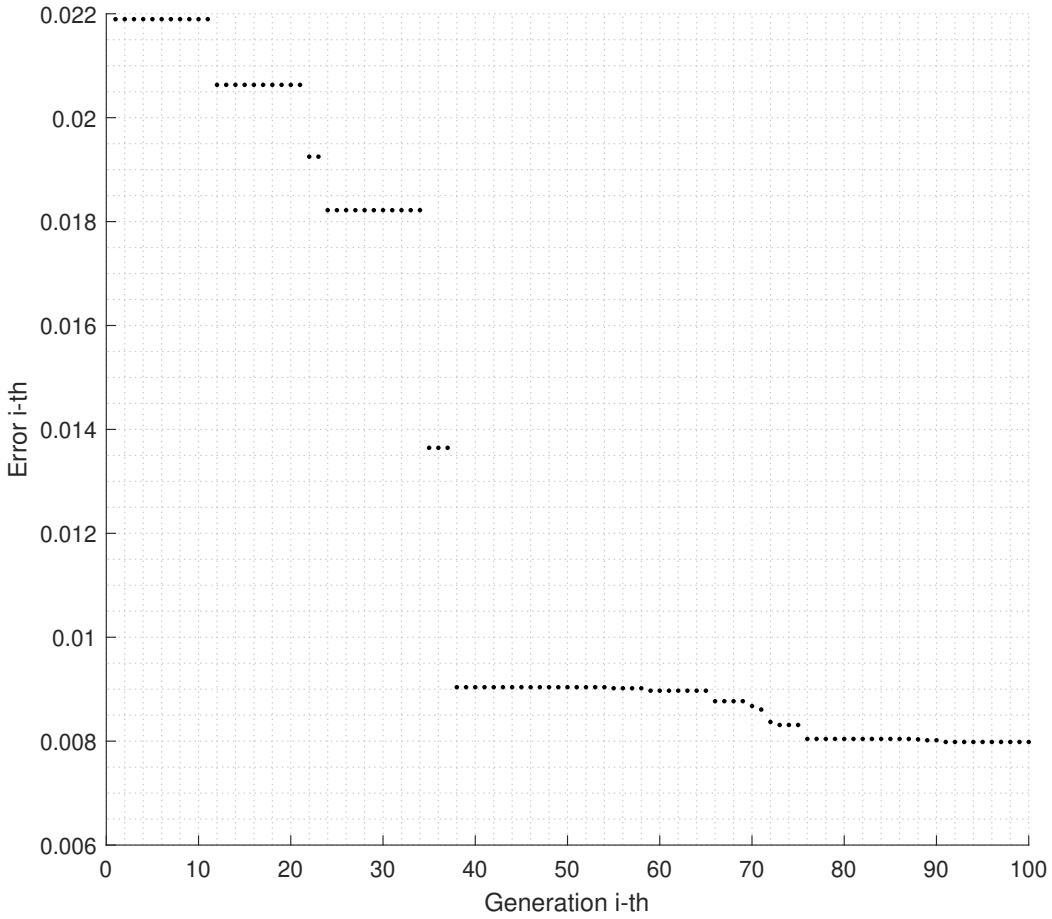

Figure 4.1: Error trend at different generations

Specifically, in the genetic algorithm implemented in this thesis work, it was fixed:

- a 50% probability of having a random mutation of one of the fifth genes in an individual,
- a probability of 30% of having a mutation by algebraic sum between the genes of two different individuals, i.e., that offspring are generated by an algebraic

sum of the parents' alleles (this solution helps to narrow down the search for the optimal solution more and more as if it were a true bisection method),

- a 70% probability of having a crossover, that is, that the offspring inherit one or more random genes from the father and the rest of the genes from the mother.

In addition, it was also chosen to generate $\frac{1}{4}$ of new random population at each generation both to have a well-distributed population avoiding the presence of similar individuals, and also because this allows the algorithm to be able to explore other parts of the universe in terms of combinations of the 5 parameters, so that it will be able to get out of a local minimum by evolving toward another local minimum perhaps characterized by a smaller error in absolute value.
In addition to keeping track of the error, the genetic algorithm is structured to plot, at each generation, the 5 alleles of the best individual according to the order $[\Delta V, \theta, \varphi, t_f, \Delta\theta]$ and the various errors that the final conditions (which are obtained by propagating the initial conditions defined by these 5 parameters) will have with respect to the target conditions, according to the following order:

- err1: represents the dimensionless difference between the norm of the vector containing the information about the final radius reached by the S/C and the norm of the target radius vector defined as $\frac{r_{SOI}}{DU}$.
  Having an err1 $\to 0$ means that the satellite have arrived at the boundaries of the SOI of Mars.

- err2: represents the dimensionless difference between the norm of the vector containing the information about the final velocity reached by the S/C and the V_∞.
  To also have an err2 $\to 0$ means that the satellite arrived at the boundaries of the SOI of Mars with exactly the modulus of the velocity it takes to make the Hohmann ellipse and return to Earth.

- err3: represents the ΔV relative to the initial conditions, so the genetic algorithm, given two initial conditions that meet the first two constraints, will tend to reward the one with the minimum ΔV.

Finally, the variable err will be defined as the sum of these two errors and will represent the main parameter to be tended to zero by the genetic algorithm.

4.1 Constraint on minimum distance to moons during flyby

A very important observation to make at this point is this: the parametric analysis that has been carried out predicts going to increase the mass of the moons of Mars up to as much as 7 orders of magnitude over their actual mass. It is obvious that in addition to simulating an increase in the μ parameter, an increase in the radii of the moons of Mars should also be simulated at the same time.
Strictly speaking, in fact, the term "moons" would not be correct since the value of their radii is $R_{Ph} = 11{,}267\,\text{km}$ and $R_{De} = 6{,}2\,\text{km}$, respectively; which is why it would be more appropriate to speak of asteroids. It is obvious, therefore, that a situation in which, for example, Phobos had a mass increased by 6 orders of magnitude, while maintaining the same actual radius value of just over 10 km, would not be realistic at all, since Phobos, under such conditions, would look more like a black hole than a moon.
It is good to emphasize this aspect because in the simplified model implemented in this work no assumption is made about how the radius of secondary and tertiary bodies varies as a function of the gravity parameter μ. However, two additional constraints have been inserted, which are not part of the definition of the error that the genetic algorithm will try to minimize[1], but which will allow for results consistent with the simplified model chosen. That is, constraints have been imposed on the minimum distance at which the probe can arrive in the vicinity of Phobos and Deimos during their respective flyby maneuvers: this minimum distance is defined as the respective scaled radius plus a safety coefficient consisting of 10% of the moon's radius. Thus the trajectory followed by the S/C will be able to pass at most a dimensional distance of 12,4 km from the center of mass of Phobos and 6,82 km from the center of mass of Deimos.

4.2 Optimal phasing

There is, however, another important consideration to make: analyzing the problem in the synodic reference system, one will have to impose that the angle θ_{Phobos} describing the angular position of Phobos along its circular orbit is always zero (by definition of a synodic system), so, the only variable that one could choose to vary would be the angle θ_{Deimos} describing the angular position of Deimos in its circular orbit.

[1] the goal is not to pass as close as possible to the moons of Mars during the flyby maneuvers, but rather to, once the initial conditions are set, pass at the right distance, such that the S/C arrives at the SOI of Mars with the right final velocity.

In reality, however, from the point of view of the synodic system, what matters is the variable Δ_θ defined as θ_{Deimos} - θ_{Phobos} because when this variable cancels out (i.e., when Phobos and Deimos are along the same line conjunct) it will mean that it will be possible to have a launch window.
For this reason, a study was first conducted to measure how many times during the course of a year the situation $\Delta\theta = 0$ occurs: the results are shown in the graph 4.2, which illustrates that, given the angular velocities of Phobos and Deimos, the optimal phasing condition occurs 855 in a year, i.e., more than twice a day.

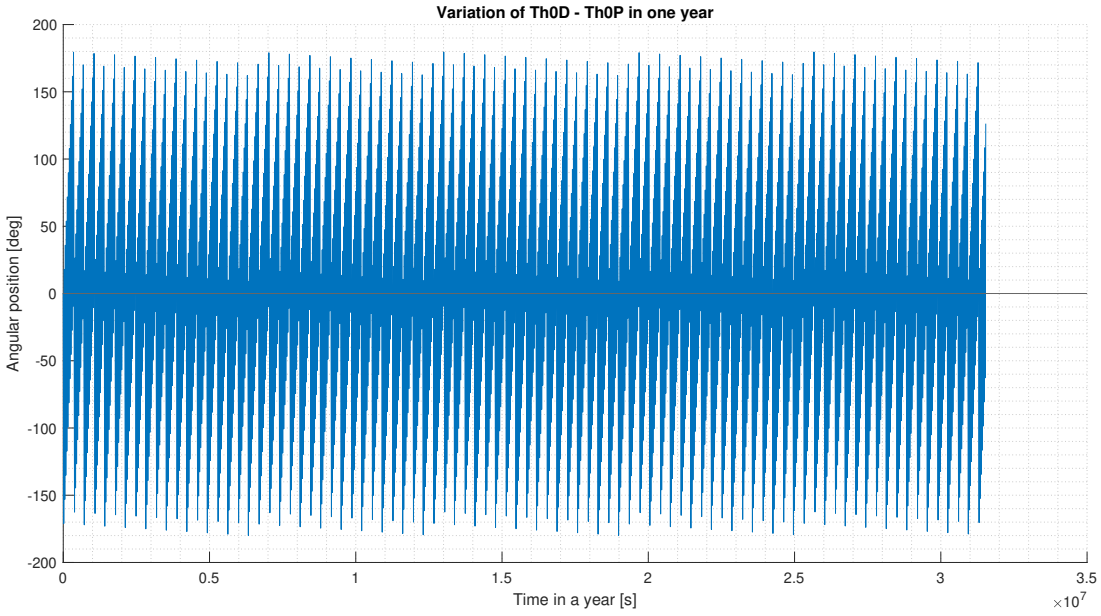

Figure 4.2: Launch windows in the synodic system

In this way, it is possible to justify the assumption, which will be adopted throughout this paper, of optimal phasing, for the trajectories that will be shown in the chapter 5, avoiding adding an additional constraint on the direction of the exit velocity once the S/C has reached the Mars SOI.

Chapter 5

Mars-Phobos-Deimos Results

This chapter will report the results obtained through the modeling of the Mars-Phobos-Deimos system in the *Matlab* environment and the implementation of the genetic algorithm analyzed in the chapter 4 and the four-body model analyzed in Refs. [29, 30].
Specifically, the genetic algorithm generates random initial conditions (but always within each established range of values for individual alleles) that are then integrated over time, providing the final conditions on which constraints are imposed. The task of the genetic algorithm will be precisely to find the trajectory, described by one of many random initial conditions, characterized by an error (defined in detail in chapter 4) that is the minimum possible value.
Therefore, to help in the convergence of the model, it is appropriate to choose appropriate initial guesses, that is, to define what are the ranges of values within which the genetic algorithm is free to generate random values.
In particular, these limits are defined as follows:

- The ΔV can take random values between 0 and 2 km/s, so as to eliminate all possible solutions characterized by a $\Delta V > 2\,\mathrm{km/s}$.
- The θ can take on random values between 220° and 320°, this range of values is due to the fact that the ΔV will be given tangentially, and therefore at 90° relative to the angular position at which the impulse occurs, so if one want to move toward Phobos which is at $\xi = 1$ it is possible to conclude that the impulse must be given more or less when the S/C will be in this range of angular positions.
- the φ can vary only between $-5°$ and 5°, this narrow range is due to the fact that one actually already know that the minimum ΔV will occur if the trajectory is planar so it must have $\varphi = 0$.

- regarding the dimensionless time taken by the probe to complete the trajectory, having initially no idea how long it would actually take, a fairly wide range was defined between 2π (i.e., the amount of dimensionless time taken by Phobos to complete a 360° turn around Mars) and 40π.

The trajectories that will be analyzed will be classified into four different categories:

1. Direct hyperbolic escape maneuvers,
2. Assisted escape maneuvers through the flyby of Phobos,
3. Assisted escape maneuvers through the flyby of Deimos,
4. Assisted escape maneuvers through the combined flyby of Phobos and Deimos.

The results will be presented both in graphical form through the appropriate plots (trajectories will be shown in both the synodic and inertial systems so as to compare not only the trajectory itself but also the positions of the tertiary bodies during the various flyby maneuvers) and in schematic form through the tables 5.1 and 5.2 that summarize, respectively, the optimal initial conditions that integrated over time allow for that particular trajectory and the errors in terms of the position vector (err1) and modulus (err2) of the velocity vector.
The planar trajectories described by the EOMs of the *PBCR4BP* will be shown in both the synodic and inertial systems, so as both to get a complete and as detailed as possible view into the trajectory traversed by the S/C and to make a comparison between the two reference systems.
In the plots, the dimensions of Mars are those actually possessed by the red planet (only dimensionalized with respect to DU) while the dimensions of Phobos and Deimos were voluntarily increased to make their positions visible during trajectory propagation.

5.1 Best direct escape

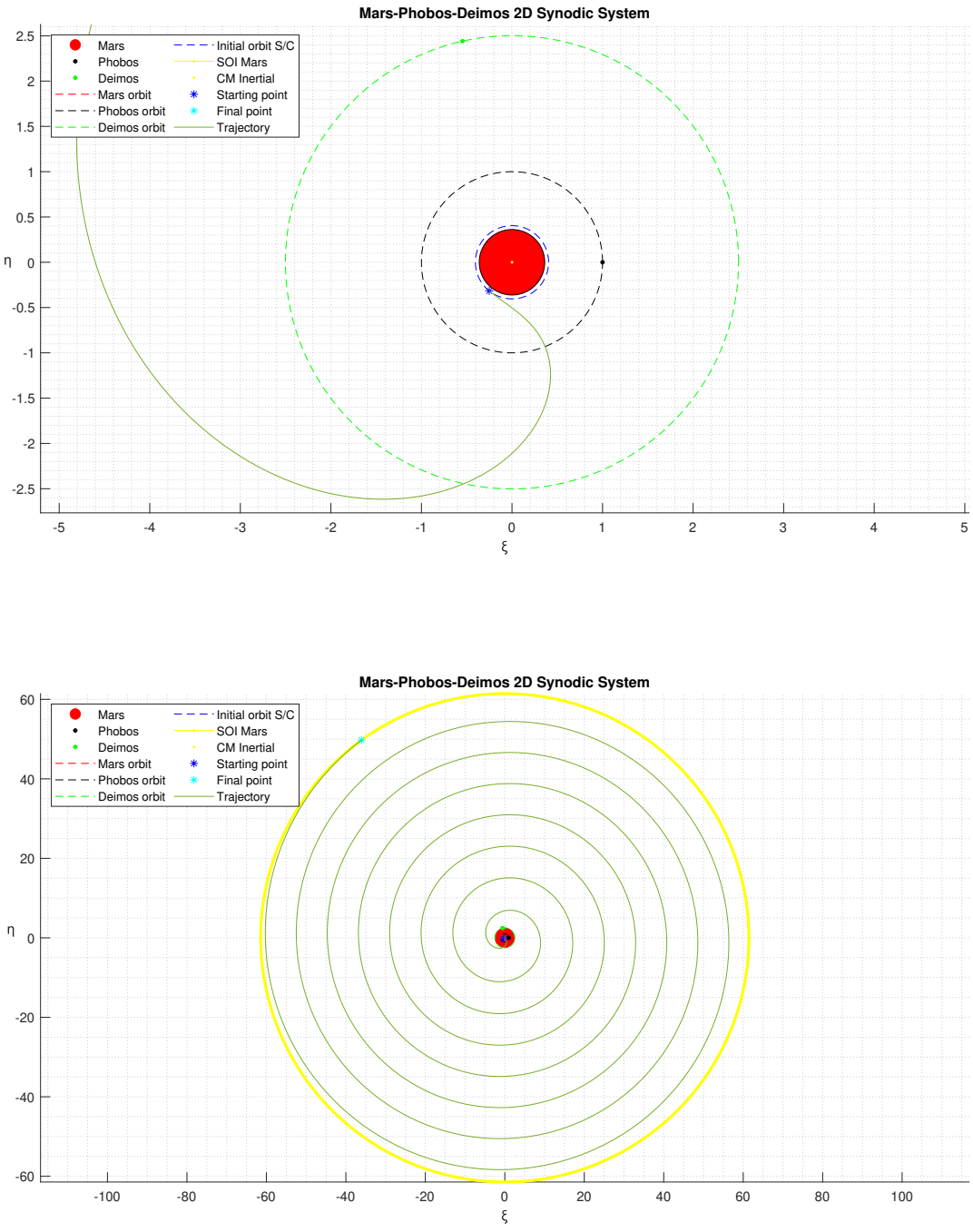

Figure 5.1: Mars-Phobos-Deimos synodic system direct escape

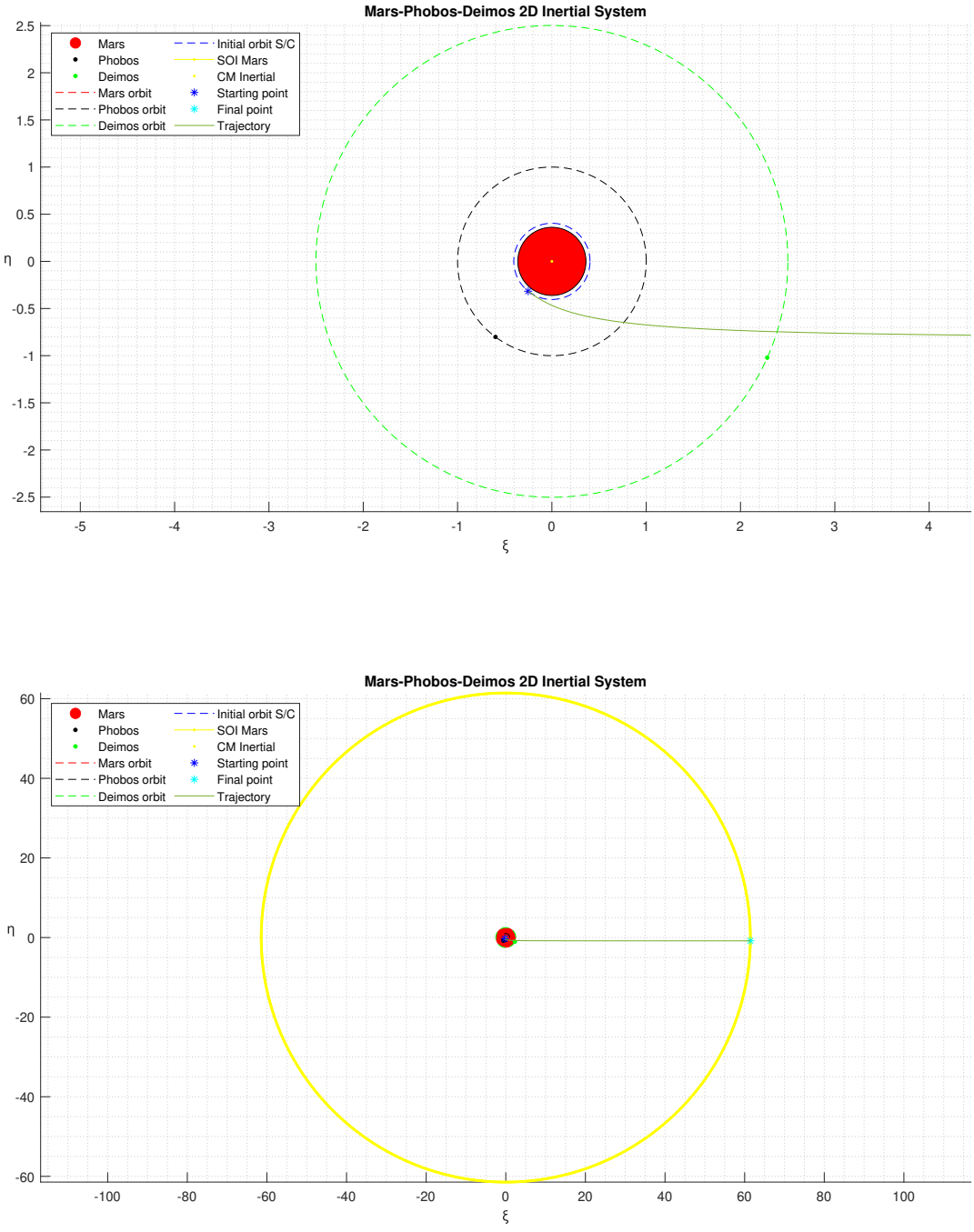

Figure 5.2: Mars-Phobos-Deimos inertial system direct escape

As can be visualized of the plots in Figs. 5.1 and 5.2, as well as from the table 5.1, the optimal direct escape trajectory is obtained by providing a ΔV of 1,2036 km/s in the tangential direction when the S/C is at an angular distance of 231,54°. The trajectory has a dimensionless duration equal to the time it takes Phobos to make a rotation of 48.054 radians around Mars; this means that, since Phobos has an angular velocity of equal to ω_{syn}, it will take the probe $2{,}1088 \times 10^5$ s to arrive at the SOI boundaries of Mars, which is about 58 hours and 48 minutes. On the other hand, from the table 5.2 it is possible to visualize how well the genetic algorithm worked, talking about an overall error of the order of 1×10^{-10} so it is possible to conclude that the trajectory described by the S/C will very accurately meet all constraints listed in chapter 4, representing a very reliable trajectory. Moreover, the intent of the next two figures is to show the flyby maneuvers with Phobos and Deimos, not graphically, as was done above, but this time from a point of view of both energy and velocity possessed by the space probe.
Thus is presented in the figure 5.3 what will be the reference graph, that is, the trend of velocities (along x-axis, along y-axis and the absolute value) in the inertial reference system that the S/C possesses during its trajectory. As a first thing, however, it must be specified that there is talk about dimensionless velocities; the horizontal asymptote represents in fact the dimensionless value of V_∞, i.e.:

$$\frac{V_\infty}{VU} = \frac{2.6490}{2.1370} = 1.2396 \tag{5.1}$$

The two vertical lines in green, on the other hand, represent the time instants during which the probe is at its minimum distance from, respectively, Phobos and Deimos. This is a very useful piece of information, as it is precisely at these temporal instants that, in cases where flyby maneuvers with the moons of Mars will be analyzed, the velocity possessed by the space probe will undergo a sudden change, an unmistakable sign of the interaction between the probe and the moons of Mars. In the case of Figure 5.3, however, it can be seen that there was no interaction, as is to be expected from a direct escape maneuver.

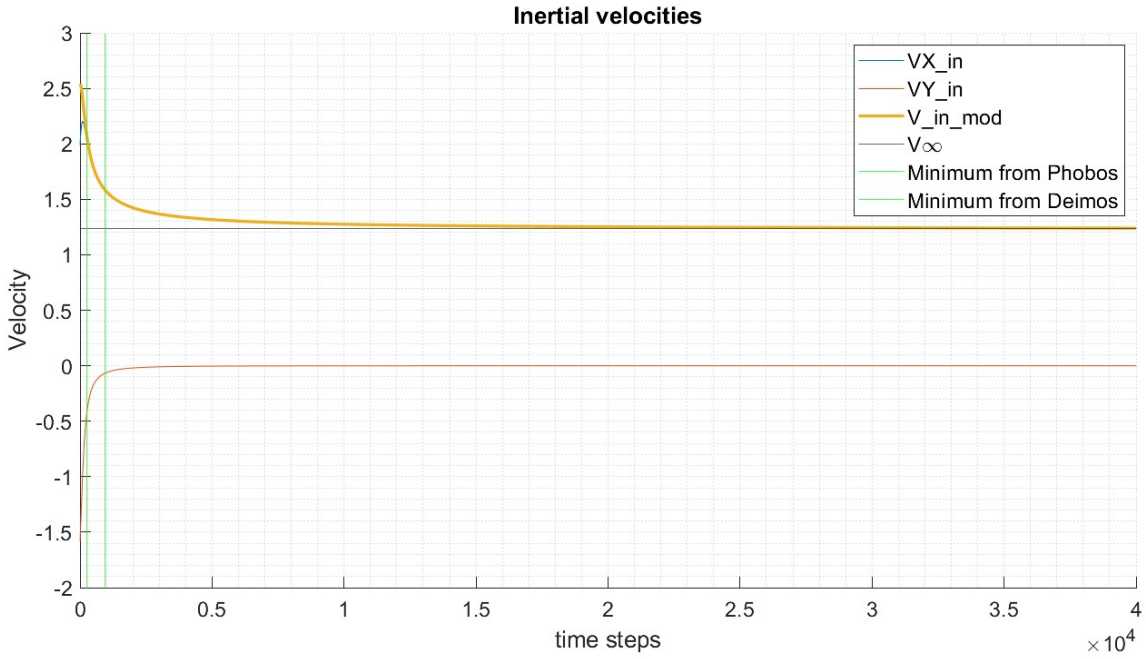

Figure 5.3: Best Direct Escape - Inertial velocities

For a complete understanding of the trajectory, the next figures also show the energy trend of the trajectory followed by the S/C. In a two-body model, the energy of a trajectory remains constant; in this case, however, having implemented a four-body model, a perturbation can be expected, which, as shown by Figure 5.4, concerns the sixth decimal place (to give an example that is as concrete as possible, this is the same order of magnitude as the perturbative action that the Sun has toward a satellite that is at an Earth-Sun distance from the latter), demonstrating how microscopic Phobos and Deimos are and how their gravitational effects are insignificant but still measurable.
The gravitational interaction between the satellite and the moons of Mars can also be appreciated from an energy point of view, as the energy trend graphs will show in cases where flyby maneuvers with one or both moons of Mars will be analyzed. Specifically, these graphs refer to the flyby maneuvers previously discussed, energy is calculated using the equation 2.24, using the norm of the dimensional velocity evaluated in the inertial system, the norm of the vector radius also dimensional and evaluated in the inertial system, and using the dimensional value of Mars' gravitational parameter as the μ parameter. On the other hand, with regard to the energy trend in the figure 5.4 it can be seen that, apart from small perturbations, there are no major variations, as can be expected from a direct escape maneuver.

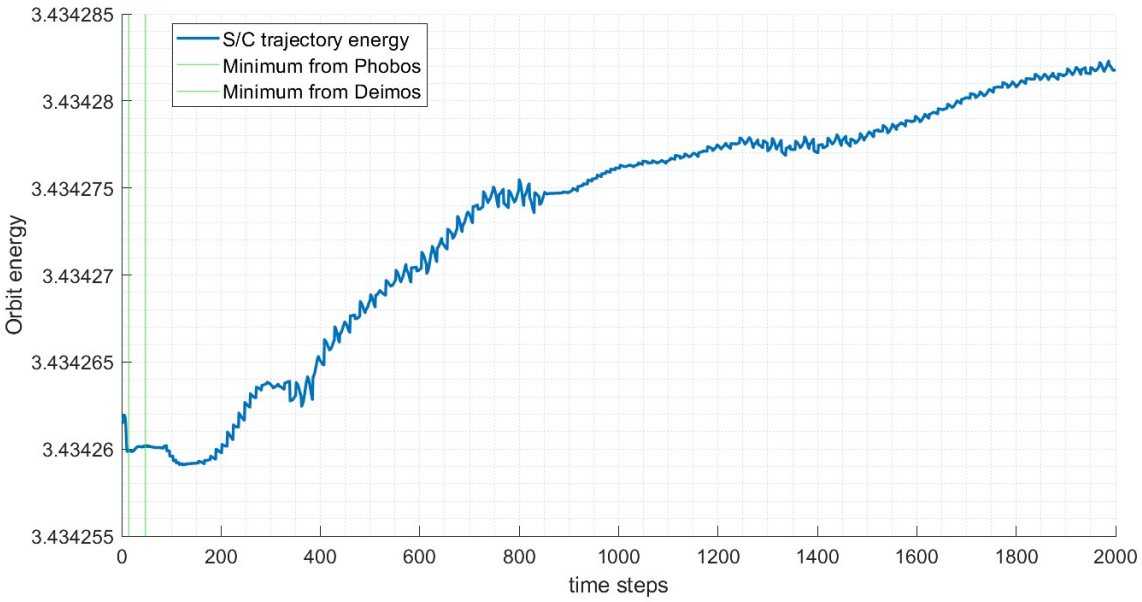

Figure 5.4: Best Direct Escape - Energy plot

5.2 Best Phobos flyby

Regarding the flyby with Phobos and Deimos, it is important to point out at the outset that the study conducted has shown how the gravitational assist effect of both of Mars' moons is absolutely negligible: Indeed, by modifying only the θ angle in an appropriate way such that a flyby of one or the other satellite is implemented, the result in terms of ΔV does not change, and the reason is due to the fact that, as can already be easily guessed, they are too unmassive to actually change the trajectory described by the probe in a non-negligible way.
For this reason, it was decided to conduct a parametric analysis by implementing a flyby maneuver by going from time to time to increase the effective mass of Phobos and Deimos by an order of magnitude, so that it will be possible to estimate what the order of magnitude of a planet's moons should be in order to actually gravitationally exploit them profitably. Although the mass of Phobos and Deimos will be increased, no consideration will be given instead to the size of Mars' moons, which will be regarded as dots and not as three-dimensional spherical bodies in flyby maneuvers.
Furthermore, it should be explained that in order to implement the flyby maneuver it will be necessary to act on two fundamental parameters:

1. Vary appropriately the angle θ that establishes the angular position in the

plane from which to start the S/C trajectory,

2. Vary appropriately the angle θ_{Phobos} and θ_{Deimos} representing, respectively, the angular distance measured counterclockwise with respect to the ε axis from which to start the two Mars moons so that, defined by their angular velocity, they meet the probe at the exact moment it passes through their circular orbit.

Obviously, these two angles will be defined in the inertial system, where both Phobos and Deimos rotate with their respective non-zero angular velocity, while in the synodic system, which is the reference system in which the EOMs of the *PBCR4BP* are solved, θ_{Phobos} will always be zero while for Deimos it will be important to define the difference $\theta_{Phobos} - \theta_{Deimos}$.
At the code level, the case $\theta_{Phobos} \neq 0$, which can be implemented in the inertial system, may in fact be misleading since it cannot have a mirror counterpart in the synodic system, since in the latter reference system Phobos will be located at any time instant at an angle $\theta_{Phobos} = 0$.
The optimal phasing hypothesis thus allows not only to simplify the problem by setting the variable θ_{Phobos} to zero in both reference systems but also to eliminate the parallelism constrain between the final velocity vector possessed by the S/C at the end of the integration time and the vector $\vec{V_\infty}$: without the optimal phasing hypothesis, in fact, the direction of the $\vec{V_\infty}$ vector in the heliocentric system would depend on the day of the year on which the space probe arrives at the Mars SOI, and consequently further study should be done to identify which launch windows are possible to meet this parallelism constraint.
As can be easily seen from the summary table 5.1, the flyby maneuver with Phobos has negligible effects up to the case with 5 orders of magnitude more than the satellite's real mass, while the significant cases would result if Phobos had a mass 5 and 6 orders of magnitude more, respectively (trajectories FBPh5 and FBPh6). This shows conclusively that in a real case a flyby maneuver with Phobos would be completely useless, due to the fact that its real mass turns out to be too low to gravitationally accelerate the probe.
In this context, the FBPh6 trajectory will be analyzed in detail, that is, the one that would occur if Phobos had a mass 6 orders of magnitude greater than it actually possessed. It is obvious that the more one increase the orders of magnitude the greater the gravitational assistance effect Phobos can offer to the probe, yet, it is good to emphasize the fact that the mass of the moons must never be greater than 25% of the mass possessed by the primary body, otherwise the concept of secondary and tertiary bodies and consequently the concept of the Mars-Phobos-Deimos system itself would be lost. For this reason, during the parametric analysis it would not make sense to go beyond the case described by the FBPh6 trajectory: the case

in which the mass of Phobos was increased by 6 orders of magnitude would in fact mean having a secondary body with a mass of the same order of magnitude as the mass of the primary body (1×10^{23} kg) in this case, causing the hypotheses of *PBCR4BP* themselves to lapse.
In particular, the FBPh6 maneuver makes it possible to arrive at the boundaries of the Mars SOI by spending a ΔV of 0,6711 km/s compared to the 1,2036 km/s of the direct escape, which means a more than significant savings of about 0,53 km/s. At this point, it would be easy to use the Tsiolkovsky rocket equation to estimate in a first approximation the amount of propellant consumed in one case and in the other: the savings in terms of propellant used will, of course, depend on the type of propellant adopted and the initial mass of the rocket.
It is possible to visualize such a maneuver either in the synodic system (figure 5.6) or in the inertial system (figure 5.7). In both cases, four subplots representing the Mars-Phobos-Deimos system "photographed" at different time instants are first shown: top left at the initial instant when the pulse is provided, top right at the temporal instant when the S/C has the shortest distance to Phobos, bottom left at the temporal instant when the S/C has the shortest distance to Deimos, and, finally, bottom right at the final instant when, that is, the S/C has reached the SOI of Mars. Next, a zoom of the trajectory is also depicted so that it is possible to visulize in detail how the trajectory followed by the probe is deflected due to the gravitational effect of Phobos.
In this ideal case in which Phobos is assumed to have a mass of $1{,}08 \times 10^{23}$ kg (i.e., 6 orders of magnitude more than its actual mass) the S/C will therefore have to give a tangential impulse of 0,6711 km/s at an angular distance of 287,15°, so as to implement a flyby maneuver from behind with Phobos that will see it, at its point of minimum relative distance, approach Mars' satellite to a minimum distance of 357 km (as is shown by fig 5.5) from its surface.
Finally, it is possible to see that the time taken for the probe to get to the SOI of Mars by implementing this flyby maneuver with Phobos is about the same as the time taken in the direct escape case, a consequence of the fact that the S/C on the one hand will start its trajectory with a lower ΔV of slightly more than half that of the direct escape, so it will initially be slower and will have to lengthen its trajectory so as to pass purposely close enough to Phobos at the right time instant but on the other hand it will also be accelerated in a free manner having implemented a flyby from behind the satellite, so it is possible to conclude that the two effects cancel each other out.
To get as complete a view as possible, it is also good to keep track of the evolution of various quantities during the propagation of the trajectory, particularly in Figure 5.5 it is possible to keep track of the relative distance between the position of the space probe that will propagate from the LMO to the SOI of Mars and the position

of Phobos and Deimos moving instead within their circular orbits around Mars, so that it is possible to easily identify the time instant at which the point of minimum distance with the moons of Mars occurs.

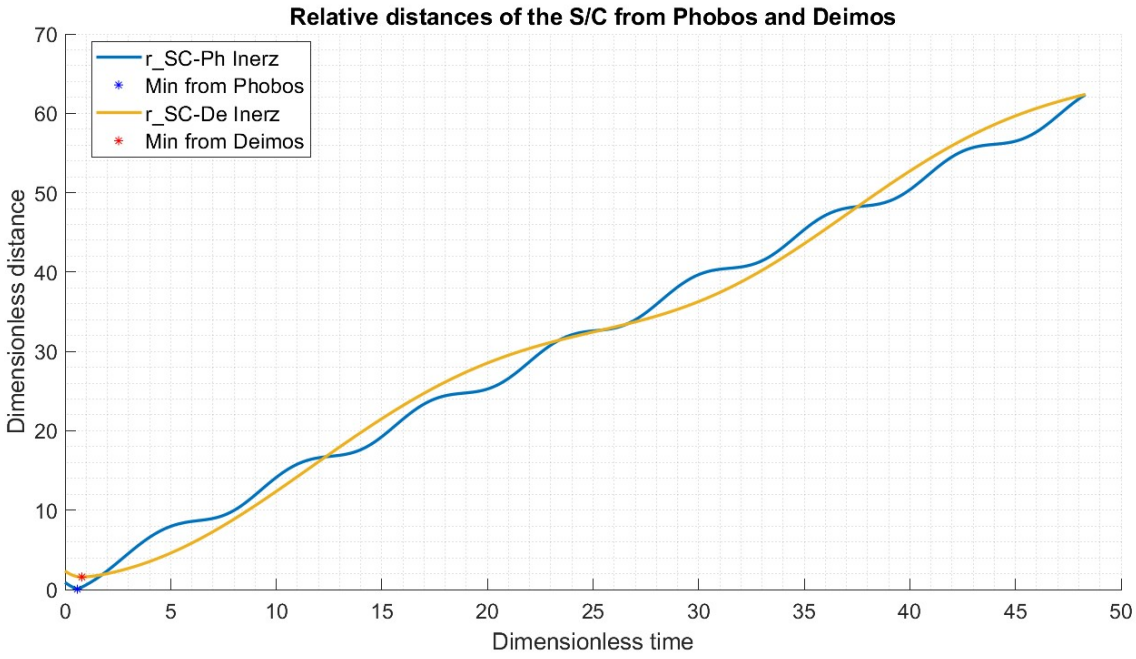

Figure 5.5: Relative distance between the probe and Phobos/Deimos

Other quantities to be taken into account are then the trend of the velocity possessed by the S/C and the trend of its energy: the implementation of the flyby maneuver in fact, in addition to being visualized in graphic form through the appropriate graphs, can also be perceived without visualizing the actual trend of the trajectory. In fact, the interaction between the probe and the moons of Mars has consequences in terms of both velocity and energy that are manifested in the form of peaks or strong variations in these quantities near the time instant at which this interaction occurs.

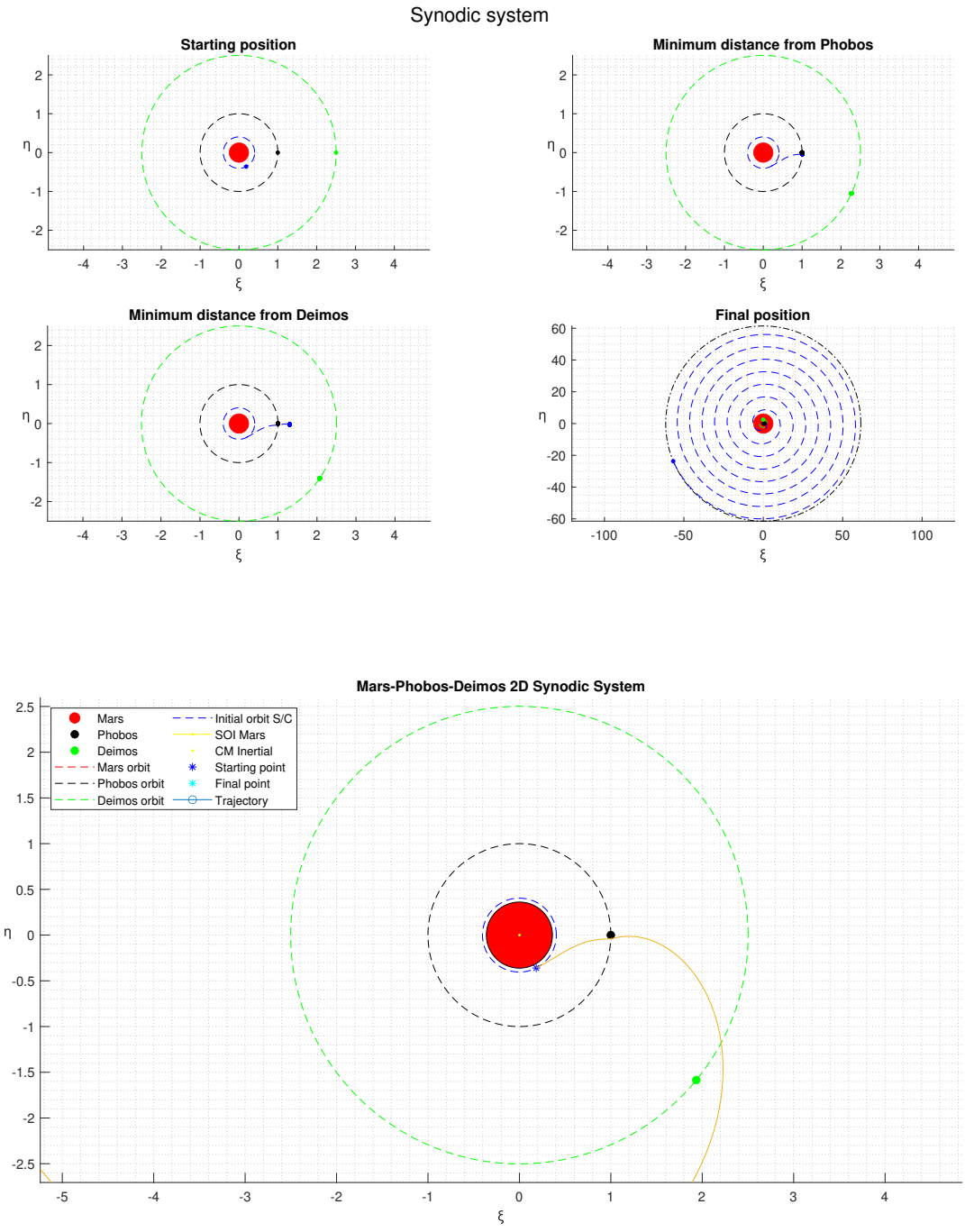

Figure 5.6: Synodic FBPh6

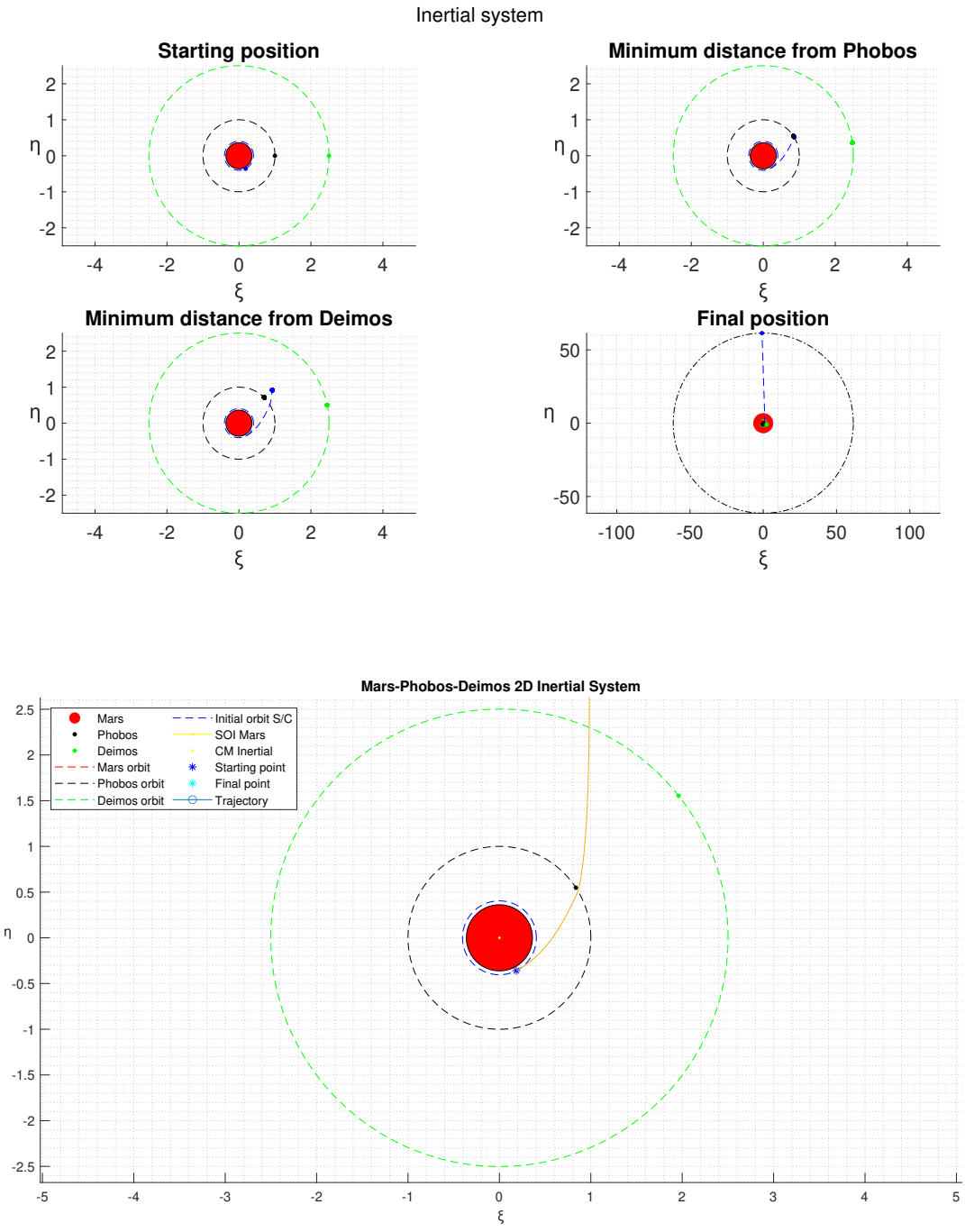

Figure 5.7: Inertial FBPh6

The next two graphs show the entire trend, respectively of velocity (5.8) and energy (5.9), related to the trajectory followed by the space probe (left), and a zoom (right) of the same graph is also shown, so as to have a clearer and more detailed view of the interaction that occurred during the flyby, which can be visualized through the presence of peaks in the variables involved.

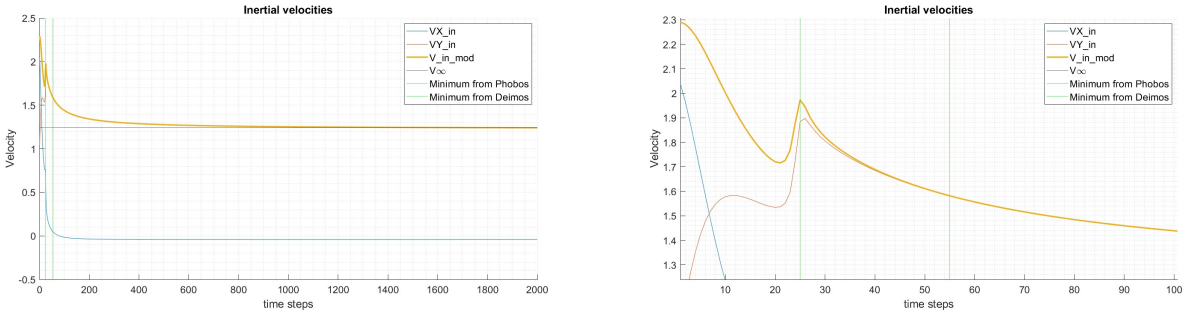

(a) **(b)**

Figure 5.8: Best Phobos Flyby FBPh6 - Inertial velocities

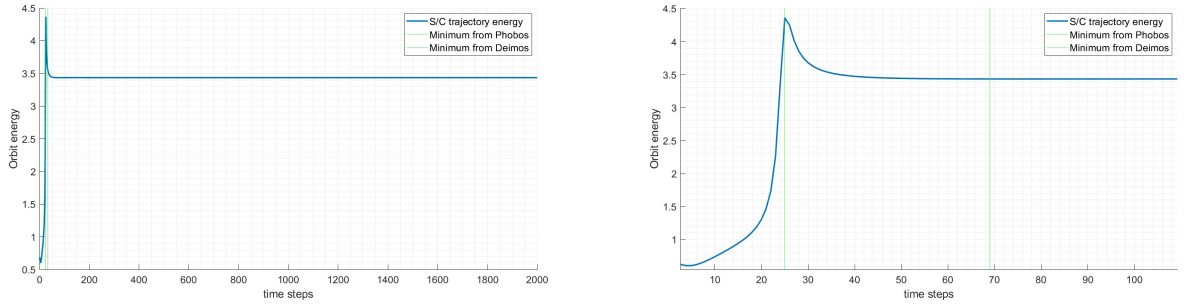

(a) **(b)**

Figure 5.9: Best Phobos Flyby FBPh6 - Energy plot

5.3 Best Deimos flyby

Concerning the flyby maneuver with Deimos, the trajectory FBDe7 (corresponding to the ideal case in which Deimos had a mass 7 orders of magnitude more than its actual mass) will be analyzed in more detail. Again, it is possible to visualize the trajectory both in the synodic system (figure 5.11) and in the inertial system (figure 5.12). As can be visualized from the table 5.1, the best possible case is implemented by giving an impulse in the tangential direction equal to 0,8032 km/s when the S/C is at an angular distance equal to 263,69°, allowing a savings in terms of ΔV of about 0,4 km/s compared to the direct escape maneuver.
This propellant savings is achieved at the expense of a slightly longer trajectory duration of $2{,}1766 \times 10^5$ s, i.e., about 60 hours and 26 minutes.
Specifically, again there will be a flyby of Deimos from behind in which the probe will arrive at a minimum distance of 503 km from the satellite's surface as it can be seen in Figure 5.10 showing the dimensionless relative distance between the S/C and the moons of Mars.

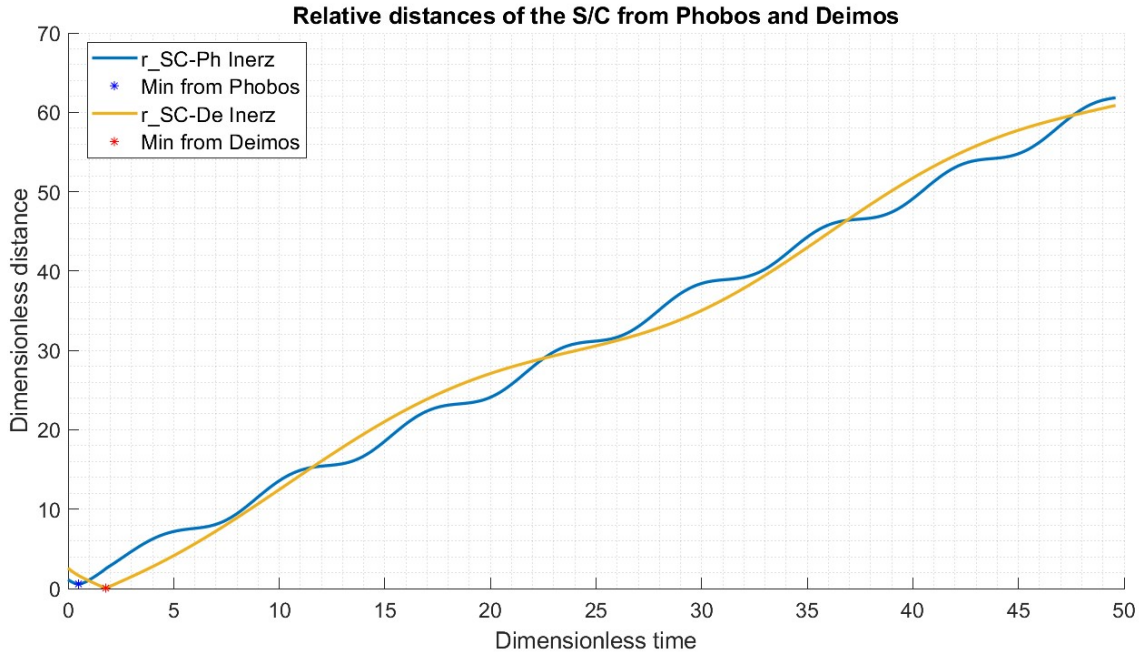

Figure 5.10: Relative distance between the probe and Phobos/Deimos

This information, as well as in the case of the flyby of Phobos analyzed above, must however be taken with caution since analyzing a nonreal case in which, in order to visualize the gravitational effects of the Mars moons, the aim is to intentionally increase their mass so that the trajectory followed by the probe can actually be

curved in the vicinity of their presence but no assumption has been made about the size in terms of radius that Phobos and Deimos should have as a result of having fictitiously acquired mass. Strictly speaking, in fact, one would have to specify that the minimum relative distances between the S/C and Phobos/Deimos (357 km and 503 km, respectively) refer, not so much to their surface, but to their center of mass, so logically these values should be subtracted from the value in kilometers in radius that Phobos and Deimos would have if they actually had a mass of $1{,}08 \times 10^{22}$ kg and 2×10^{22} kg.
Since the aspect related to how the radius value of both moons of Mars would increase as their masses increase as the parametric analysis proceeds in this thesis work has not been considered, in order to obtain a model consistent with the assumptions that have been made, two additional constraints related to the minimum allowable distance at which the space probe can arrive in the vicinity of Phobos and Deimos have been imposed, and this minimum distance has been imposed as respectively the value of their true radius (i.e. 11,26 km in the case of Phobos and 6,2 km in the case of Deimos) plus a 10% of the value of their radius as a safety coefficient.
Because of the microscopic value of their radii, in fact, Phobos and Deimos would be assimilated to two asteroids and the definition of 'moons' of Mars would not be so appropriate given their real size. In the various figures presented in this paper, however, the choice has been made to make their positions in the various time steps easily visible, consciously increasing their sizes relative to those they actually possessed; this choice was necessary due to the fact that the trajectory plots show dimensionless magnitudes so that if the choice of representing Phobos and Deimos with their real sizes had been carried forward, they would have turned out to be too small to allow their visualization in terms of position.

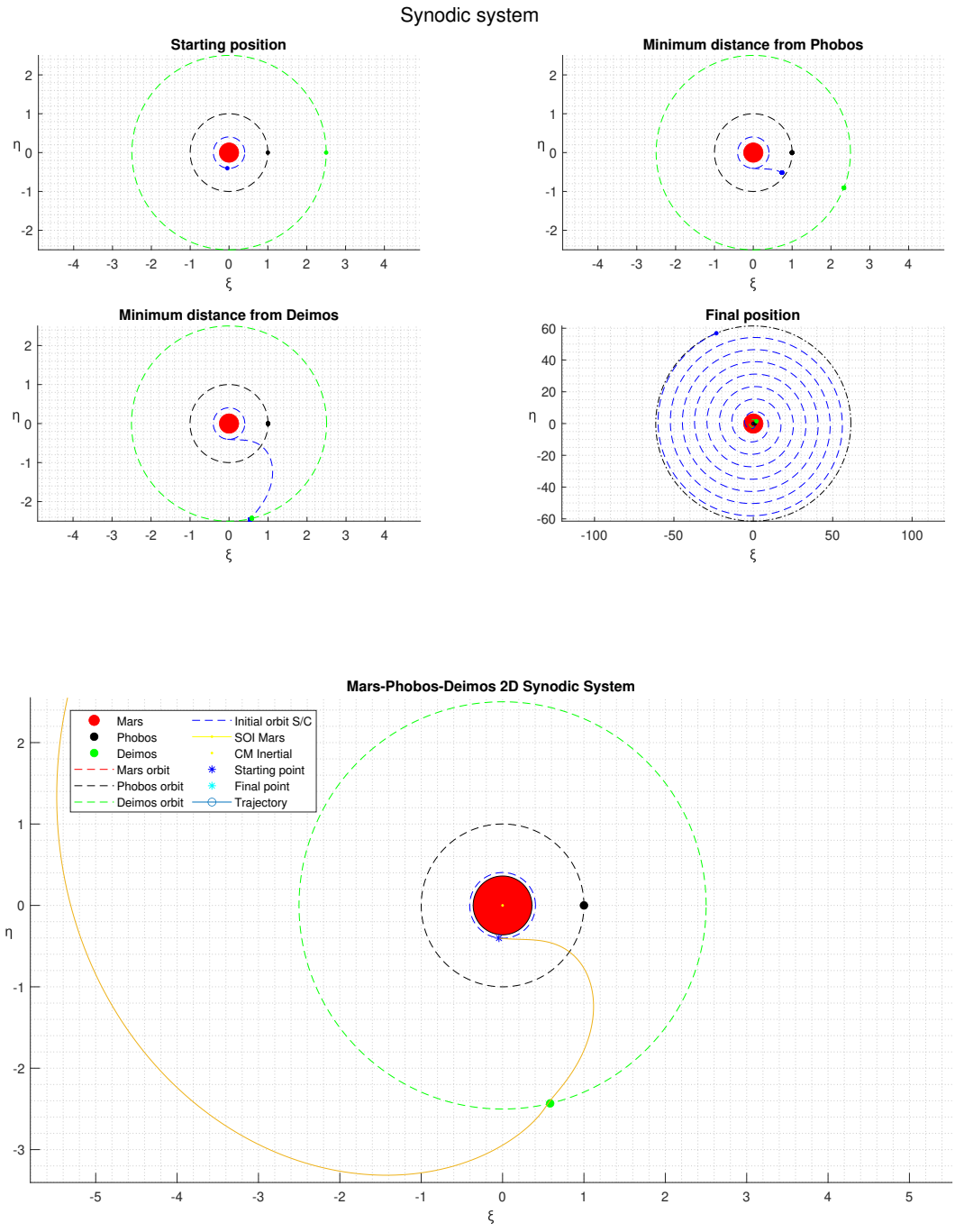

Figure 5.11: Synodic FBDe7

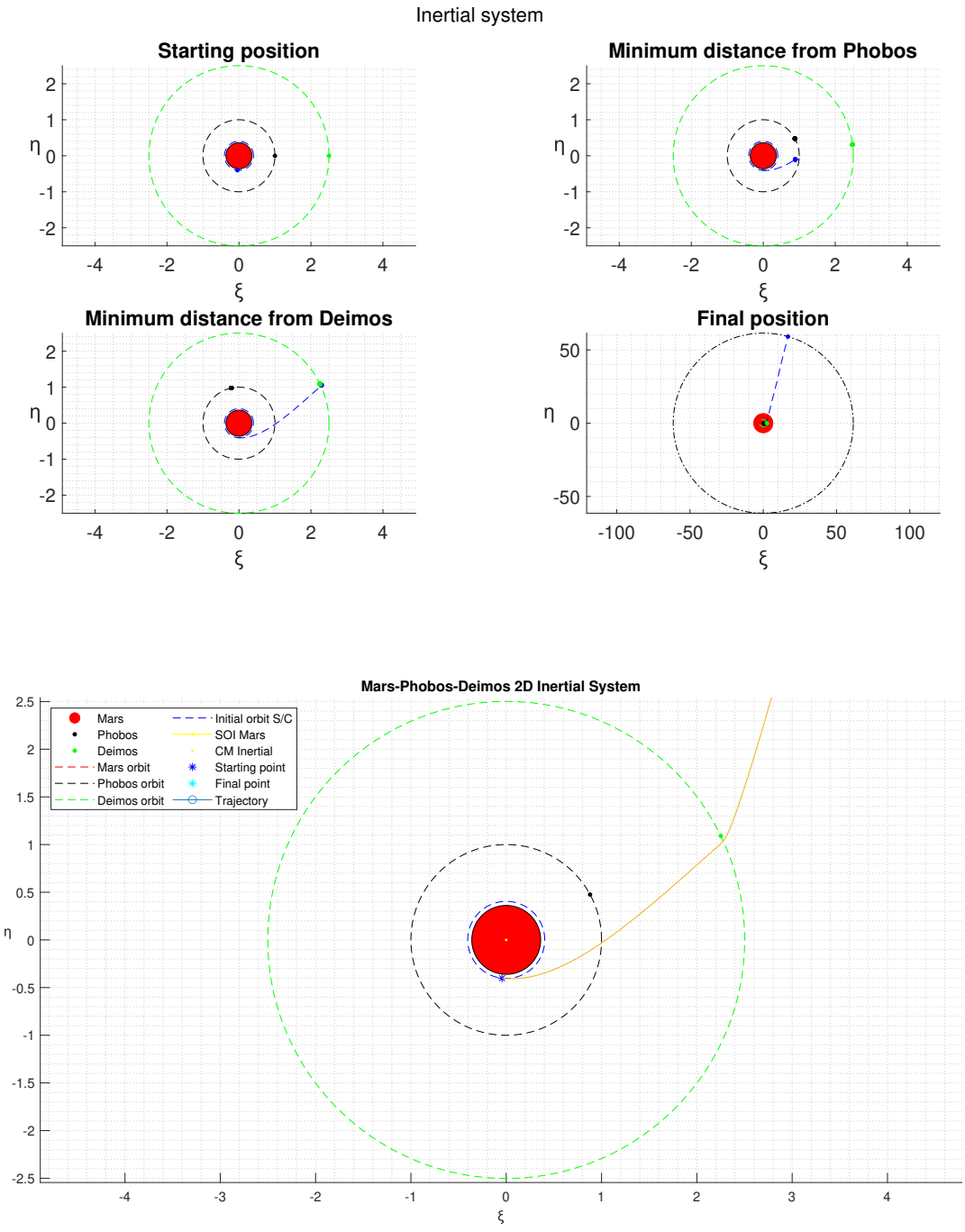

Figure 5.12: Inertial FBDe7

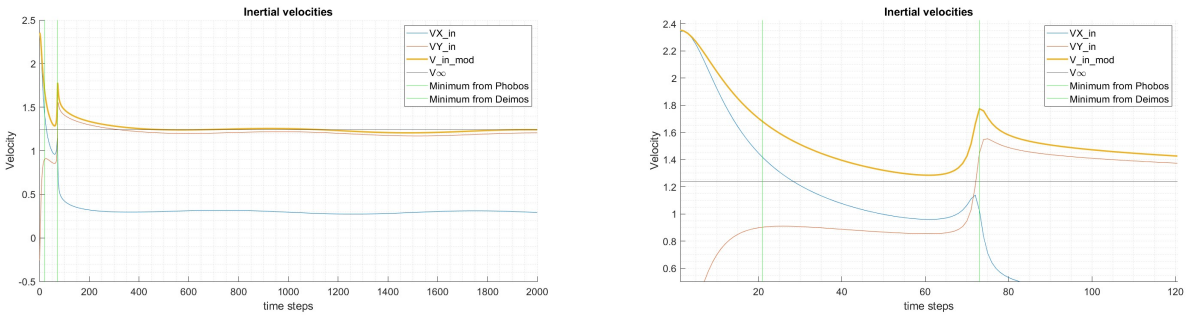

(a) **(b)**

Figure 5.13: Best Deimos Flyby FBDe7 - Inertial velocities

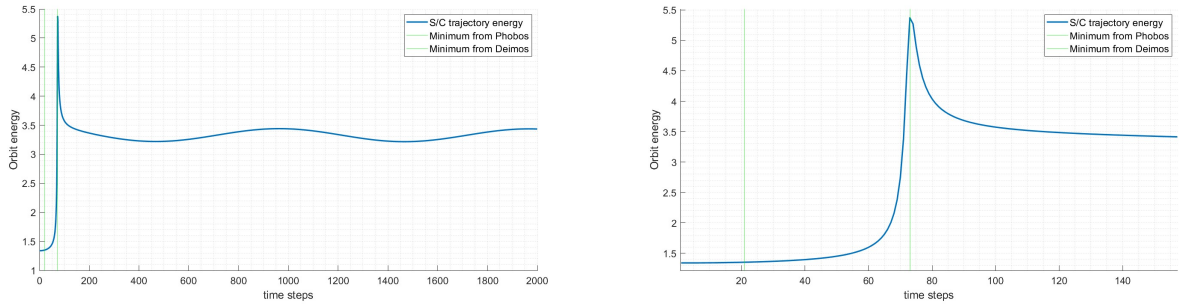

(a) **(b)**

Figure 5.14: Best Deimos Flyby FBDe7 - Energy plot

5.4 Best combined flyby

In this section, the combined flyby maneuver with both of Mars' moons is shown and analyzed. In order to implement this maneuver, an initial angle θ_{Phobos} equal to 0° and an initial angle θ_{Deimos} equal to 61° was imposed so that the trajectory followed by the S/C and curved by the Phobos flyby could also pass in the vicinity of Deimos. In addition, following the parametric study implemented for the individual flybys, it was decided to combine the FBPh6 and FBDe7 cases. As can be visualized from the summary table 5.1 the optimal case is obtained by generating a tangential pulse equal to 0,6275 km/s when the S/C is at an angular position of 298,61°: the first flyby will take place from behind with Phobos greatly accelerating the probe as the latter will pass, at its point of minimum distance from the satellite, at a distance equal to 34 km (fig 5.15) from its surface; subsequently, the second flyby with Deimos will instead occur from in front, so in this case

Deimos will decelerate the S/C, which, at its point of minimum distance, will be at a distance equal to 340 km from its surface. The fact that this is a flyby first from behind to accelerate and then from in front to brake should not be surprising since the goal of the mission is not only to arrive at the boundaries of the SOI of Mars, but also to get there with the right velocity in terms of modulus, which is why it is necessary for Deimos to slow down the S/C to allow it to arrive at the SOI with exactly the modulus of V_∞.
Finally, it is important to remind that for a better understanding of the figure 5.15 to obtain the dimensional distance expressed in kilometers one has to multiply the corresponding dimensionless value by the DU, while to obtain the dimensional time expressed in seconds one has to divide the corresponding dimensionless value by the angular velocity (expressed in radians per second) characteristic of the Mars-Phobos ω_{syn} synodic system.

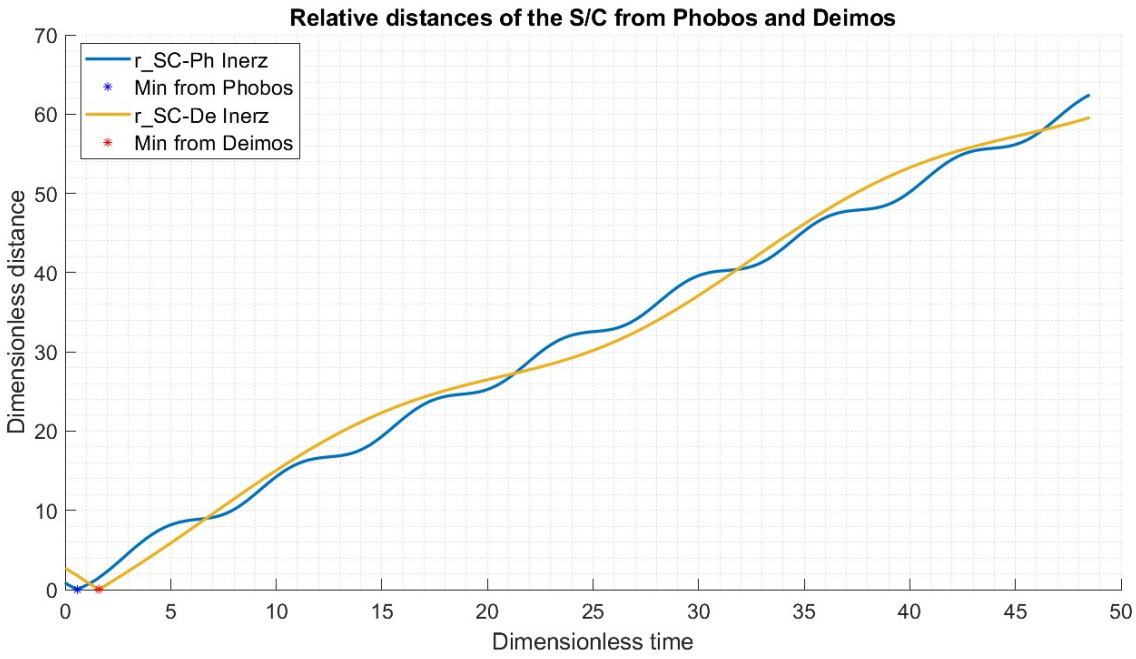

Figure 5.15: Relative distance between the probe and Phobos/Deimos

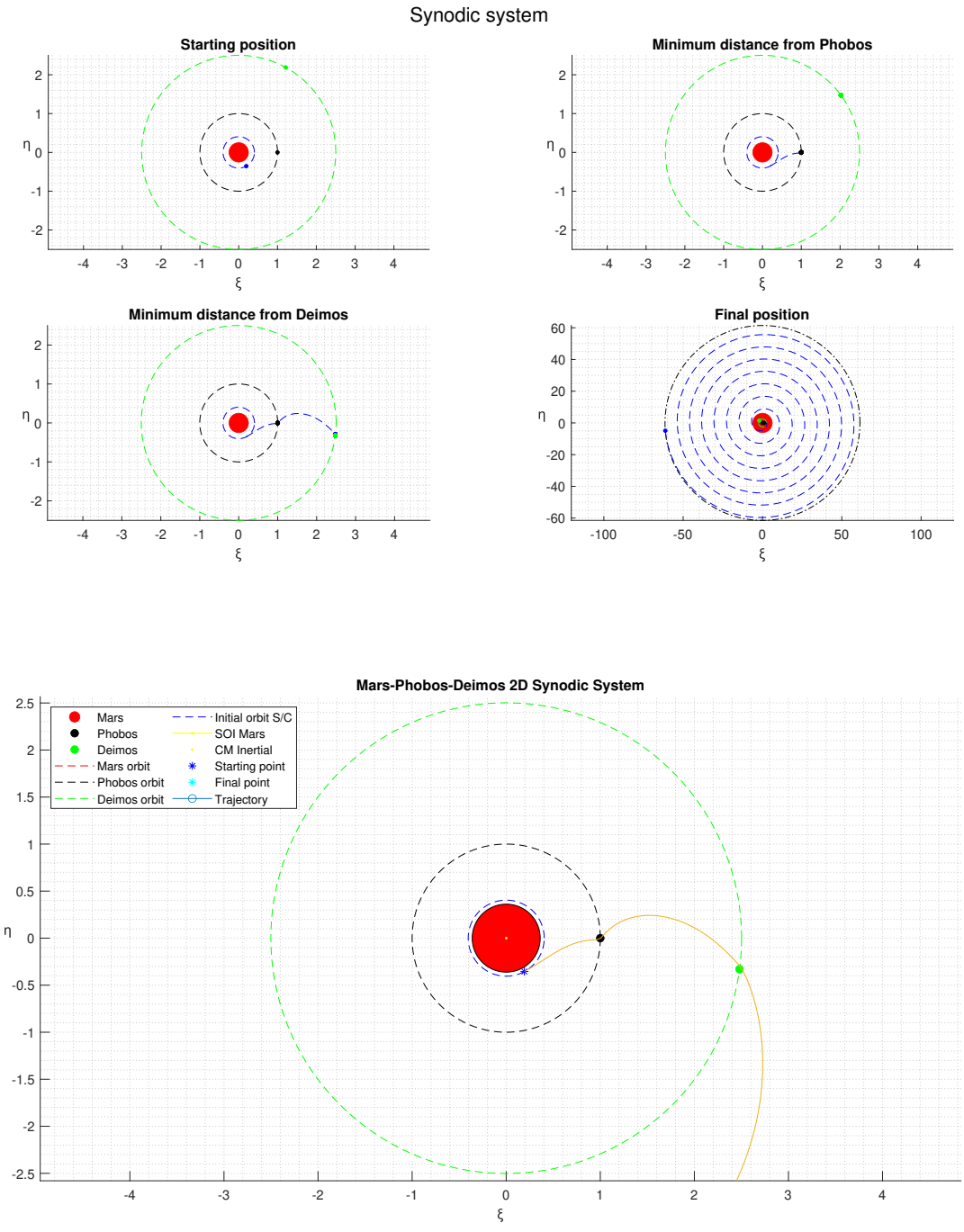

Figure 5.16: Synodic BCFB

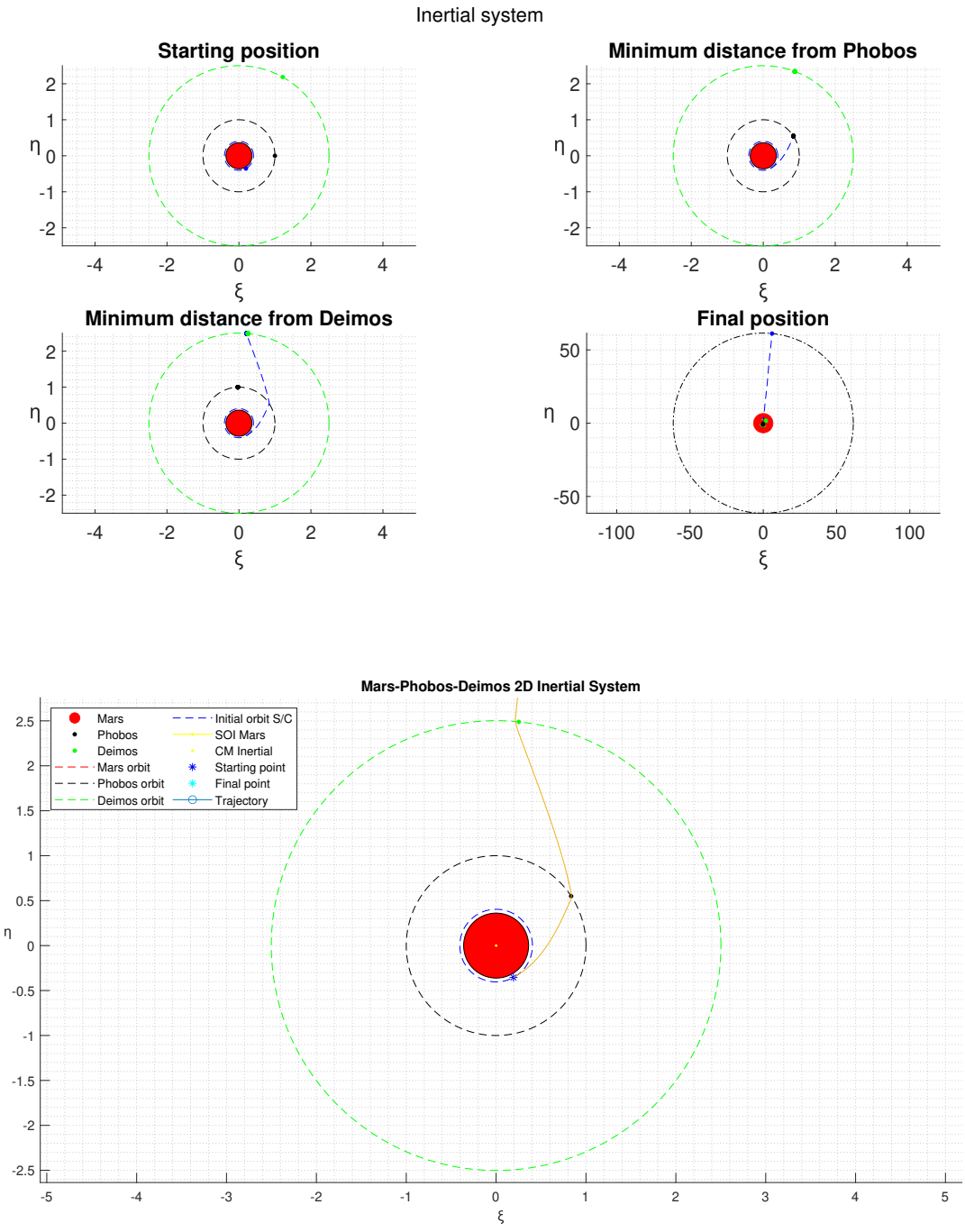

Figure 5.17: Inertial BCFB

The following two graphs clearly clarify what happens during this combined flyby maneuver: in fact, it can be seen from the figure 5.18b how the velocity trend undergoes two peaks, the first at the flyby with Phobos causing a marked increase in the velocity vector norm, and subsequently, a second flyby this time with Deimos braking, which causes a more slight decrease in the velocity vector norm. A similar trend can also be seen from the energy behavior depicted in Figure 5.19.

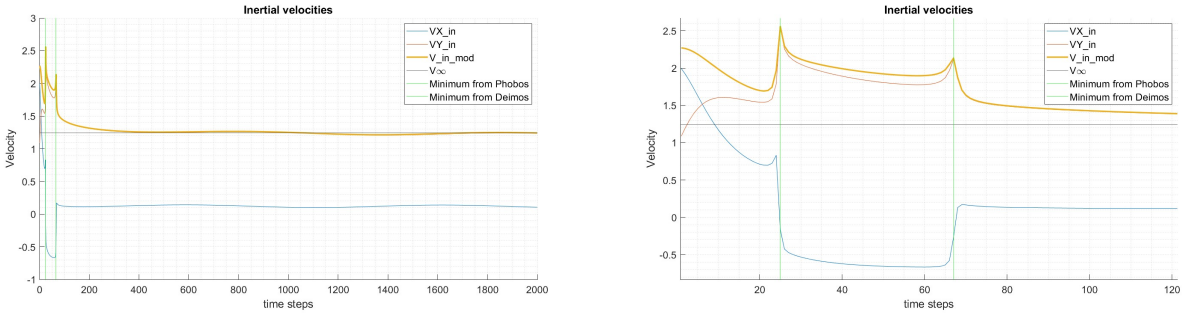

(a) **(b)**

Figure 5.18: Best Combined Flyby BCFB - Inertial velocities

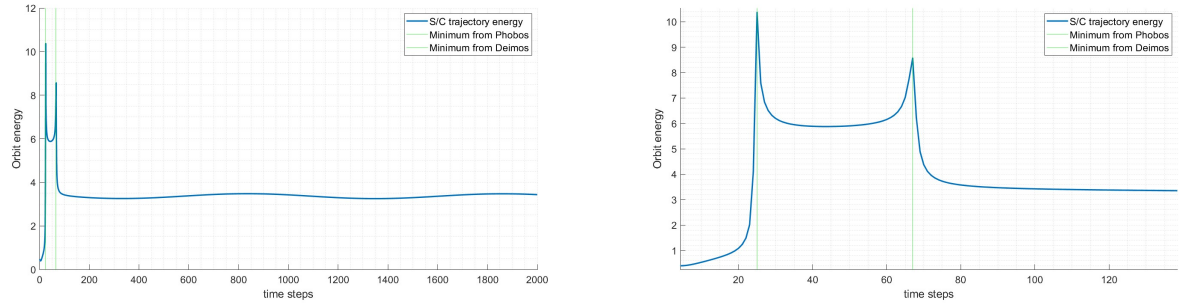

(a) **(b)**

Figure 5.19: Best Combined Flyby BCFB - Energy plot

5.5 Summary of trajectories and final results

The following table summarizes in schematic form the results obtained. Specifically, a parametric analysis was conducted in which the gravitational parameter μ (defined as per the equation 3.4) of a generic binary system was varied from a minimum value of $1{,}6606 \times 10^{-8}$, which represents the real case of the Mars-Phobos binary system, to a maximum value of $1{,}6606 \times 10^{-1}$, with the purpose of going to investigate what the minimum binary gravitational ratio must be in order for it to make sense to talk about a gain of at least 1 m/s compared to the ΔV that is needed instead to make a direct escape without any gravitational assistance from a planet's moons. Note that, for example, in the case of the Jupiter-Ganymede binary system (which represents the most massive of Jupiter's many moons) the gravitational parameter μ is worth $7{,}8065 \times 10^{-5}$, while in the more common case of the Earth-Moon binary system it is worth 0,0122, which is why, this parametric analysis should not be seen as descriptive only of the Mars-Phobos binary system, but on the contrary, the Mars-Phobos system represents only one of the possible combinations of optimization of the gravitational parameter, which, varying in the range just described, allows to describe any binary system in the solar system.
The upper limit is due to the fact that it has been shown that it is useless to talk about a generic binary system if the mass ratios are greater than 1/4, otherwise the system will not be self-stable. In reality, however, there is no binary system with a value of μ above the value of 0,0122, which is the characteristic value of the Earth-Moon system, which is why it was decided to choose $1{,}6606 \times 10^{-1}$ as the upper limit of the parametric analysis, so that our binary system would also be included.
The code provides the possibility of being able to parametrically set the distance between the secondary and tertiary as well, so that any ternary system can be analyzed, since the distance between the primary and secondary will always be fixed and unity. In particular, the study was conducted by setting a dimensionless length range between the secondary and tertiary between 1 and 2.5: in this way it was possible to incorporate within the analysis the real cases of both the Mars-Phobos-Deimos tertiary system, characterized by a distance of 2,5015 between Phobos and Deimos, as well as the case of the tertiary Jupiter-Ganymede-Callisto system characterized by a distance between secondary and tertiary equal to 1,7589.

Label	**Trajectory [kg]**	**μ [/]**	**ΔV [km/s]**	**θ [deg]**	**φ [deg]**	**tf [rad]**
BDE	M_{Ph} and M_{De}	$1{,}6606 \times 10^{-8}$	1,2036	231,54	0	48,054
FBPh0	$M_0 = M_{Ph}$	$1{,}6606 \times 10^{-8}$	1,2036	299,77	0	48,054
FBPh1	$M_1 = 10^1 \cdot M_{Ph}$	$1{,}6606 \times 10^{-7}$	1,2036	300,13	0	48,054
FBPh2	$M_2 = 10^2 \cdot M_{Ph}$	$1{,}6606 \times 10^{-6}$	1,2036	299,55	0	48,054
FBPh3	$M_3 = 10^3 \cdot M_{Ph}$	$1{,}6606 \times 10^{-5}$	1,2010	299,69	0	48,055
FBPh4	$M_4 = 10^4 \cdot M_{Ph}$	$1{,}6606 \times 10^{-4}$	1,1888	299,34	0	48,061
FBPh5	$M_5 = 10^5 \cdot M_{Ph}$	$1{,}6606 \times 10^{-3}$	1,0352	299,04	0	48,138
FBPh6	$M_6 = 10^6 \cdot M_{Ph}$	$1{,}6606 \times 10^{-2}$	0,6711	297,15	0	48,314
FBPh7	$M_7 = 10^7 \cdot M_{Ph}$	$1{,}6606 \times 10^{-1}$	0,1944	291,56	0	48,268
FBDe0	$M_0 = M_{De}$	$1{,}6606 \times 10^{-8}$	1,2036	269,91	0	48,054
FBDe1	$M_1 = 10^1 \cdot M_{De}$	$1{,}6606 \times 10^{-8}$	1,2036	270,59	0	48,054
FBDe2	$M_2 = 10^2 \cdot M_{De}$	$1{,}6606 \times 10^{-8}$	1,2036	269,74	0	48,054
FBDe3	$M_3 = 10^3 \cdot M_{De}$	$1{,}6606 \times 10^{-8}$	1,2036	269,84	0	48,054
FBDe4	$M_4 = 10^4 \cdot M_{De}$	$1{,}6606 \times 10^{-8}$	1,2029	269,64	0	48,055
FBDe5	$M_5 = 10^5 \cdot M_{De}$	$1{,}6606 \times 10^{-8}$	1,1928	269,77	0	48,074
FBDe6	$M_6 = 10^6 \cdot M_{De}$	$1{,}6606 \times 10^{-8}$	1,1452	268,85	0	48,197
FBDe7	$M_7 = 10^7 \cdot M_{De}$	$1{,}6606 \times 10^{-8}$	0,8032	263,69	0	49,599
BCFB	M_{Ph} and M_{De}	$1{,}6606 \times 10^{-2}$	0,6275	298,61	0	48,518

Table 5.1: Mars-Phobos-Deimos results

In contrast, the table 5.2 shows the errors related to a trajectory. In particular, the column *err* refers to the dimensionless sum between *err1* (which determines how accurately the S/C has arrived at the boundaries of Mars' SOI) and *err2* (which determines how accurately the final velocity of the S/C is close to V_∞): as one can easily visualize these are very low errors, even negligible compared to the magnitudes involved. The second column, on the other hand, allows us to visualize the error on the final position expressed in a dimensional way, however: as can be seen there is talk about errors that in the worst case are of the order of 10 m, while as for the third column, which shows the error on the velocity expressed in a dimensional that in the worst case is of the order of 10 mm/s.
This accuracy of the results is to be attributed to the robustness of the genetic

algorithm described in Chapter 4, which allows for errors that are all the lower the more the number of generations performed is increased. In the specific case, these results were obtained by setting a number equal to 100 generations, where each generation consists of a population consisting of 1000 individuals.

Label	**err [/]**	**err1 [mm]**	**err2 [mm/s]**
BDE	$8{,}5413 \times 10^{-10}$	0,0179	0,0012
FBPh0	$9{,}3178 \times 10^{-9}$	12,3649	0,0171
FBPh1	$1{,}1113 \times 10^{-7}$	418,4932	0,1421
FBPh2	$3{,}4383 \times 10^{-6}$	$1{,}0667 \times 10^{4}$	4,9173
FBPh3	$6{,}9397 \times 10^{-6}$	$1{,}8829 \times 10^{3}$	14,4012
FBPh4	$2{,}5879 \times 10^{-7}$	219,0044	0,5031
FBPh5	$2{,}0811 \times 10^{-7}$	$1{,}8926 \times 10^{3}$	0,0135
FBPh6	$9{,}1285 \times 10^{-8}$	815,9516	0,0091
FBPh7	$6{,}1177 \times 10^{-8}$	234,1968	0,0774
FBDe0	$2{,}1488 \times 10^{-9}$	3,1715	0,0039
FBDe1	$2{,}0766 \times 10^{-8}$	46,0572	0,0339
FBDe2	$1{,}6945 \times 10^{-7}$	871,8633	0,1634
FBDe3	$1{,}9950 \times 10^{-7}$	$1{,}4160 \times 10^{3}$	0,1037
FBDe4	$1{,}2254 \times 10^{-8}$	114,9180	0,0026
FBDe5	$3{,}3416 \times 10^{-6}$	$2{,}2982 \times 10^{3}$	6,6173
FBDe6	$3{,}9164 \times 10^{-12}$	0,0335	$7{,}3169 \times 10^{-7}$
FBDe7	$1{,}2346 \times 10^{-12}$	0,0014	$2{,}3195 \times 10^{-6}$
BCFB	$4{,}0593 \times 10^{-7}$	737,5047	0,6994

Table 5.2: Mars-Phobos-Deimos errors

The following plot in Fig. 5.20 compares the binary gravitational parameter μ with the ΔV required to reach the SOI of Mars by passing in the vicinity of Phobos: it is possible to see how for low values of μ the ΔV is concentrated around the range centered in 1,2 km/s, a sign that in practice there would be no convenience in implementing a flyby maneuver in the case of the real ternary Mars-Phobos-Deimos system (characterized by a binary parameter of $1{,}6606 \times 10^{-8}$).
As mentioned, the figure 5.20 was obtained by sweeping the parameter μ in a range from $1{,}6606 \times 10^{-8}$ to $1{,}6606 \times 10^{-1}$, which is why, in order to understand the order of magnitude of the parameter μ from which one can appreciate nonnegligible ΔV gains, one must zoom in to the initial part of the graph, which is shown in figure 5.21. From that graph it is therefore possible to conclude that the gain in terms of ΔV begins to be relevant from a value of μ equal to $0{,}3 \times 10^{-3}$ onward, since it is from this value that, sporadically, we can begin to have ΔV that are about half as large as the 1,2 km/s of direct escape, and that this advantage gradually becomes more convenient, following a law in with the ΔV decreases hyperbolically as the parameter μ increases.

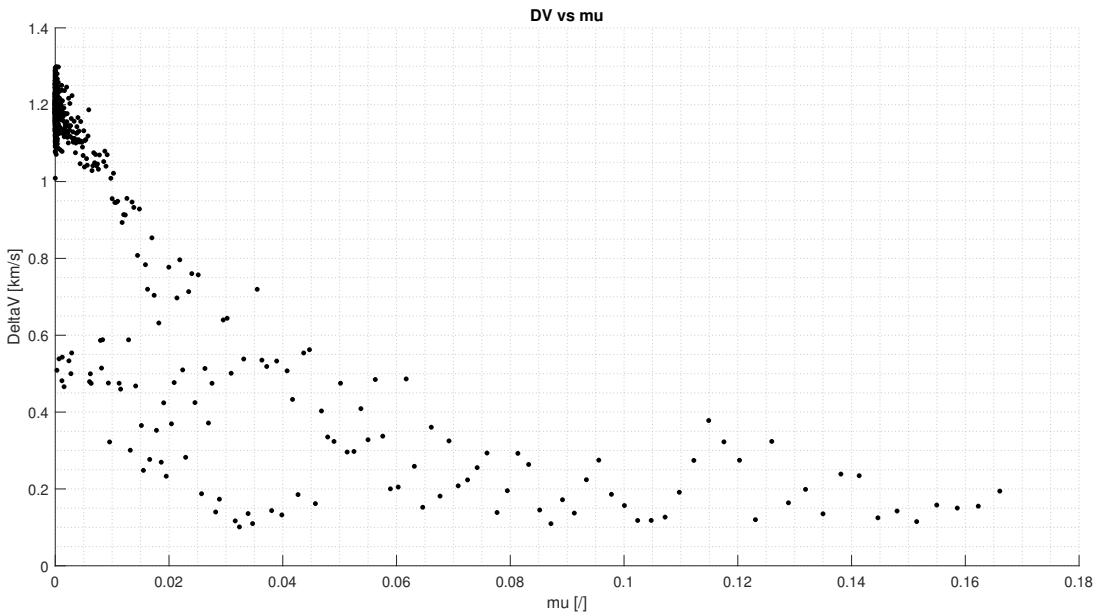

Figure 5.20: μ vs ΔV comparison

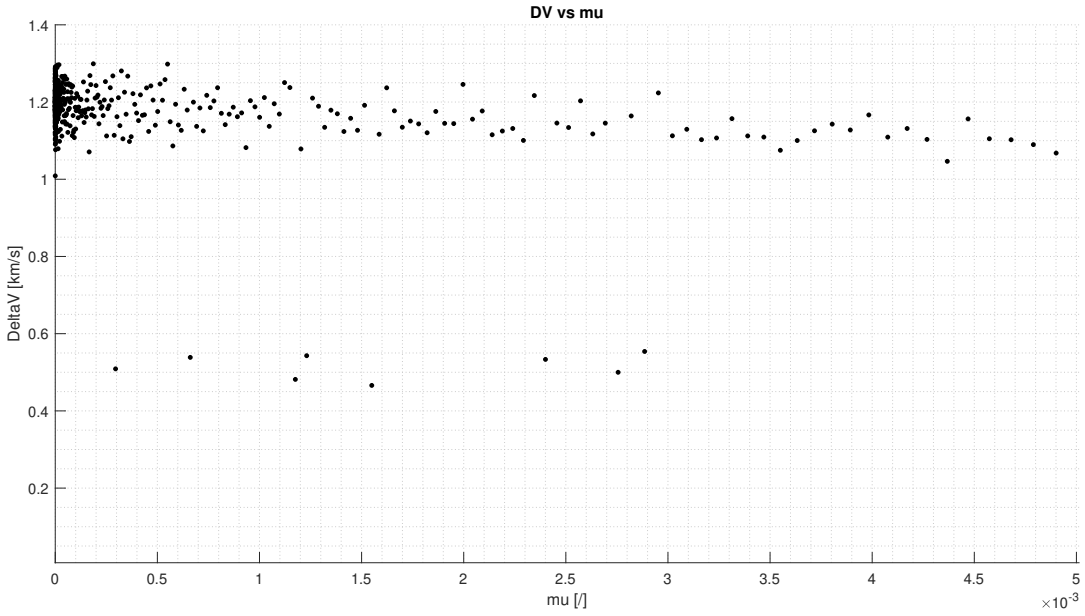

Figure 5.21: μ vs ΔV comparison (zoom)

5.6 Generic ternary system

This section will present the results of the parametric analysis aimed at simulating any ternary system. The analysis consists of the implementation of a triple cycle *for* in which, from time to time, the following are made to vary:

- the gravitation parameter of the binary system μ_{12}, it will be made to vary from a minimum value of $1{,}6606 \times 10^{-8}$, which represents the Mars-Phobos system as well as the minimum value this parameter can take, up to a maximum value of $1{,}6606 \times 10^{-1}$ so as to also encompass the maximum value this parameter can reach, i.e., of 0,0122 in the case of the Earth-Moon system, with steps of one order of magnitude each.

- the mass of the tertiary body m_3, it will be made to vary from a minimum value of 2×10^{15} kg representing the case of the microscopic mass of Deimos, up to a maximum value of 2×10^{23} kg, so as to also encompass the mass of Ganymede, which with its mass of $1{,}4819 \times 10^{23}$ kg represents the most massive moon in the solar system, with steps of an order of magnitude each.

- the dimensionless distance d_{12-3} between the barycenter of the binary system and the tertiary body, it will be made to vary from a minimum value of 1 (having a parameter d_{23}=1 will thus mean that the tertiary body is at a unit distance from the center of the synodic reference system, and rotates in its circular orbit together with the secondary body) to a maximum value of 2.5 with steps of 0.25, so as to encompass most of the existing ternary systems, such as even the Mars-Phobos-Deimos system that sees Deimos at a dimensionless distance equal to 2,5015 or even the Jupiter-Ganymede-Callisto system that sees Callisto at a dimensionless distance equal to 1,7589.

To obtain the following results, it was decided to implement a *while* loop so that the genetic algorithm could iterate until, for each case considered, i.e., for each trajectory defined by the triple [μ_{12},m_3,d_{12-3}], the following conditions occurred simultaneously:

- the error 1 on the final position reached by the probe once it arrived at the boundaries of Mars' sphere of influence less than 0.1, which in dimensional terms means an error at most 937,80 km.

- the error 2 on the final velocity reached by the probe less than 0.1, which in dimensional terms means an error of plus or minus 0,2137 km/s with respect to V_∞

- for each trajectory is recorded the vector ray followed by the probe and the one related to the position of Phobos and Deimos within their circular orbit: the minimum value of the difference between these two vector rays will thus represent the minimum distance at which the probe will pass in the vicinity of both moons of Mars.
  Two additional constraints were imposed on this parameter so as to exclude those trajectories that perhaps meet both error 1 relating to final position and error 2 relating to final velocity but passing too far from Phobos and Deimos for which, effectively, there would be no gravitational assistance.

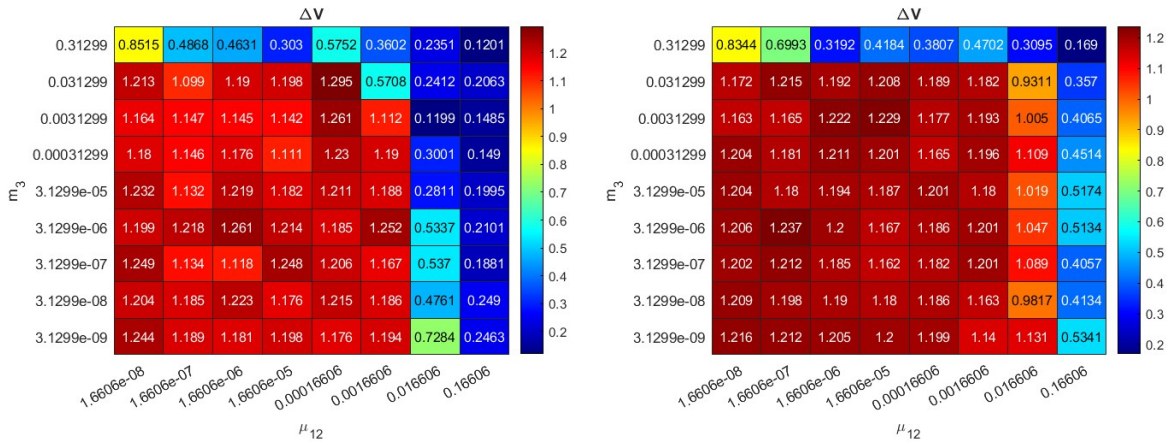

(a) d=1.25

(b) d=1.5

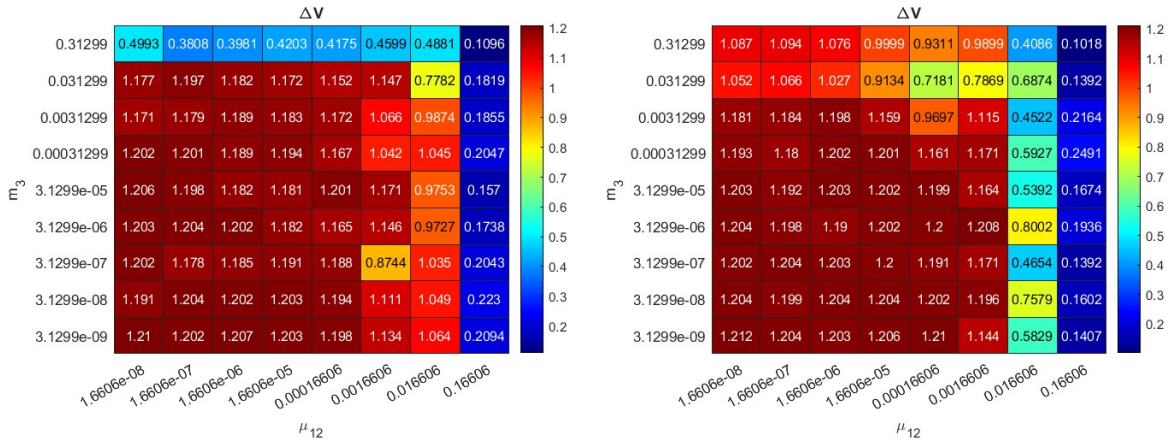

(c) d=1.75

(d) d=2

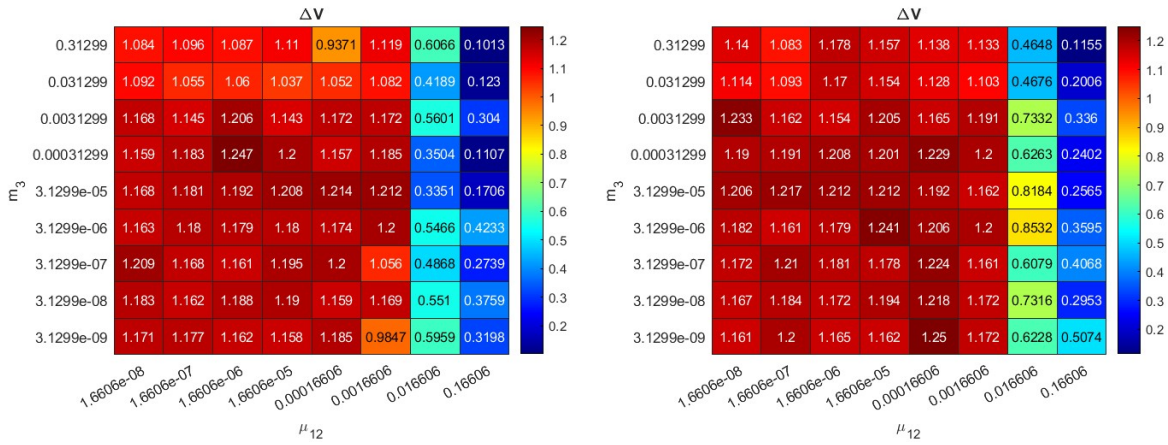

(e) d=2.25

(f) d=2.5

Figure 5.22: Parametric analysis at fixed distance

As can be clearly seen, the cases of greatest interest, where a visible and effective decrease in ΔV can be seen, are those in which the third body has a dimensionless mass equal to $m_3 = 0.31299$ and the secondary body is characterized by a gravitational parameter equal to $\mu_{12} = 0.0166$ and/or $\mu_{12} = 0.166$.
A more careful analysis of the tables, however, would allow one to see that from the d=2 case onward the gravitational effect given by the third body becomes progressively weaker, causing an increase in the ΔV relative to the line characterized by $m_3 = 0.31299$. This effect should not be surprising since it confirms what could be regarded as one of the fundamental rules of astrodynamics. In fact, as explained in detail in Chapter 2 of this paper, it is convenient to thrust at low radii when the velocity is high, and in this case a similar reasoning applies: the gravitational effect of the third body, which allows the probe to receive "free" acceleration, is maximized if the probe is already fast, that is, if the third body is at a relatively small distance from the initial orbit of the probe. As the third body is moved away, the probe will arrive in its vicinity with decreasing speed, so the advantage in implementing the flyby maneuver becomes weaker and weaker.
In conclusion, I would like to mention that, while in the case of the parametric analysis involving the particular case of the Mars-Phobos-Deimos ternary system with only the gravitational parameter μ varying and the other two parameters involved in the parametric analysis remaining fixed, the best possible trajectories were shown, and therefore the value of ΔV was the minimum possible value; in this case where the parametric analysis focuses on simultaneously varying in a combined way all three fundamental parameters involved, the ΔV referred to each individual trajectory will not necessarily be the minimum, since searching for the point of minimum of each individual trajectory would have implied a very high cost and computational time, but it will certainly represent a valid value of the parameter ΔV that allows to obtain a valid escape trajectory respecting the requirements described above and that, at the same time, allows to visualize the general trend of ΔV as the parameters involved vary. In this sense, a possible future work could in fact be to search for the minimum value of ΔV for every single combination of the triple $[\mu_{12}, m_3, d_{12-3}]$, so as to build a parametric model that allows to evaluate the point of optimum in every possible combination of the involved parameters.

Chapter 6

Conclusion

In summary, in this thesis work, the Mars-Phobos-Deimos system was presented as a particular case of a parametric analysis to simulate any ternary system. In order to go into more detail and actually evaluate how convenient it is to exploit the gravitational effects of the moons of a generic planet, a simplified parametric analysis was conducted, adapted to the case of Mars and its two moons, whereby only the gravitational parameter of the Mars-Phobos binary system and the mass of the ternary body were varied. Under these assumptions, it was possible to identify the best flyby maneuvers with the individual moons and subsequently with both, and the effect of the interaction between them and the space probe were highlighted both in graphical form through visualization of the trajectory itself and in the form of velocity and energy trends, which allow, although not as directly as in the case of the trajectories, to be aware of the consequences that such flyby maneuvers have on the probe itself.
The results showed that it is possible to have significant benefits in terms of ΔV from a minimum value of the gravitational parameter μ equal to $0{,}3 \times 10^{-3}$ onward. In particular, as shown by the graph 5.21, it is from this value onward that it is possible to have optimal solutions characterized by a value of ΔV of about $0{,}5\,\mathrm{km/s}$. However, even considering only the area of the graph characterized by values of the gravitational parameter μ greater than $0{,}3 \times 10^{-3}$, it can be seen from the trend of the solutions that the genetic algorithm stabilizes at suboptimal solutions characterized by a much higher ΔV around $1{,}2\,\mathrm{km/s}$. For this reason, with a view to future studies, it might be interesting to be able to train the genetic algorithm to make the optimal solutions even more elitist, in order to help stabilize around the optimal solution, once one has been found.
Next, the parametric analysis was extended in its most general case possible by going to vary all three fundamental parameters involved in the definition of a ternary system (thus also adding the possibility of varying the relative distance between secondary and tertiary bodies), and the results in terms of ΔV were shown

in the form of heatmaps in figure 5.22.
In light of the results obtained and analyzed in the previous chapter, it is possible to draw some very important conclusions, and more importantly, to justify why this analysis was conducted.
The construction of an orbiting station around the Moon emerges as a crucial prospect in the field of space exploration and lunar missions [31, 32], both because in the first place the Moon is large enough to be able to keep a possible space station on a stable orbit, and because it offers a significant advantage in terms of ΔV, allowing a significant reduction in the energy requirements for launching and recovering space missions. Launching a mission from the lunar surface requires a significant amount of energy to overcome lunar gravity and reach lunar orbit. An orbiting station could be placed in a stable and relatively low orbit around the Moon, thus reducing the ΔV needed to reach it from a mission from Earth or the Moon itself. This means that less energy is required to reach the orbiting station compared to a direct launch to other deep-space destinations.
Well, by the time mankind succeeds in colonizing Mars, the results obtained show that it is futile to hope that on Phobos and Deimos it makes sense to do something similar, both because they are too small (it would be correct to call them asteroids and not moons, given the size of their radii) and therefore would not be able to maintain a hypothetical space station on a stable orbit around them, and because they would not give any advantage in terms of ΔV.

Acknowledgements

In one of my first lessons at the Polytechnic, Professor Marco Mezzalama, chair of the Computer Science course to first-year students in Aerospace Engineering, said, "Guys, it is important to be engineers, but the most important thing is to be men." This phrase has guided me through these five years of study, and I can finally say that today I have become both.
Therefore, I would like to thank first and foremost my family who supported me throughout this journey and above all shaped what I call "being a man" in these lines. Thank you mom and thank you dad for making me the person I am today.
On the other hand, as far as "being engineers" is concerned, surely I should thank myself for never having given up even in the most difficult moments that this path has put in front of me, for having more or less easily managed to get back on my feet and for having continued to move forward more determined than before; but I do not like to be the center of attention so I will pause briefly to thank the whole Polytechnic understood as a combination of places and people who have shared this journey with me and who, each in his or her own way, have made it special.
Finally, I would like for a heartfelt thank you to the person who believed that I could pursue this thesis work before I could even believe it myself, I admit to you only now that at the beginning of this journey I thought I couldn't do it, but I think you had already figured it out and at every meeting you never failed to add a motivational speech to keep me from giving up; I appreciated it so much, thank you very deeply Luigi.

Bibliography

[1] A. Brown and Erik Gregersen. *Curiosity.* URL, last accessed on 2023-10-15. 2023.

[2] NASA. *NASA's Perseverance Rover Sees Mars in a New Light.* URL, last accessed on 2023-10-15. 2023.

[3] Sydney Do et al. "An Independent Assessment of the Technical Feasibility of the Mars One Mission Plan – Updated Analysis." In: *Acta Astronautica* 120 (2016), pp. 192–228.

[4] European Space Agency. *Mars sample return.* URL, last accessed on 2023-10-15. 2023.

[5] K. Muirhead Brian et al. "Mars Sample Return Campaign Concept Status". In: *Acta Astronautica* 176 (2020), pp. 131–138.

[6] Jeffrey V. Bowles, Loc C. Huynh, and Veronica M. Hawke. *Mars Sample Return: Mars Ascent Vehicle Mission and Technology Requirements.* URL, last accessed on 2023-10-15. 2023.

[7] Kazuhisa Fujita et al. *Nonstop Mars Sample Return System Using Aerocapture Technologies.* URL, last accessed on 2023-10-15. 2009.

[8] European Space Agency. *Space for Kids - Phobos and Deimos - ESA.* URL, last accessed on 2023-10-15. 2010.

[9] Roger R. Bate, Donald D. Mueller, and Jerry E. White. *Fundamentals of astrodynamics.* Vol. 1. Courier Dover Publications., 2020.

[10] Fundamentals of Astrodynamics and Applications. *Vallado, D. A., & McClain,* Space Technology Library, 2001.

[11] Cornelisse J.W., Schöyer H.F.R., and Wakker K.F. *Rocket Propulsion and Spaceflight Dynamics.* Pitman, London, 1979.

[12] Wang Sang Koon et al. *Dynamical Systems, the Three-Body Problem, and Space Mission Design.* Marsden Books, 2006. ISBN: 978-0-615-24095-4. DOI: 10.1142/9789812792617_0222.

[13] U. Walter. *Astronautics:* vol. 3. Springer International Publishing, 2018.

[14] Orbital Mechanics for Engineering Students. *H. D. Curtis.* Vol. 3. Butterworth-Heinemann, 2014.

[15] Diane Davis Kenza Boudad Kathleen Howell. *Energy and Phasing Considerations for Low-Energy Transfers from Cislunar to Heliocentric Space.* URL, last accessed on 2023-10-15. 2021.

[16] L. Abolfazl e J. Ceberio. J. Shirazi. *Spacecraft trajectory optimization: A review of models, objectives, approaches and solutions.* URL, last accessed on 2023-10-15. 2018.

[17] David W. Dunham et al. *Morph the gateway into an Earth-Mars cycler? Trajectories to/from Mars.* URL, last accessed on 2023-10-15. 2020.

[18] Brian P. McCarthy and Kathleen C. Howell. *Quasi-periodic orbits in the Sun-Earth-Moon Bicircular Restricted Four-Body Problem, Purdue University.* URL, last accessed on 2023-10-15. 2021.

[19] Topputo F. "On Optimal Two-Impulse Earth–Moon Transfers in a Four-Body Model". PhD thesis. Politecnico di Milano, Milan, Italy., 2013.

[20] Jacob A. Dahlke. *Optimal Trajectory Generation in a Dynamic Multi- Body Environment using a Pseudospectral Method,* URL, last accessed on 2023-10-15. 2018.

[21] Victor Szebehely and E Grebenikov. "Theory of Orbits-The Restricted Problem of Three Bodies." In: *Soviet Astronomy, Vol. 13, p. 364* 13 (1969), p. 364.

[22] June Barrow-Green. *Poincaré and the three body problem.* 11. American Mathematical Soc., 1997.

[23] Henri Poincaré. "Sur le problème des trois corps et les équations de la dynamique". In: *Acta mathematica* 13.1 (1890), A3–A270.

[24] R. C. Domingos, R. Vilhena de Moraes, and A. F. Bertachini De Almeida Prado. "Third-Body Perturbation in the Case of Elliptic Orbits for the Disturbing Body". In: *Mathematical Problems in Engineering* 2008 (2008). DOI: 10.1155/2008/763654.

[25] Daniel J. Grebow. "Generating Periodic Orbits in the Circular Restricted Three-Body Problem with Applications to Lunar South Pole Coverage". MA thesis. Purdue University, 2013.

[26] Martin Lara. "On Perturbation Solutions in the Restricted Three-Body Problem Dynamics". In: *Acta Astronautica* 195 (2022), pp. 596–604. ISSN: 0094-5765. DOI: 10.1016/j.actaastro.2022.01.022.

[27] Daniel J. Grebow. "Generating Periodic Orbits in the Circular Restricted Three-Body Problem with Applications to Lunar South Pole Coverage". MA thesis. Purdue University, 2013.

[28] Luigi De Maria. *Planar Bicircular Restricted 4-Body Problem (PBR4BP)*. URL, last accessed on 2023-10-15. 2023.

[29] Thomas A. Pavlak. "Trajectory Design and Orbit Maintenance Strategies in Multi-Body Dynamical Regimes". PhD thesis. Purdue University, 2013.

[30] Brian P. McCarthy and Kathleen C. Howell. "Trajectory Design Using Quasi-Periodic Orbits in the Multi-Body Problem". In: *Proceedings of the AIAA/AAS Astrodynamics Specialist Conference*. AAS 19-329. Portland, ME, USA, Aug. 15, 2019.

[31] ESA Earth Observation Portal (eoPortal). *Lunar Gateway of NASA's Artemis Program*. (Retrieved: 2023-10-15). URL: `https://www.eoportal.org/other-space-activities/lunar-gateway`.

[32] NASA. *The Artemis Plan*. NASA's Lunar Exploration Program Overview, Technical Report NP-2020-05-2853-HQ. (Retrieved: 2023-10-15). URL: `https://www.nasa.gov/sites/default/files/atoms/files/artemis_plan-20200921.pdf`.